

Leibniz-Institut für Katalyse e.V.

an der Universität Rostock

**Late transition metal complex catalyzed
dehydrogenation of hydrazine borane and other
primary amine boranes**

Kumulative Dissertation

Zur Erlangung des akademischen Grades

doctor rerum naturalium (Dr. rer. nat.)

der Mathematisch-Naturwissenschaftlichen Fakultät
der Universität Rostock

vorgelegt von

M. Sc. Delong Han

geb. am 05. 01. 1989 in P. R. China

Rostock, April 2018

Die vorliegende Arbeit wurde im Zeitraum von November 2014 bis März 2018 am Leibniz-Institut für Katalyse e.V. an der Universität Rostock im Arbeitskreis von PD Dr. Torsten Beweries angefertigt.

1. Gutachter:

PD. Dr. Torsten Beweries

Leibniz-Institut für Katalyse e. V. an der Universität Rostock

2. Gutachter:

Prof. Dr. Rüdiger Beckhaus

Institute für chemie, Universität Oldenburg

Tag der Einreichung: 28. March. 2018

Tag der Verteidigung: 26. June. 2018

Acknowledgement

I would like to express my most sincere thanks to my supervisor *PD Dr. Torsten Beweries* for offering me such a value opportunity studying under his guidance. Throughout the past four years, what I learn from him is not just limited to professional knowledge and an attitude towards research, but also German customs and practices. Without his illuminating suggestion, inspired encouragement and patient supervision, this dissertation would not have been possible. Additionally, I am also grateful him for his kindness and consideration in daily work, which gives me chances to promote myself in the future.

I am deeply indebted to *Prof. Dr. Uwe Rosenthal* for enrolling me working as a member in such an outstanding institute and giving me so much useful advices on my study.

I do appreciate *PD Dr. Haijun Jiao* and *Prof. Dr. Yongwang Li* from the bottom of my heart, because their suggestions and help brought me to the turning point of my life and a prospect to extend my horizon. Except that, I would like to thank *Dr. Jiao* and his wife (*Mrs. Yihua Zhang*) for always doing their best to provide supports to me in academy as well as life from the day I came to Rostock.

My gratitude also goes to each dear member of my group, *Dr. Christian Godemann, Dr. Laura Dura, Dr. Marcus Klahn, Dr. Markus Joksche, Felix Anke, Benjamin Andres, Patrick Hasche, Dr. Hemlata Agarwala* and *Dr. Michael Trose* for providing kind and hospitable assistance and such a comfortable and pleasant working atmosphere. Working with all of you is the most unforgettable period in my life. Besides, my German teammates are good teachers for my German learning. However, it still needs to improve a lot. A thank you also goes to all members of the coordination chemistry and catalysis group.

I sincerely thank *Dr. Anke Spannenberg, Dr. Wolfgang Baumann* for their excellent collaboration and obliging discussions.

I would also like to sincerely thank all my friends and colleagues companying me when having spent wonderful moments in LIKAT, Rostock. There are *Dr. Tao Wang, Dr. Xinxin Tian, Tian Xia, Pim Puylaert, Dr. Kaiwu Dong, Dr. Qiang Liu, Dr. Xinjiang Cui, Dr. Jie Liu, Dr. Chaoren Shen, Dr. Jianbo Feng, Dr. Xianjie Fang, Dr. Wu Li, Dr. Dengxu Wang, Dr. Feng Chen, Ronald A. Farrar Tobar, Shaoke Zhang, Dr. Shaoli Liu, Dr. Yun Shi, Zhihong Wei, Teng Li, Dr. Lin Wang, Yun Zhao, Yahui Li, Wei Zhou, Zechao Wang, Dr. Jiawang Liu, Dr. Martha Hoehne, Dr. Yuehui Li, Yuya Hu, Rui Sang, Ji Yang, Xin Liu, Dr. Bern Mueller, Dr. Haoquan Li.*

I am gracious to *Dr. Christine Fischer, Mr. Andreas Koch, Mrs. Astrid Lehmann, Mrs. Susanne Buchholz* and other colleagues of analytic department for their precise analysis and generous support.

Last but not least, I would like to thank my parents and wife. I am proud as the son of my parents, they brought me up and taught me to be a man as the first teachers of my life. I am also fortunate to meet

my wife, she is such a nice girl, brings me colorful and joyful life, as well as wise ideas that benefit my career. My appreciation that I want to express to them are beyond any word.

Abstract

The content of this thesis is presented into two parts. The first part mainly focuses on exhibiting high efficiency and selective pincer complexes employed as catalysts for dehydrogenation to obtain hydrogen from potential hydrogen storage materials, hydrazine borane. The first series of pincer catalysts used for dehydrogenation of hydrazine borane is Brookhart's well-described catalysts as well as their 3,5-substituted analogs with electron withdrawing and electron donating groups. Then, iron(II) complexes bearing a PNP backbone were also utilized for dehydrogenation of the same substrate. Apart from the dehydrogenation reactions, the BN materials as coupling result of dehydrogenating amine boranes were characterized. Analyzing the BN materials shows that the structures of BN materials have relationship with dehydrogenation degree. Evolving one equivalent H_2 from amine boranes may produce linear BN polymer. However, when much more H_2 released, cyclic BN product could be synthesized. Additionally, synthesis and characterization of a PPN ligand, 2-[bis(diisopropylphosphino)methyl]-6-methylpyridine and its complexes with selected 3d metals.

Zusammenfassung

Der Inhalt der vorliegenden Arbeit ist in zwei Teile gegliedert. Im ersten Abschnitt liegt der Schwerpunkt auf der Darstellung von hocheffizienten und selektiven Pinzettenkomplexen, die als Katalysatoren für die Dehydrierung von Hydrazin-Boran eingesetzt wurden, um Wasserstoff aus potentiellen Wasserstoffspeichermaterialien zu erhalten. Dabei ist Brookharts Dehydrierungskatalysator der erste Pinzettenkomplex, der für die Dehydrierung von Hydrazinboran angewandt wurde. Es folgen weitere Untersuchungen, die den Einfluss von elektronziehenden und elektronschiebenden Substituenten an der 3,5-Position am Arylgerüst des Katalysators auf diese Reaktion erfassen. Anschließend wurden Eisen(II)-Komplexe mit einem PNP-Rückgrat für die Dehydrierung des gleichen Substrates verwendet. Darüber hinaus sind die bei der Dehydrierung anfallenden BN-Materialien charakterisiert worden und legen einen Zusammenhang zwischen der Struktur des BN-Materials und dem Dehydrierungsgrad nahe. Bei der Entwicklung von einem Äquivalent an Wasserstoff entsteht vorwiegend ein lineares Polymer. Die Bildung zyklischer Produkte ist bevorzugt, wenn mehr als ein Äquivalent Wasserstoff freigesetzt wird. Der zweite Abschnitt beschreibt die Synthese und Charakterisierung eines PPN-Liganden, 2-[Bis(diisopropylphosphino)methyl]-6-methylpyridin und dessen Komplexierung mit ausgewählten 3d Übergangsmetallen.

Abbreviation

DOE	The united states department of energy
AB	Ammonia borane
HB	Hydrazine borane
MAB	Methylamine borane
DMAB	Dimethylamine borane
<i>n</i> Bu	<i>n</i> -Butyl
<i>t</i> Bu	<i>tert</i> -Butyl
<i>i</i> Pr	Isopropyl
Dipp	Diisopropylphenyl
Me	Methyl
Et	Ethyl
THF	Tetrahydrofuran
TMS	Trimethylsilane
Cp	Cyclopentadienyl
Cp*	Pentamethylcyclopentadienyl
NMR	Nuclear Magnetic Resonance
Ph	Phenyl
TOF	Turnover frequency
TON	Turnover number
ebthi	1,2-ethylene-1,1'-bis(η^5 -tetrahydroindenyl)
OFLP	organometallic frustrated Lewis pairs
CTB	borazine cyclotriborazane
Cy	Cyclohexyl
NPs	Nanoparticles
IR	Infrared
NMR-MAS	Nuclear magnetic resonance magic-angle spinning
MQ MAS	Multiple quantum magic-angle spinning
KIE	Kinetic isotope effects
NHC	N-heterocyclic carbene
OAc	Acetoxy

COD	1,5-cyclooctadiene
Xantphos	4,5-bis(diphenylphosphino)-9,9-dimethylxanthene
K	Kelvin
DFT	Density functional theory
EA	Elemental analysis
GPC	Gel permeation chromatography
DLS	Dynamic light scattering
PDI	Highly polydispersity index
TGA	Thermogravimetric analysis
FLPs	Frustrated Lewis pairs
PS	Proton sponge
9-BBN	Diborane 9-borabicyclo[3.5.1]nonane
EPR	Electron paramagnetic resonance

Table of contents

1. Introduction.....	1
2. Dehydrogenation of amine boranes	4
2.1. Research background.....	4
2.2. Main group metal complex catalyzed dehydrogenation of amine boranes	5
2.2.1. Category 1 Complexes	5
2.2.2. Category 2 complexes	6
2.2.3. Group 14 complexes.....	8
2.3. Transition metal complex catalyzed dehydrogenation of amine boranes.....	8
2.3.1. Group 3 complexes.....	8
2.3.2. Group 4 complexes.....	10
2.3.3. Group 6 complexes.....	13
2.3.4. Group 7 complexes.....	14
2.3.5. Group 8 complexes.....	17
2.3.6. Group 9 complexes.....	30
2.3.7. Group 10 complexes.....	38
2.3.8. Group 11 complexes.....	41
2.4. Metal-free catalytic dehydrogenation of amine boranes.....	42
2.4.1. Frustrated lewis pairs (FLP)	42
2.4.2. Acid-catalyzed dehydrogenation	43
2.4.3. Based-catalyzed dehydrogenation	43
3. Objectives of this work	44
4. References	45
5. List of publications.....	51
5.1. Iridium(III) hydrido complexes for the catalytic dehydrogenation of hydrazine borane.....	53
5.2. Formation of high-molecular weight polyaminoborane by Fe hydride catalyzed dehydrocoupling of methylamine borane	63
5.3. Synthesis and coordination chemistry of the PPN ligand 2-[bis(diisopropylphosphanyl)methyl] 6-methylpyridine	71
5.4. Fe(II) hydrido complex catalysed dehydrogenation of hydrazine borane and insights on the products structure using solid-state NMR and XPS analysis.....	81
6. Curriculum Vitae.....	91
7. Compounds in the dissertation.....	93

1. Introduction

From the last few centuries to now, fossil fuels have always been the main energy sources that constantly drive prosperity and development of human society. However, numerous problems, such as environmental destruction, release of greenhouse gases, poor recyclability and so on, rise up significantly. Moreover a huge amount of fossil fuels is being consumed. Thus, at present, except fossil fuels, a growing number of economically friendly and regenerable alternatives are also adopted in terms of scale and forms.^[1] Among these potential alternatives, hydrogen, undoubtedly, is a fascinating candidate because of its apparent advantages in 1) high energy density (120 kJ/kg, which is almost three times as much as that of gasoline), 2) abundant natural storage and 3) water as the only product after consumption, all of these make building up a hydrogen economy highly desirable.^[2] Nevertheless, there are critical problems like low volumetric energy density (in liquid form is 8 kJ/L which is only a quarter of that of gasoline) setting barriers for realization of a hydrogen economy.^[3] Thus, divergent physical-based and chemical-based hydrogen storage methods were proposed to solve these problems.^[4] For the former method, the hydrogen is usually stored under special conditions which are needed to cool the systems or take a lot of extra energy to compress and liquefy hydrogen. Also hydrogen leakage may occur to a certain extent. To make matters worse, considering the weight of container and cooling system, the hydrogen storage capacity is in fact much lower.^[5] In contrast, storage of hydrogen via chemical bonds owns merits such as good stability, convenient storage conditions, higher gravimetric capacity making it chosen as a promising candidate by the American Department of Energy (DOE) for a future long-term pathway.^[6]

To date, numerous potential hydrogen storage compounds have been studied in laboratories for the long-term target, including N-ethylcarbazole,^[7] nitrogen heterocycles,^[8] ethanol and formic acid and such on.^[9] Comparing these chemical hydrogen storage compounds, it is not difficult to see that amine boranes have stand-out advantages regarding facile synthesis and storage, higher gravimetric capacity (Figure 1), and long term stability. Optimization of synthesis procedures and hydrogen evolution conditions has been done many years in various ways under non transition metal complex catalyzed conditions (i.e. thermolysis and hydrolysis) and still is being done at the moment.^[10] In recent years, except from aforementioned pathways to release hydrogen from ammonia borane (AB), numerous noble transition metal complexes designed to catalyze the dehydrogenation of AB were presented as well, which will be introduced in the next sections. In contrast, analogous reports on dehydrogenation of another hydrogen-rich molecule, hydrazine borane (HB) that utilizing transition metal complex as catalysts are rare, which makes exploring transition metal complex catalyzed dehydrogenation of HB promising in terms of basic research and application.^[11] Nevertheless, an issue that the dehydrogenated amine boranes only can be regenerated under harsh conditions narrows the usage of these materials to single-use H₂ storage materials or as bench-stable H₂ sources and needs much more focuses to overcome these issues.

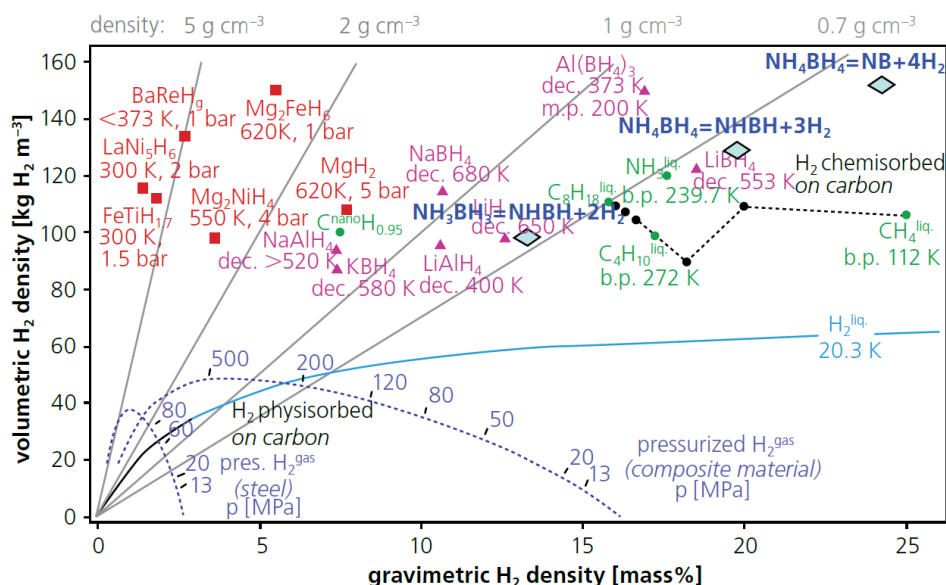


Figure 1. Comparison of gravimetric and volumetric densities of various hydrogen storage materials. ^[12]

It is noteworthy that transition metal catalysts bearing pincer ligands are employed for stoichiometric and catalytic applications and are thus well-described.^[13] Variations of ligand backbones and the metal centers can tune the electronic and steric properties of pincer complexes nicely and makes this type of organometallic compounds suitable for different kinds of reactions (Figure 2). Accordingly, since pincer complexes were first reported by Shaw in the 1970s^[14] they have been widely well practiced, e.g. for nitrogen activation,^[15] hydrogenation of CO₂,^[16] olefins,^[17] ketones,^[18] imines,^[17a] and esters,^[19] dehydrogenation of alcohols,^[20] N-heterocycles^[21] and used for the dehydrogenation of amine boranes as well.

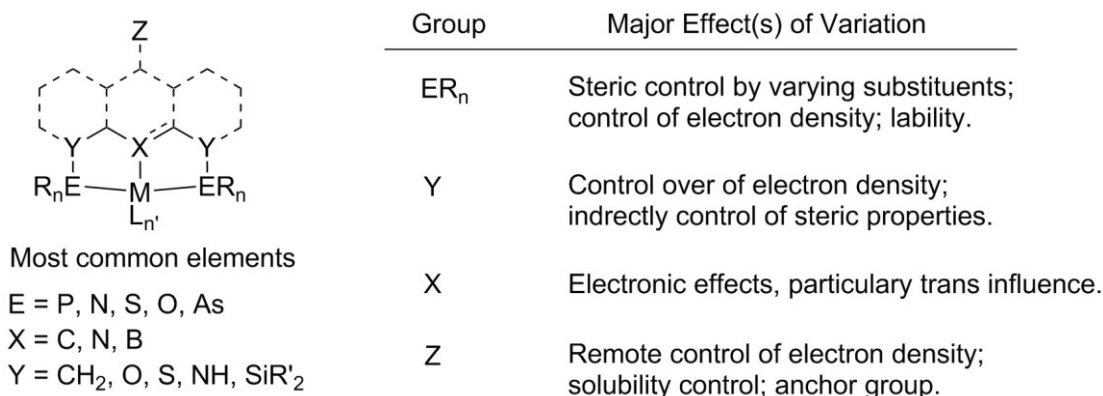
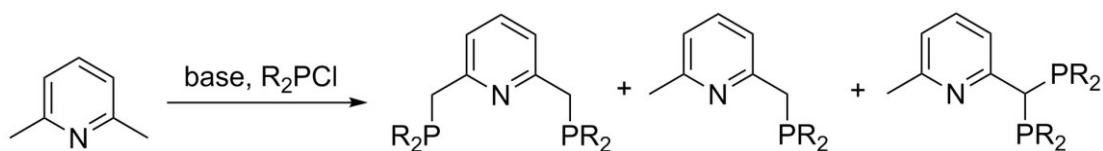


Figure 2. Variations of pincer ligand parameters for control of the steric and electronic properties. ^[13c, 22]

Generally speaking, these pincer complexes are easily synthesized or commercially available. However, when it comes to the pyridine-based aromatic PNP catalysts, one common synthesis method for building carbon-phosphorous arms is the reaction of 2,6-lutidine with *n*BuLi at low temperature,^[23] which not only gives pyridine-based PNP ligands but PPN ligands and PN ligands that result from

partial deprotonation of one-side methyl groups (Scheme 1). As having theoretically multiple binding modes, PPN ligands can be regarded as hetero-functionality containing analogs of the well-known short-bite angle ligand dppm (i.e. bis(diphenylphosphino)methane).^[24] Then, it also can be treated as PN ligands binding to catalysts which are metal ligand cooperative.^[25] Thus, it is worthy to developing PPN ligands and related transition metal complexes for practice.



Scheme 1. General pathways for the synthesis of aromatic PNP ligands, giving also PN and PPN ligands.

2. Dehydrogenation of amine boranes

2.1. Research background

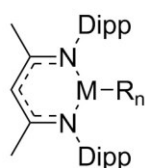
Amine boranes are ideal materials for a lot of areas. For example, AB and HB have relatively high gravimetric hydrogen capacity (approximately 19.6 wt% and 15.4 wt%, respectively), so that they are very suitable for hydrogen storage and hydrogen transfer reactions.^[26] Apart from that, a compound containing boron-nitrogen bonds is isoelectronic to compounds containing carbon-carbon bonds, but unlike the bond between two carbon atoms, the different electronegativity of boron and nitrogen makes BN compounds polar which can significantly alter molecular and solid-state electronic and optical properties of the system and the intermolecular interactions present in solid phases.^[27] These properties make boron nitrogen containing compounds interesting for polymer chemistry, optoelectronic devices, elastomers and biomaterials^[28] with special characteristics that their all-carbon analogs do not have.^[29]

From the aspect of our research, the thesis mainly focuses on the dehydrogenation of amine boranes. The details of various methods for release of hydrogen from amine boranes are depicted in the next sections. Meanwhile, it is unneglectable that dehydrogenation is a dehydrocoupling process as well. That is to say, amine borane derivatives such as methylamine borane (MAB), dimethylamine borane (DMAB), aniline borane and N,N-diisopropylamine borane except from being used as hydrogen storage materials or as models to give a better insight into mechanisms of dehydrogenation reactions of more hydrogen-rich AB,^[30] could also serve as precursors of linear or cyclic oligomers or polymers via catalytic dehydrogenation and coupling. MAB as an example is suitable substrate for dehydrogenation, mechanistic studies as well as for polymer formation. Manners and co-workers synthesized a soluble, poly(N-methylaminoborane), $[\text{MeNH-BH}_2]_n$ with high molecular weight (M_w up to 160,000) using Brookhart's Ir(III) pincer catalyst $[(\text{POCOP})\text{IrH}_2]$ (**1**) ($\text{POCOP} = [\kappa^3\text{-2,6-(OP}^t\text{Bu}_2)_2\text{C}_6\text{H}_3]$).^[31] Weller and co-workers first reported a relatively stable iridium aminoborane complex $[\text{Ir}(\text{PCy}_3)_2(\text{H})_2(\eta^2\text{-H}_3\text{B}\cdot\text{NMeH}_2)][\text{BAR}^{\text{F}}_4]$ (**2**) via adding one equivalent of MAB to the dihydrogen complex $[\text{Ir}(\text{PCy}_3)_2(\text{H})_2(\text{H}_2)_2]$ (**3**). After that, addition of a second equivalent of MAB, formation of the simplest oligomer of MAB, $\text{H}_3\text{B}\cdot\text{NMeHBH}_2\cdot\text{NMeH}_2$ was observed, which gave insights into what role a metal center of catalyst may play during the dehydrocoupling process.^[32] Our group also chose MAB to make dehydrocoupling products mediated by $[(\text{PNHP})\text{Fe}(\text{BH}_4)(\text{CO})(\text{H})]$ (**4**) ($\text{PNHP} = \text{HN}(\text{CH}_2\text{CH}_2\text{P}^i\text{Pr}_2)_2$) pincer complex with slightly more than one equivalent of hydrogen gained.^[33] We found that the polymerization process occurs after dehydrogenation, accordingly, polymerization of MAB catalyzed by the iron complex actually is an off-metal process and how much hydrogen produced is partial decided by catalyst. Dehydrocoupling, as aforementioned, is so closely related to dehydrogenation that it also necessary to be introduced in the next sections.

2.2. Main group metal complex catalyzed dehydrogenation of amine boranes

For now, two categories of general coordination patterns of main group 2 and 13 metals displayed in Figure 3 (transition metal Zn shows category 1 type coordination,^[34] Sc and Y show category 2 type coordination^[35]) have been mentioned by several groups for dehydrogenation and dehydrocoupling of ammonia borane and amine boranes and investigation of interactions between these complexes and substrates.^[36]

Category 1 - heteroleptic



M = Mg, Ca, Zn (n = 1),
Al (n = 2)
R = N(SiMe₃)₂, CH(SiMe₃)₂,
H, *n*Bu
Dipp = 1,2-*i*Pr₂-C₆H₃

Category 2 - homoleptic



M = Mg, Ca, Sr, Ba (n = 2),
Sc, Y, Al (n = 3)
R = N(SiMe₃)₂, CH(SiMe₃)₂,
*t*Bu, N(SiHMe₂)₂, NMe₂

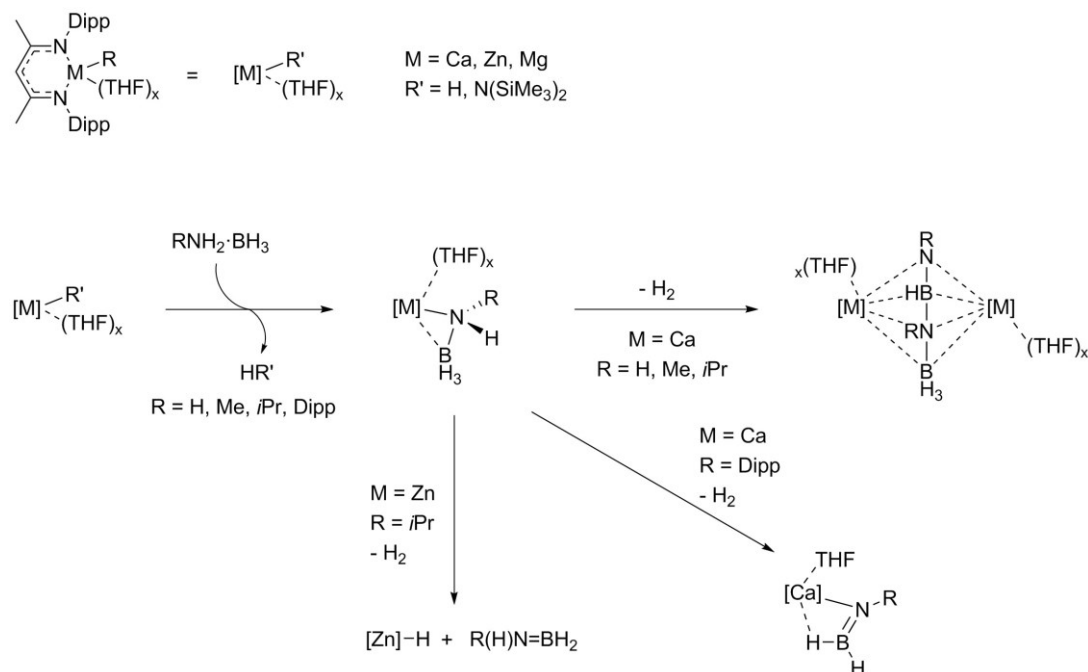
Figure 3. Two coordination patterns of main group precatalysts for dehydrogenation reactions.

2.2.1. Category 1 complexes

Two Mg complexes with nacnac type ligands [(Dipp-nacnac)Mg(*n*Bu)] (Dipp = 2,6-Diisopropylphenyl) (**5**) and [(Dipp-nacnac)MgN(SiMe₃)₂] (**6**) (Dipp-nacnac = CH{(CMe)N(2,6-*i*Pr₂C₆H₃)₂}), (Dipp-nacnac)Mg = [Mg]) were reported by Hill's and Harder's groups, individually.^[36c, 36f] Stoichiometric reaction of the [Mg]*n*Bu complex with two equivalents of DMAB produced the [Mg] ligated with anion [NMe₂BH₂NMe₂BH₃][−] which converted to [NMe₂-BH₂]₂ (20% yield) after heating for 16 hours at 60 °C with concomitant formation of a small quantity of dimeric magnesium hydride {[Mg]H(THF)₂]₂ (**7**). When using a loading of 5 mol% **6**, (Dipp)NH₂·BH₃ could be obtained quantitatively and was cleanly transformed to HB[NH(Dipp)]₂, BH₃ and H₂ in toluene at 20 °C. [Mg]NH(DIPP)BH₃ (**8**) and {[Mg]BH₄]₂ (**9**) were characterized as active catalyst and a possible intermediate, respectively.

Ca amidoborane complexes (Dipp-nacnac)CaNHRBH₃ synthesized by reaction of [(Dipp-nacnac)CaH(THF)]₂ (**10**) ((Dipp-nacnac)Ca = [Ca]) and AB, MAB, *i*PrNH₂·BH₃ and DippNH₂·BH₃ with H₂ evolution were reported by Harder's group (Scheme 2).^[36d, 36g] Analogous mono- and bimetallic Mg amidoborane complexes for supplying valuable insight into the thermal release of hydrogen from metal amidoboranes were published by the same group as well.^[37] For Ca coordinating to amine boranes with small substituents, heating in benzene gave dimerized products [(Dipp-

nacnac)Ca(THF)_n]₂(RN-BH-NR-BH₃) (R = H (**11**), *i*Pr (**12**), R = Me (**13**)). With sterically demanding amine substituent Dipp, an amidoborane complex [(Dipp-nacnac)CaBH₂=NDipp(THF)] (**14**) is formed. Secondary Ca amidoborane complex [(Dipp-nacnac)Ca(NMe₂BH₃)(THF)] (**15**) did not react with amine boranes even using an excess of the substrate.^[36c] In contrast to Mg and Ca complexes mentioned before, reaction of (Dipp-nacnac)AlH₂ (**16**) and DippNH₂·BH₃ gave (Dipp-nacnac)Al(BH₄)₂ (**17**) and DippNH₂, no H₂ was released from this reaction.^[36a] It should be emphasized that when reacting with AB, partial (Dipp-nacnac)AlH₂ can dissociate two hydrides and chelate to a ligand [HN(BH=NH)₂]²⁻ which is a dianion, isoelectronic with a β-Diketiminato.^[38]

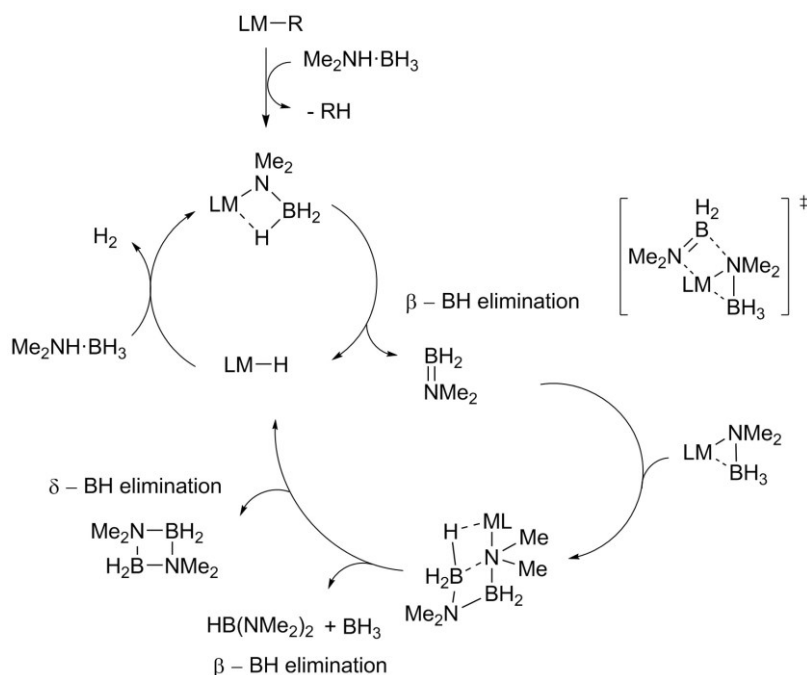


Scheme 2. Overview of the formation and decomposition of main group metal amidoborane complexes.

2.2.2. Category 2 complexes

The dehydrogenation of amine boranes using homoleptic category 2 complexes is summarized in Table 1. In dehydrogenations of DMAB using Mg[CH(TMS)₂]₂ (TMS = trimethylsilyl), formation of the anionic ligand [NMe₂BH₂NMe₂BH₃]⁻ takes place as result of dimerization of the substrate (Scheme 3).^[36c] Although the corresponding Ca complex can consume the same substrate, there was no triplet resonance assignable to the appearance of [NMe₂BH₂NMe₂BH₃]⁻. ¹¹B NMR spectra of DMAB dehydrogenation experiments promoted by Ca and Mg were similar. The authors, based on the dehydrogenation ability of the metals, proposed that efficacy of this insertion and subsequent β- or δ-hydride elimination steps is assumed to be dependent upon the charge density and polarizing capability of the participating group 2 centers. A catalytic cycle for B-N bond formation was proposed. Other two group 2 elements strontium and barium were also tested.^[36e] Mg[N(SiMe₃)₂]₂ can extract hydrogen from DMAB and *i*Pr₂NH·BH₃ in high yields via δ-hydride elimination. Reactions of secondary amine boranes with Sr and Ba complexes gave metal amido-borane complexes of the type M-NMe₂BH₃ or

M-NiPr₂BH₃, no further reaction was observed. When Al(III) category 2 complexes Al(NiPr₂)₃ and Al(NMe₂)₃ were employed to dehydrogenate DMAB, *i*Pr₂NH·BH₃ and *t*BuNH₂·BH₃^[36h] both of them show better catalytic capability on consuming amine boranes with smaller substituents. In addition to that, the authors also isolated [H₂Al(μ-NiPr₂)]₂ (**18**) from a reaction of Al(NiPr₂)₃ and *i*Pr₂NH·BH₃. Complex **18**, according to the authors, probably is the real catalyst of reaction and can transform the substrate *i*Pr₂NH·BH₃ as well.



Scheme 3. Proposed mechanism for the catalytic dehydrocoupling of DMAB by main group metal complexes.^[35]

Table 1. Main group catalyzed dehydrogenation of amine boranes.^[36c, 36e, 36h]

Substrate	Catalyst	Loading (mol %)	Product	Conversion (%)	Condition (°C, h, solvent)	TOF (h ⁻¹)
DMAB	Mg[CH(TMS) ₃] ₂	5	[NMe ₂ BH ₂] ₂	100	60, 72, C ₆ D ₆	0.28
<i>i</i> Pr ₂ NH·BH ₃	Mg[N(SiMe ₃) ₂] ₂	5	<i>i</i> Pr ₂ NBH ₂	100	25, 1, C ₆ D ₆	20.00
DMAB	Al(NMe ₂) ₃	8	[NMe ₂ BH ₂] ₂	80	25, 120, C ₇ D ₈	0.08
DMAB	Al(NMe ₂) ₃	5	[NMe ₂ BH ₂] ₂	100	50, 48, C ₇ D ₈	0.42
<i>i</i> Pr ₂ NH·BH ₃	Al(NiPr ₂) ₃	2	<i>i</i> Pr ₂ NBH ₂	100	20, 2, C ₇ D ₈	25.00
<i>i</i> Pr ₂ NH·BH ₃	Al(NiPr ₂) ₃	10	<i>i</i> Pr ₂ NBH ₂	100	60, 2, C ₆ D ₆	5.00
<i>i</i> Pr ₂ NH·BH ₃	[H ₂ Al(μ-NiPr ₂)] ₂	0.5	<i>i</i> Pr ₂ NBH ₂	50	20, 96, C ₇ D ₈	1.04
<i>t</i> BuNH ₂ ·BH ₃	Al(NMe ₂) ₃	3	[<i>t</i> BuNBH] ₃	13	20, 96, C ₆ D ₆	0.05

TOF = (mol substrate converted)/(mol.cat × time) = (conversion/loading)/time.

2.2.3. Group 14 complexes

Dehydrocoupling of AB, $t\text{BuNH}_2\cdot\text{BH}_3$ and DMAB promoted by tin catalysts was presented by Waterman and co-workers.^[39] Three Sn compounds Cp^*SnCl_2 , Ph_2SnCl_2 and SnCl_2 were examined in the catalytic dehydrogenation of amine boranes. By comparing NMR spectra and dehydrogenation profiles of amine boranes catalyzed by three tin catalysts, the authors concluded that the oxidation state of the metal does not affect the nature of catalytic dehydrocoupling of amine boranes. Only the relative rate of dehydrocoupling is affected.

Table 2. Dehydrocoupling of amine boranes using tin catalysts.^a

Substrate	Cp^*SnCl_2		Ph_2SnCl_2		SnCl_2	
	Conversion (%)	Time (d)	Conversion (%)	Time (d)	Conversion (%)	Time (d)
AB	100 ^b	1	100 ^b	1	100 ^c	~ 18 h
$t\text{BuNH}_2\cdot\text{BH}_3$	95	5	93	4	84 ^c	5
DMAB	69	6	47	4	23	5

^a reaction conditions: at 65 °C, 10 mol% loading, Sn(IV) in C_6D_6 , Sn(II) in $\text{THF}-d_8$. ^b reaction in $\text{THF}-d_8$. ^c 5 mol% loading.

2.3. Transition metal complex catalyzed dehydrogenation of amine boranes

2.3.1. Group 3 complexes

After having published works on Mg and Ca complexes, Hill's group further investigated DMAB dehydrogenation mediated by $[\text{Sc}\{\text{N}(\text{SiMe}_3)_2\}_3(\text{THF})_2]$ and $\text{Y}[\text{N}(\text{SiMe}_3)_2]_3$ in 2010, for getting better insight into relationship between catalytic activity and cationic charge density and radius.^[35] Full consumption of DMAB is observed in benzene at 60 °C after twelve hours when using 3 mol% of $\text{Y}[\text{N}(\text{SiMe}_3)_2]_3$. The cyclic dimer $[\text{NMe}_2\text{-BH}_2]_2$ is formed in 90% yield. In contrast, for $\text{Sc}[\text{N}(\text{SiMe}_3)_2]_3$ case, dehydrocoupling of DMAB occurs almost quantitatively in only one hour and selectively gives the same product. In both cases, ^{11}B NMR spectra show ambiguous signals probability due to $[\text{NMe}_2\text{BH}_2\text{NMe}_2\text{BH}_3]^-$ according to similar experiments using Mg and Ca complexes (see chapter 2.2.2). To shed light on the dehydrocoupling mechanism of both group 3 complexes, a stoichiometric reaction between the Sc amide complex and four equivalents of DMAB was carried out and lead to a new pseudo-pyramidal Sc(III) complex that contains an amide ligand $\text{N}(\text{SiMe}_3)_2$ and two $[\text{NMe}_2\text{BH}_2\text{NMe}_2\text{BH}_3]^-$ ligands that were formed by dehydrodimerization of two molecules of DMAB. The authors concluded that activity of metals is qualitatively ordered as $\text{Sc} > \text{Y} > \text{Mg} > \text{Ca}$. Meanwhile, these metals dehydrogenate DMAB in a similar mechanism.

In 2013, Chen's group presented an extremely active 1-methylboratabenzene yttrium alkyl catalyst for dehydrocoupling of DMAB after it was synthesized by their group.^[40] The reported TOF value of yttrium complex $(\text{C}_5\text{H}_5\text{BMe})_2\text{YCH}(\text{SiMe}_3)_2$ (**19**) of up to 1000 h^{-1} in benzene solvent at 50 °C with 0.5

mol% loading is higher than for any other early transition metal catalysts. Over 99% of substrate was transformed into the cyclic dimer $[\text{NMe}_2\text{-BH}_2]_2$. $^{11}\text{B}\{^1\text{H}\}$ NMR spectra indicated that linear dimer $\text{BH}_3\text{-NMe}_2\text{-BH}_2\text{-NHMe}_2$ as intermediate arose during reaction and was gradually converted into $[\text{NMe}_2\text{-BH}_2]_2$. Apart from that, a Lu complex bearing the same ligand (**20**) and boratabenzene Y (**21**) and Lu (**22**) alkyl complexes containing a more electron donating NMe_2 group on boratabenzene (Figure 4) were also tested in this paper. All of them showed far less activity. Evidently, catalytic capability of rare-earth metal complexes is highly depended on the identity of ligands and metal ions. Systematic studies on structure-activity relationships are however rare.

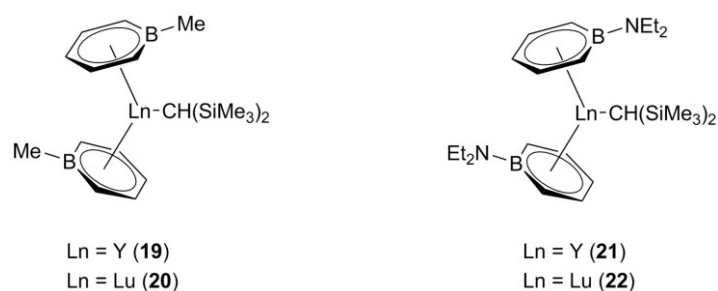


Figure 4. Rare-earth metal boratabenzene complexes for DMAB dehydrogenation.

Rare-earth-metal hydrides $[\{(1,7\text{-Me}_2\text{TACD})\text{LnH}\}_4]$ ($1,7\text{-Me}_2(\text{TACD})\text{H}_2=1,7\text{-dimethyl-1,4,7,10-tetraazacyclododecane}$, $\text{Ln}=\text{La}$, (**23**) Y (**24**)) (Figure 5) were shown to catalyze the dehydrogenation of secondary amine borane DMAB by Okuda, Maron and co-workers in 2013.^[41] All DMAB dehydrogenation reactions were performed at 60 °C in THF and monitored by ^{11}B NMR spectroscopy. It took Y hydride complex 48 hours to convert 95% of substrate into the cyclic dimer $[\text{NMe}_2\text{-BH}_2]_2$ (75%) and diamineborane $(\text{NMe}_2)_2\text{BH}$ (25%). Most remarkably, complete transformation of the same substrate into products $[\text{NMe}_2\text{-BH}_2]_2$ (79%) and $(\text{NMe}_2)_2\text{BH}$ (21%) via La hydride complex is possible within only two hours. To better explore the dehydrogenation process, complex **23** was reacted with two, eight and twelve equivalents of DMAB, respectively and gave a series of structurally characterized intermediates which gave evidence for the coordination and activation modes of DMAB and intermediates for its dehydrogenation that were trapped in the coordination sphere of a rare-earth metal center.

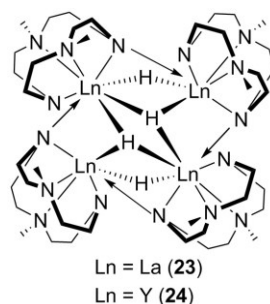
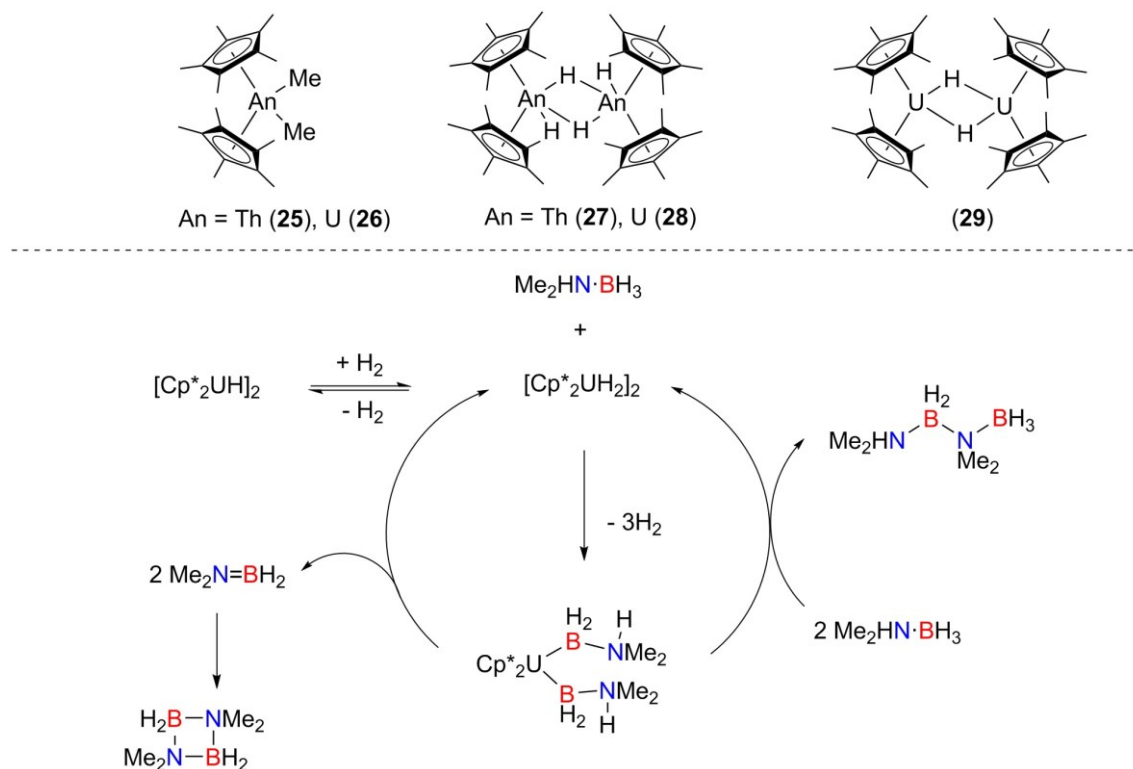


Figure 5. Rare-earth metal hydride complexes for DMAB dehydrogenation.

More recently, five examples of highly active Th and U metallocene complexes were explored for DMAB dehydrogenation by Erickson and Kiplinger (Scheme 4).^[42] All complexes exhibited outstanding activity in benzene under the same conditions. At catalyst loading of 0.5 mol%, TOF values of up to 200 h⁻¹ (complex **25**) and 400 h⁻¹ (complex **26**) were observed. These values are among the highest for DMAB dehydrogenation catalysts and demonstrate similarities in catalytic activity between (1) Th versus U catalysts, (2) dialkyl versus hydride catalysts, or (3) U(III) versus U(IV) hydride catalysts. A mechanism for dehydrogenation of DMAB by the five complexes was proposed as well (Scheme 3).

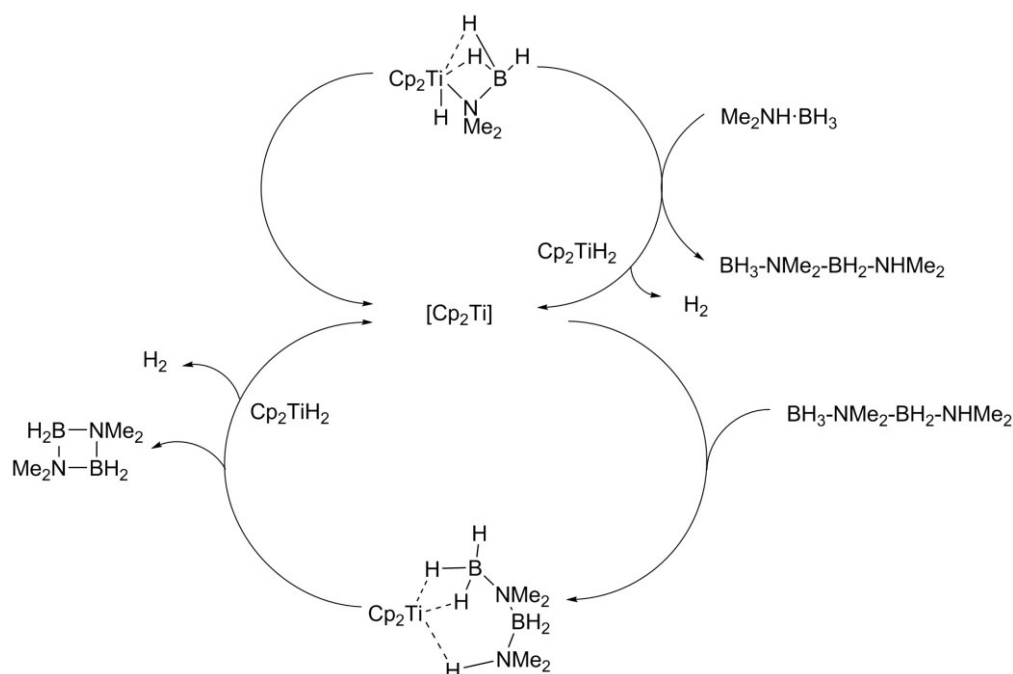


Scheme 4. Actinide complexes for the catalytic dehydrogenation of DMAB and proposed dehydrogenation cycle.

2.3.2. Group 4 complexes

A titanocene system was reported by Manners and co-workers for dehydrocoupling of DMAB after it was successfully put into dehydrocoupling of secondary silanes by Corey and co-workers.^[43] The results showed that the titanocene complex generated *in situ* from Cp_2TiCl_2 (**30**) and $n\text{BuLi}$ was suitable for dehydrogenative coupling reaction of DMAB (Scheme 5), or more sterically encumbered $i\text{Pr}_2\text{NH}\cdot\text{BH}_3$ in toluene with 2 mol% loading at 20 °C. Substrates were completely consumed and transformed into $[\text{BH}_2\text{-NMe}_2]_2$ and diisopropylamino borane in four hours and one hour, respectively. Next, the catalytic capabilities of group 4 metallocene fragments $[\text{Cp}_2\text{M}]$ (M= Ti, Zr, Hf) and derivatives which were generally synthesized by Cp_2MCl_2 and $n\text{BuLi}$ was tested. Also, $(\text{Cp}_2\text{Ti}(\text{PMe}_3)_2)$ (**31**) was investigated in the dehydrocoupling of DMAB and $i\text{Pr}_2\text{NH}\cdot\text{BH}_3$.^[44] From the collected catalytic data for using these group 4 complexes, phenomena were rationalized. First, decrease in

catalytic activity can be associated with descending the group. This was pointed out before by Chirik and co-workers as well in their report on titanocene and zirconocene catalyzed DMAB dehydrogenation, in which the TOF of a titanocene system was more than 430 h^{-1} at 23°C . In contrast, TOF values for similar zirconocene complexes for substrate dehydrogenation were less than one under the same conditions.^[45] Sterically demanding substituents have a negative effect on the dehydrogenation as well. Moreover, the secondary amine boranes neither react with Ti(0) nor Ti(III) complexes supporting the presence of a catalytically active Ti(II) complex. Analysis of ^{11}B NMR spectra of catalytic reactions showed that DMAB is first transformed to linear dimeric $\text{BH}_3\text{-NMe}_2\text{-BH}_2\text{-NHMe}_2$, and then converted into the cyclic dimer $[\text{BH}_2\text{-NMe}_2]_2$ on the metal center, which was also reported by description of Weller and co-workers for DMAB dehydrocoupling using a $[\text{Rh}(\text{PCy}_3)_2]^+$ catalyst.^[46] The catalytic cycle depicted in Scheme 5 was also computed by Luo and Ohno, however, the presence of the intermediate Cp_2TiH_2 was not confirmed experimentally.



Scheme 5. Proposed catalytic cycle of DMAB dehydrogenation using titanocene.

Titanocene and zirconocene alkyne complexes of the type $\text{Cp}_2\text{M(L)}(\eta^2\text{-Me}_3\text{SiC}_2\text{SiMe}_3)$ [$\text{Cp} = \eta^5\text{-cyclopentadienyl}$; $\text{M} = \text{Ti}$, no L (**32**); $\text{M} = \text{Zr}$, $\text{L} = \text{pyridine}$ (**33**)]^[47] (Figure 6) and their derivatives were applied to dehydrogenation of DMAB by our group in 2011.^[48] All reactions were conducted at 24°C in toluene with 2 mol% catalyst loading. Unlike the active species $[\text{Cp}_2\text{M}]$ *in situ* activated from Cp_2MCl_2 and $n\text{BuLi}$, metallocene complexes used by our group could dehydrogenate DMAB. Yields of hydrogen gas in 16 hours were 86% ($\text{M} = \text{Ti}$) and 42% ($\text{M} = \text{Zr}$). Sterically more demanding Cp^* complexes were not active for dehydrogenation. Experimental phenomena observed here were similar to those reported by Manners. Additionally, two amide complexes $\text{Zr}(\text{NMe}_2)_4$ and $\text{Ti}(\text{NMe}_2)_4$ were employed with good hydrogen yields (86% and 87%). However, $\text{Ti}(\text{OiPr})_4$ and TiCl_4 showed no

activity which indicates that the amido functionality plays a crucial role for the performance of the catalyst and how important a key group is to undergo insertion reaction to initiate the catalytic cycle. In a later report, dehydrogenation of HB was described using 2 mol% concentration of these complexes at 25 °C and 50 °C in THF.^[11a] Among them, $(i\text{PrC}_5\text{H}_4)_2\text{Ti}(\eta^2\text{-Me}_3\text{SiC}_2\text{SiMe}_3)$ (**34**) showed the best performance and can completely decompose HB to H_2 and N_2 in 32 hours at 50 °C. Using an *in situ* synthesized titanocene hydrido complex $(\text{Cp}^*_2\text{TiF}_2/i\text{Bu}_2\text{AlH})$ ($\text{Cp}^* = \text{Pentamethylcyclopentadienyl}$) and dimeric zirconocene dihydride complex $[\text{rac}(\text{-ebthi})\text{ZrH}(\mu\text{-H})_2]$ (**35**) ($\text{ebthi} = 1,2\text{-ethylene-1,1'-bis}(\eta^5\text{-tetrahydroindenyl})$) also gave full conversion of HB and indicates that a metal hydride complex may play an important role as intermediate.^[49] Nevertheless, there are drawbacks of these Ti and Zr complexes for HB dehydrogenation. First, they cannot selectively extract H_2 from substrate, N_2 is always liberated during dehydrogenation. Then, to date, regenerating spent HB is impossible. Last but not least, evolving H_2 from these Ti and Zr catalyzed systems is too slow to be applicable.

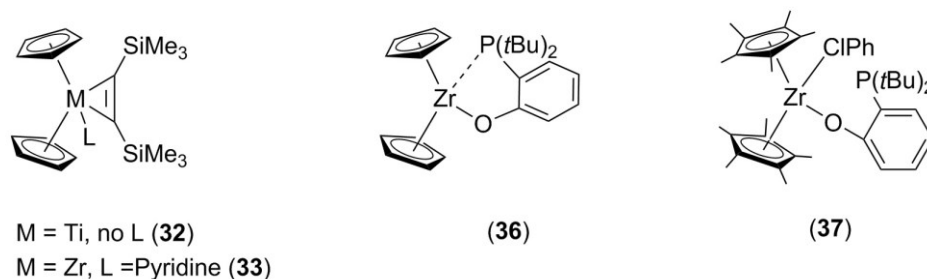
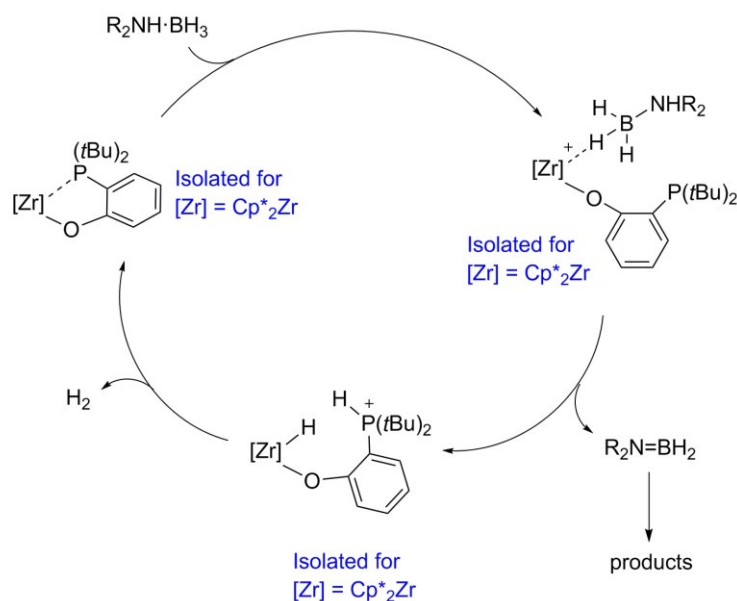


Figure 6. Group 4 metallocene complexes for dehydrogenation of amine boranes (anion portion of **36** and **37** are omitted).

In 2013, two organometallic frustrated Lewis pairs systems (OFLP) $[\text{Cp}'_2\text{ZrOC}_6\text{H}_4\text{P}(t\text{Bu})_2][\text{B}(\text{C}_6\text{F}_5)_4]$ [$\text{Cp}' = \text{Cp}$ (**36**) or Cp^* (**37**)] based on cationic zirconium Lewis acids with phosphorus bases were reported by Wass and co-workers (Figure 5).^[50] Treatment of AB with 5 mol% of **36** and **37** in fluorobenzene at room temperature gave the main product linear polyaminoborane and trace amounts of borazine. Complex **36** is capable of dehydrogenating diisopropylamine borane under the same conditions resulting in a monomeric aminoborane after three hours with 100% conversion. It is noteworthy that DMAB can be 100% converted to the cyclic dimer $[\text{NMe}_2\text{-BH}_2]_2$ using 1 mol% of **36** within ten minutes, presenting exceptional activity (TOF is 600 h^{-1}) among known group 4 catalysts. Its Hf analogue was also active for DMAB dehydrogenation (99% yield after one hour at 1 mol% loading). The mechanism proposed by the authors is shown in Scheme 6.



Scheme 6. Proposed catalytic cycle for amine borane dehydrogenation by zirconocene complexes.

More recently, titanium analogues of Zr OFLPs were synthesized by our group for dehydrogenation of DMAB (Figure 7).^[51] Two conditions were used: dehydrogenation of DMAB in toluene solvent at 25 °C as well as dehydrogenation of a DMAB melts without additional solvent. Among these titanocene complexes, **38** has the highest activity under solvent-free conditions after 24 hours (TOF is 43 h⁻¹) and was stable enough to run long-term experiments by adding fresh substrate several times. Measurement of EPR spectroscopy under the best condition exhibited that paramagnetic Ti(III) species was present throughout the dehydrogenation process. These titanocene complexes also show that the sterically bulky substituents on phosphine moiety and cyclopentadienyl ligand have a significant negative effect on the catalytic activity.

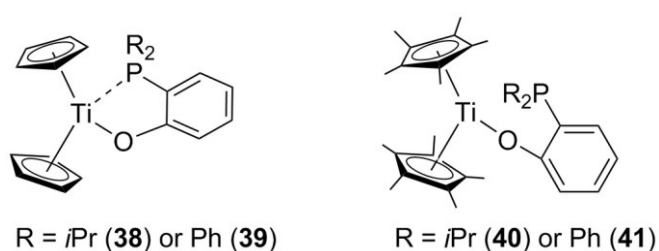
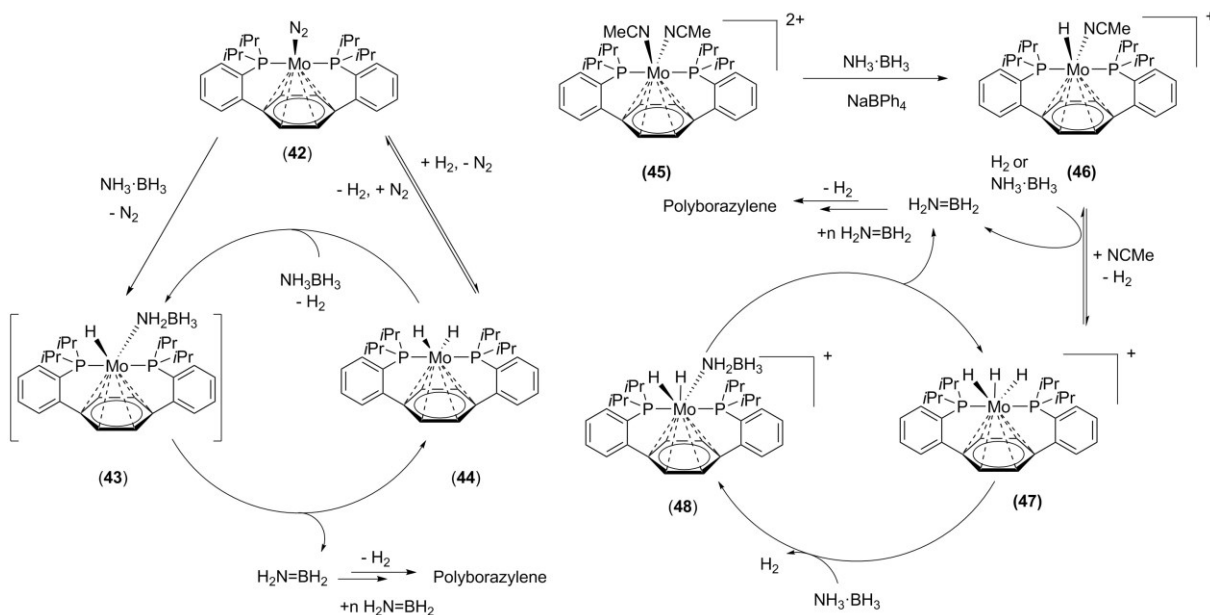


Figure 7. Titanocene complexes for dehydrogenation of DMAB.

2.3.3. Group 6 complexes

In 2014, two Mo complexes containing a *p*-terphenyl diphosphine ligand were presented by Agapie's group, both of which were able to abstract more than one equivalent of hydrogen from AB (Scheme 7).^[52] Using the corresponding Mo(0) dinitrogen complex (**42**) (5 mol%) in diglyme at 70 °C, two equivalents of hydrogen were released in 6.5 hours, 2.5 equivalents were released in 15 hours. During the catalysis, complex **42** was transformed into a Mo(H)(NH₂BH₃) (**43**) intermediate via N-H

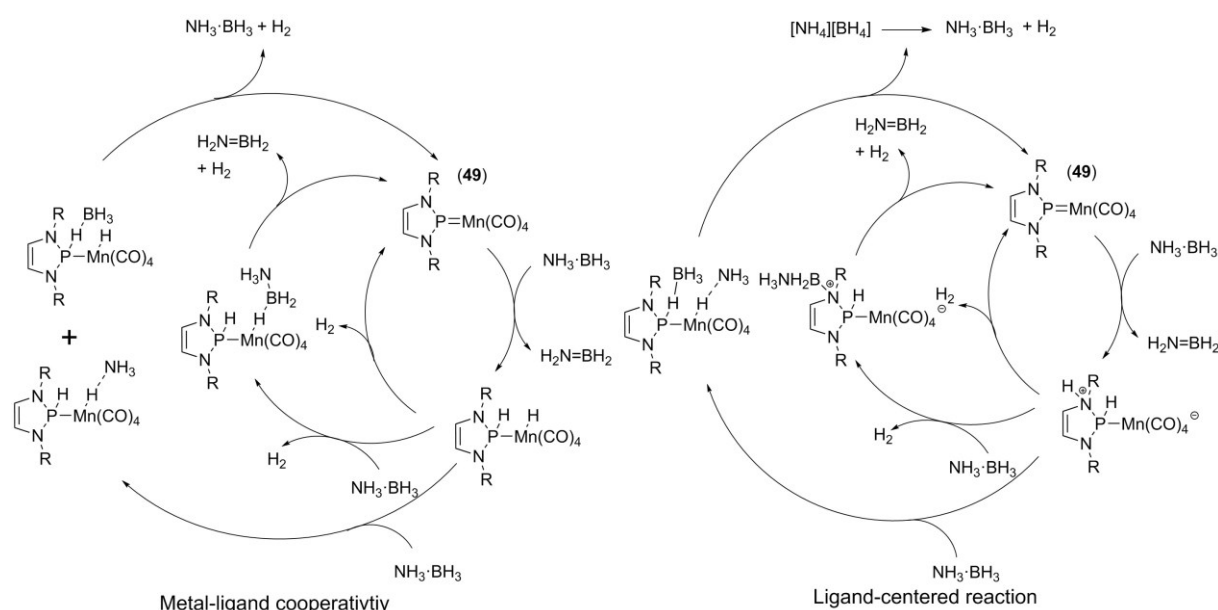
boranes under photocatalytic conditions by Kawano and co-workers.^[54]

Scheme 7. Proposed mechanism for Mo(II) (right) and Mo(0) (left) catalyzed AB dehydrogenation.

2.3.4. Group 7 complexes

In 2017, a new neutral N-heterocyclic phosphonium (NHP) complex of manganese (**49**) was synthesized and characterized by Gudat and co-workers (Scheme 8).^[55] The authors first postulated that in a reaction with AB the manganese phosphonium complex may bind the H⁺/H⁻ pair to the Mn-P double bond in one-step, however they observed that the complex catalyzed dehydrogenation of AB.

The results showed that 2.5 mol% NHP ligated Mn complex could completely consume AB (> 99%) within 24 hours with borazine and condensed borazine oligomer being formed when reacting at 50 °C in THF/toluene (2:1) solution. After 30 hours, the catalytic process was stopped, 1.7 equivalents of hydrogen were evolved and three dehydrocoupling products, borazine cyclotriborazane (CTB), and polyborazylene were found. During the reaction, $[\text{NH}_2=\text{BH}_2]$ was trapped using cyclohexene and the hydroborated product was observed as intermediate by $^{11}\text{B}\{^1\text{H}\}$ NMR spectroscopy. There are two reasonable pathways which, based on experimental and computational results, can explain the catalytic cycle. In the first pathway, the catalyst displays metal-ligand cooperativity, transferring proton and hydride to Mn and P individually. In the other pathway, hydride and proton are transferred to the P and N atoms in a ligand-centered reaction where Mn only plays a role as a stabilizing substituent (Scheme 8, R = Dipp). According to experimental findings, the second pathway was preferred.



Scheme 8. Calculated pathways for the catalytic dehydrogenation of AB with Gudat's Mn complex.

In 2018, Kays and co-workers published their work on dehydrogenation of DMAB using two- and three-coordinate manganese *m*-terphenyl complexes as precatalysts (Figure 8).^[56] All three precatalysts (5 mol%) can consume over 90% of substrate at 60 °C. In addition, dehydrocoupling of DMAB catalyzed by complex **50** and **51** proceeds via homogenous catalysis, however, the same reaction mediated by complex **52** is heterogeneous catalysis. The authors proposed this difference result from steric differences of the ligands, thus giving different stabilities of the Mn(0) catalyst under reaction conditions.

A manganese catalyst analogous to the Fe complex published by Manners' group^[57] was also explored for dehydrocoupling reaction of various amine boranes under photoirradiation by Kawano and co-workers.^[58] $[\text{CpV}(\text{CO})_4]$ and $[(\eta^6\text{-C}_6\text{H}_6)\text{Cr}(\text{CO})_3]$ were employed for dehydrocoupling of AB, primary and secondary amine boranes under the same conditions in this report as well.

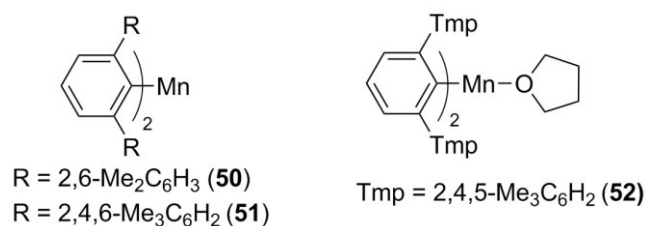
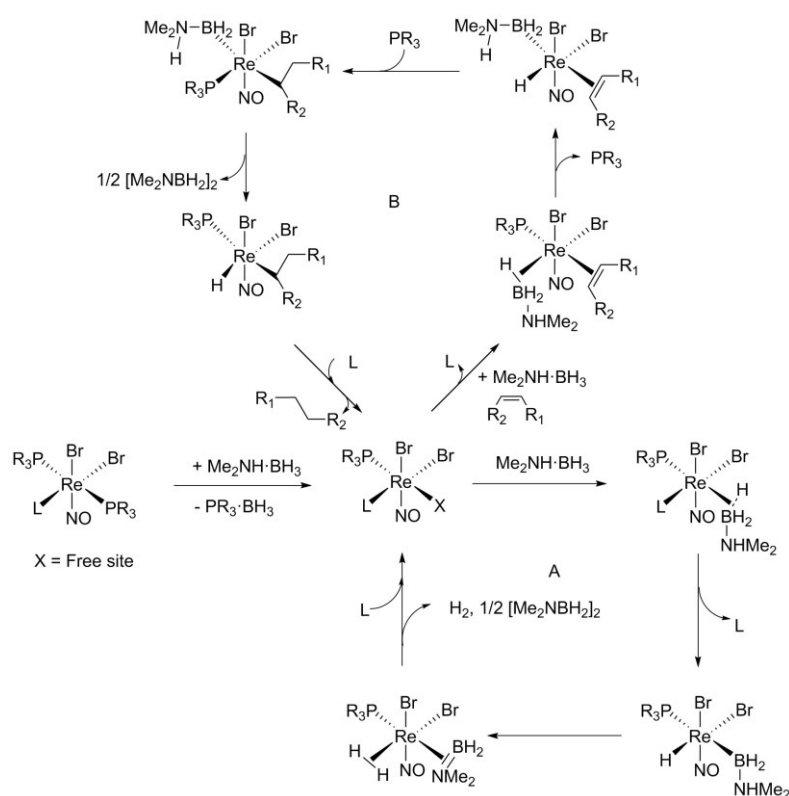


Figure 8. Manganese precatalysts for dehydrogenation of DMAB.

Since rhenium complexes are useful for catalytic C-H activation and amine boranes are isoelectronic to alkanes,^[59] Berke and Jiang presented their work on hydrogen transfer using the Re complex $[\text{ReBr}_2(\text{NO})(\text{PR}_3)_2\text{L}]$ ($R = i\text{Pr}$, $L = \text{H}_2$ (**53**), CH_3CN (**54**) and ethylene (**55**); $R = \text{cyclohexyl}$, $L = \text{H}_2$ (**56**), CH_3CN (**57**) and ethylene (**58**)) as catalyst and DMAB as hydrogen source.^[60] All reactions were carried out in dioxane at 85 °C with catalytic amounts of the Re complex (1 mol%). The conversions of DMAB in reactions mediated by different Re complexes were higher than 88% and only cyclic dimer $[\text{NMe}_2\text{BH}_2]_2$ formed as BN-product. Hydrogen thus produced by the Re catalyst can be directly transferred to alkenes to give alkanes. A mechanistic cycle of transfer hydrogenation was postulated by the authors and is shown in Scheme 9.



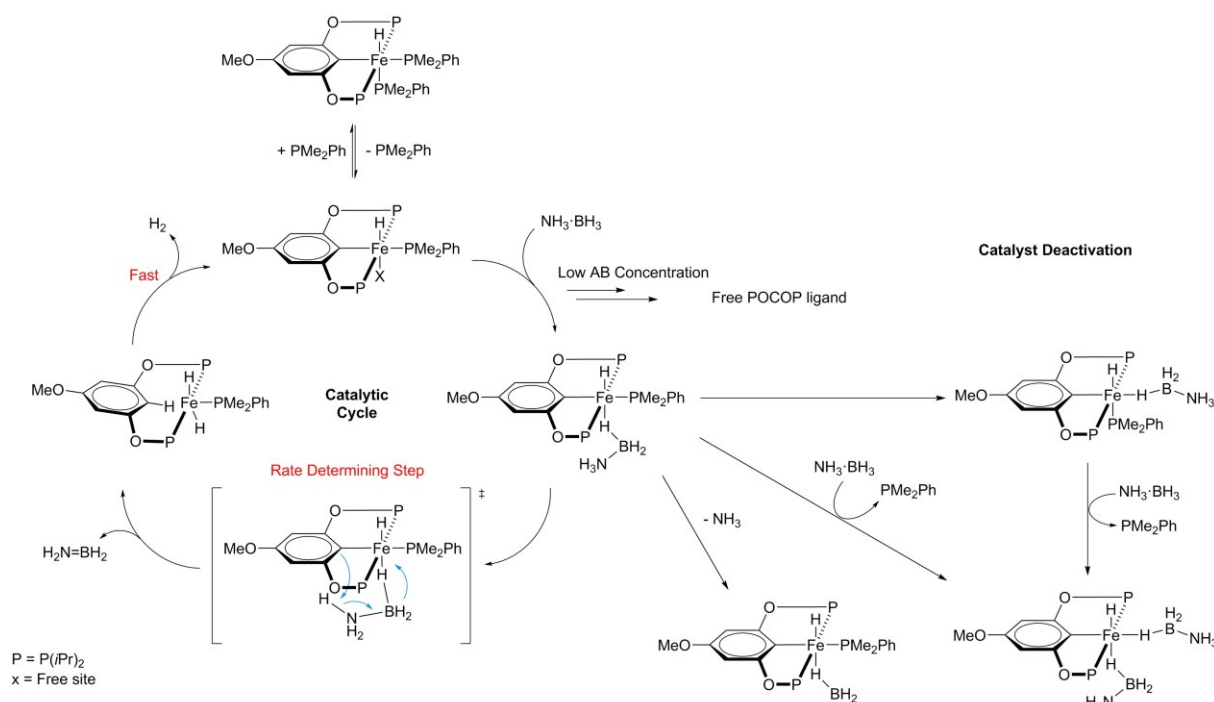
Scheme 9. Hydrogen generation (A) and transfer hydrogenation using a Re catalyst (B).

Additionally, several five-coordinate Re hydride complexes $[\text{ReBr}(\text{H})(\text{NO})(\text{PR}_3)_2]$ (**53**, **56**) were applied for dehydrocoupling of DMAB and transfer hydrogenation of olefins by Berke, Jiang and co-workers.^[61] These five-coordinate Re complexes and the corresponding NHC ligated Re complexes

were suitable catalysts with higher TOF ($R = \text{cyclohexyl}$, $\text{TOF} = 77$ and 100 h^{-1} , respectively) compared with their former report ($\text{TOF} = 24 \text{ h}^{-1}$). After catalysis, the corresponding Re dihydrogen hydride complexes were observed as the only remaining organometallic species.

2.3.5. Group 8 complexes

In 2014, Guan and co-workers presented three Fe pincer complexes bearing a POCOP ligand, $[2,6-(i\text{Pr}_2\text{PO})_2\text{C}_6\text{H}_3]\text{Fe}(\text{PMe}_3)_2\text{H}$ (**59**), $[2,6-(i\text{Pr}_2\text{PO})_2\text{C}_6\text{H}_3]\text{Fe}(\text{PMe}_2\text{Ph})_2\text{H}$ (**60**) and $[2,6-(i\text{Pr}_2\text{PO})_2-4-(\text{MeO})-\text{C}_6\text{H}_2]\text{Fe}(\text{PMe}_2\text{Ph})_2\text{H}$ (**61**).^[62] All three Fe complexes showed extraordinary catalytic activity releasing 2.3 to 2.5 equivalents of hydrogen from AB (1.0 M solution in 1:4 THF/diglyme) at 60°C within 24 hours. Among the three catalysts, complex **61** performed best in terms of rate and degree of hydrogen evolution. Measurement of the kinetic isotopic effect (KIE) for this best iron pincer catalyst suggested that proton and hydride should be transferred from substrate to catalyst simultaneously. Other details were confirmed as well, such as the presence of $[\text{NH}_2=\text{BH}_2]$ during reaction and the fact that some substrate may be dehydrogenated via significantly slower cross coupling. Also, the rate that iron catalyst consumes AB was partially determined by catalyst deactivation. A proposed catalytic cycle is depicted in Scheme 10. In our group we have tested one of Guan's complexes **60** for HB dehydrogenation and found that the complex was not suitable for HB dehydrogenation.^[63]



In 2007, Fe complex $\text{FeH}(\text{CH}_2\text{PMe}_2)(\text{PMe}_3)_3$ (**62**) was mentioned by Baker's group in the Supporting Information of a paper introducing $\text{Ni}(\text{NHC})_2$ complex for AB dehydrogenation.^[64] The iron complex

only had a moderate AB dehydrogenation ability in THF at 20 °C after four days reaction time and the conversion could not reach 100%. The iron complex then was also applied for further exploring what structures forms during the second dehydrogenation step in amine borane dehydrocoupling.^[65] It should be highly emphasized that except from formation of insoluble polyaminoboranes and polyborazylene, a soluble B-N-intermediate, the tetrameric B-(cyclotriborazanyl)amine borane can be formed as well and has in fact been isolated and characterized completely for the first time during formation of borazine derivatives and B-N cross-linked oligomers. Baker's group then tested four different amino and phosphine supported Fe dehydrogenation catalysts,^[53] namely a three-coordinate $\text{Fe}(\text{PCy}_3)[\text{N}(\text{SiMe}_3)_2]_2$ (**63**), four-coordinate $\text{Fe}(\text{DEPE})[\text{N}(\text{SiMe}_3)_2]_2$ (DEPE = 1,2-bis(diethylphosphino)ethane (**64**), a Fe complex coordinated with bidentate PP/NN ligands (**65**) and its PN analog (**66**). For complexes **63**, **64** and **66**, the amount of hydrogen released from AB was up to 1.7, 1.2 and 1.5 equivalents, respectively (Figure 9) and the B-N products formed were mixtures of polyaminoboranes and highly dehydrogenated products such as borazine and polyborazylene. By contrast, complex **65** only promoted release of one equivalent of hydrogen and linear polyaminoboranes were obtained, which according to the authors, made **65** suitable for rapid and selective polymerization of amine boranes. Besides, based on the observation of B-N bond formation in complex **65**, they also find that if these complexes are able to compare with other outstanding catalysts, the basicity at N atom in bifunctional catalysts needs to be controllable. Although complexes **63–66** were useful for dehydrogenation, identification of the catalytically active species was not possible in each case, these complexes more likely should be regarded as precatalysts that react with AB to form the catalytically active species.

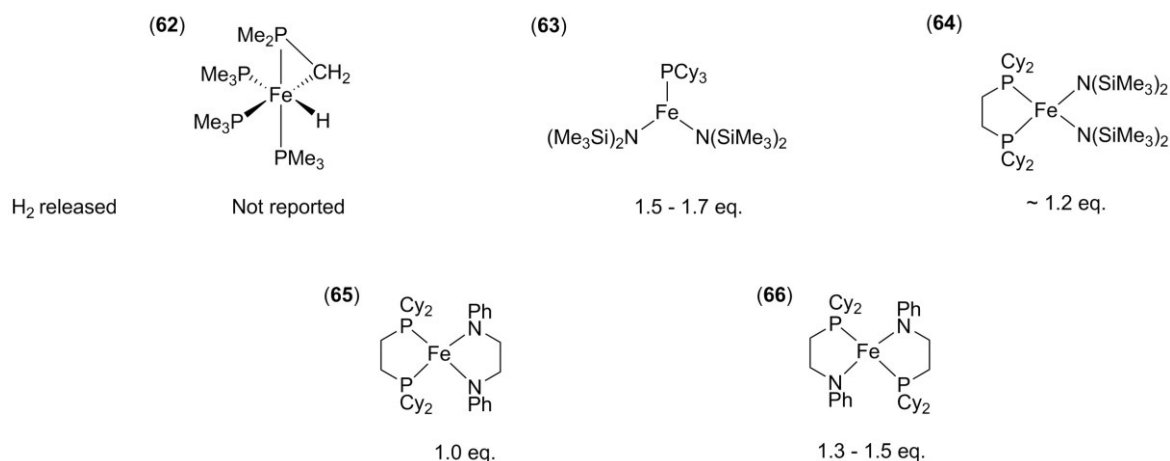
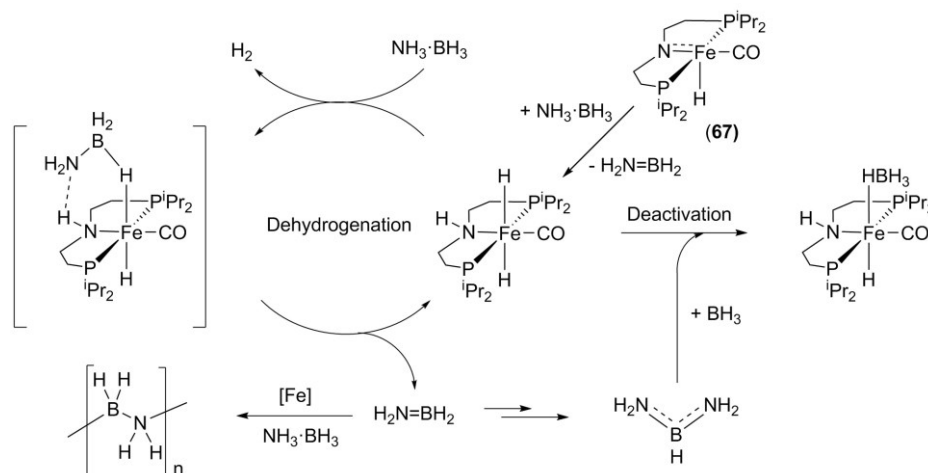


Figure 9. Fe based dehydrogenation catalysts reported by Baker and co-workers.

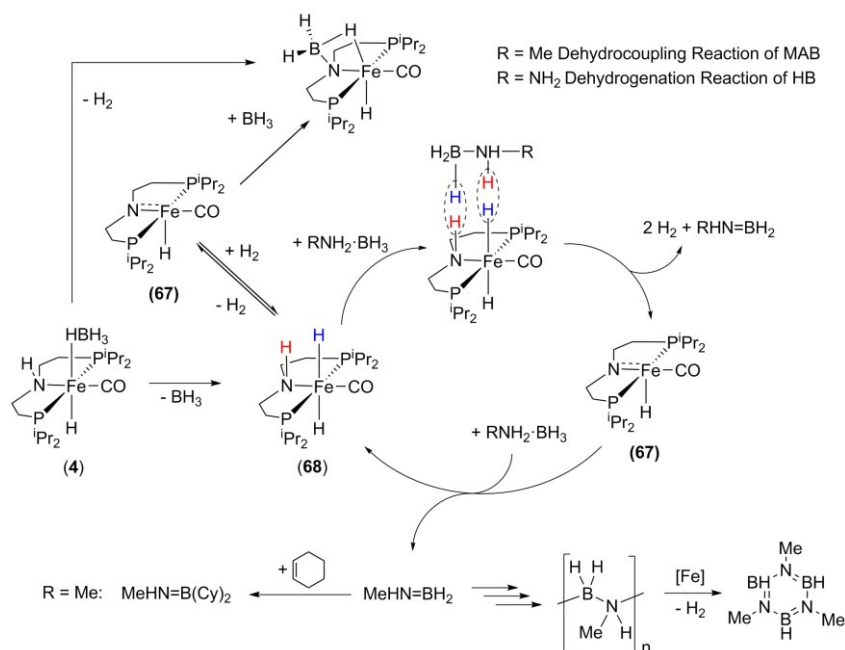
In 2015, $(\text{PNP})\text{Fe}(\text{CO})(\text{H})$ (PNP = $\text{N}(\text{CH}_2\text{CH}_2\text{P}i\text{Pr}_2)_2$) (**67**) was applied for dehydrogenation of AB at room temperature in THF by Schneider and co-workers.^[66] This well-defined base metal complex was an extraordinary catalyst and gave a high TON for AB dehydrogenation, which could even be tripled when adding NEt_3 , which captured the catalyst poison BH_3 . Even when using a catalyst loading as less

as 0.5 mol%, AB could be fully converted (TON = 200) (Scheme 11). The ^{11}B MQMAS NMR spectrum of the dehydrogenated residue suggested a polyaminoborane structure close to that of the material produced by a similar Ru complex.^[67] Taken all information together, the authors proposed a catalytic cycle for dehydrogenation that resembles that for the Ru complex. Based on direct and indirect evidence from experiments and computation, the authors suggest that polymerization occurs at the Fe center and the free borane as poison leads to diaminoborane rearrangement.



Scheme 11. Proposed mechanism for AB dehydrogenation by Schneider and co-workers.

Later, our group showed that complex **4** can serve as a precatalyst for formation of high molecular weight poly(methylaminoborane) by dehydropolymerization of MAB. Release of BH_3 from the precatalyst generates a Fe dihydride species (**68**) which was observed spectroscopically and most likely represents the resting state of the catalyst. Release of H_2 from this species forms an intermediate in which the aminoborane $[\text{MeNH}=\text{BH}_2]$ is coordinated (Scheme 12, $\text{R} = \text{Me}$). After elimination of this, formation of the polymer takes place, probably in an off-metal process with some involvement of the Fe center. This Fe complex **4** was employed to dehydrogenate HB under the same conditions by our group too,^[68] and as found before for AB, complex **67** displayed a high activity and it took 30 minutes to evolve the first equivalent of hydrogen and a maximum of approximately 2.6 equivalents of hydrogen can be extracted along with formation of a thermally unstable hydrogen deficient B-N material. Air sensitivity and thermal instability of highly dehydrogenated HB residues was reported before by Demirci.^[69] Additionally, it was confirmed by our group once more that free hydrogen could reversibly bind to **67** just as Beller's group and Guan's group mentioned in the field of hydrogen transfer^[20c, 70] and finally return to catalytically active **68** (Scheme 12, $\text{R} = \text{NH}_2$).



Scheme 12. Presumed catalytic cycle given by our group for HB dehydrogenation.

In 2011, Manners and co-workers found that the commercially available Fe complex $[\{\text{CpFe}(\text{CO})_2\}_2]$ (**69**) is suitable for catalytic dehydrogenation and dehydrocoupling reactions of ammonia borane, primary amine boranes and secondary amine boranes.^[57] It is noteworthy that this Fe complex was the first efficient system working for these purposes (the Fe complex reported by Baker et al.^[64] is just briefly introduced in Supporting Information and cannot fully convert the substrate) and must be activated by photolysis. Published data on reactions of different amine boranes with the Fe complex is summarized in Table 3. It is known that the dimeric Fe catalyst undergoes CO loss and is thus cleaved to afford mononuclear species under photolysis conditions which then generate several coordinatively unsaturated, catalytically active species during the catalytic process.^[71] As a consequence, the catalytically active form could not be identified by the authors.

Table 3. Products of dehydrogenation of different amine boranes using **69**.

Substrate	Product 1	Time (h)	Yield (%)	Product 2	Time (h)	Yield (%)
DMAB	$\begin{array}{c} \text{Me}_2\text{N}-\text{BH}_2 \\ \\ \text{H}_2\text{B}-\text{NMe}_2 \end{array}$	4	100	-	-	-
MAB	$\left[\begin{array}{c} \text{Me} \\ \\ \text{N}-\text{BH}_2 \\ \end{array} \right]_n$	3	90	$\begin{array}{c} \text{Me} \\ \\ \text{H}-\text{B}-\text{N}-\text{B}-\text{H} \\ \quad \quad \\ \text{Me}-\text{N}-\text{B}-\text{N}-\text{Me} \\ \\ \text{H} \end{array}$	13	60
AB	$\begin{array}{c} \text{H}_2 \\ \\ \text{H}_3\text{B}-\text{N}-\text{BH}_2 \\ \quad \\ \text{H}_2 \quad \text{H}_2 \end{array}$	1	65	$\begin{array}{c} \text{H} \\ \\ \text{H}-\text{B}-\text{N}-\text{B}-\text{H} \\ \quad \\ \text{H}-\text{N}-\text{B}-\text{N}-\text{H} \\ \\ \text{H} \end{array}$	1	5
		3	62	$\begin{array}{c} \text{H} \\ \\ \text{H}-\text{B}-\text{N}-\text{B}-\text{H} \\ \quad \\ \text{H}-\text{N}-\text{B}-\text{N}-\text{H} \\ \\ \text{H} \end{array}$	3	35

reaction conditions: in THF, 20 °C, photolysis, 5 mol% catalyst loading.

Later, the same group showed how the dinuclear precatalyst **69** mediates the dehydrogenation of DMAB. Apart from this, a Fe mononuclear catalyst $\text{CpFe}(\text{CO})_2\text{I}$ (**70**) and another Fe catalyst $\text{Cp}_2\text{Fe}_2(\text{CO})_3(\text{MeCN})$ (**71**) (Figure 10) which is formed by irradiation of **70** in MeCN were also employed. The authors showed that complexes **70** and **71** operate as heterogeneous catalysts, forming Fe nanoparticles (NPs, $d \leq 10$ nm) through loss of CO under UV light. These species dehydrogenate DMAB to form $[\text{Me}_2\text{N}=\text{BH}_2]$, which is finally cyclized to give the dimer $[\text{Me}_2\text{N}-\text{BH}_2]_2$. In contrast, **70** dissociated an iodide ligand and then took part in dehydrogenation and dehydrocoupling as homogenous catalyst under the same conditions. In this case, DMAB is first dehydrocoupled to give the linear dimer as a key intermediate, and then forms $[\text{Me}_2\text{N}-\text{BH}_2]_2$ as well at the second stage with release of hydrogen. Experimental and computational studies showed that the catalytic cyclization involves amine borane ligated $[\text{CpFe}(\text{CO})]^+$ as a key intermediate (Scheme 13).

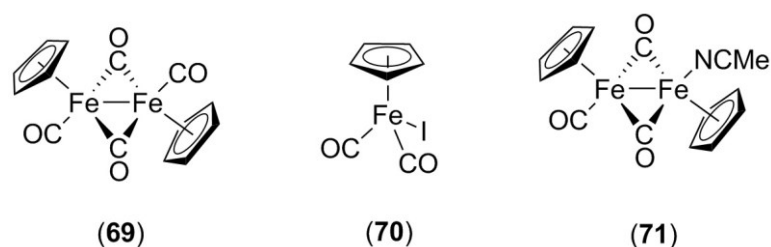
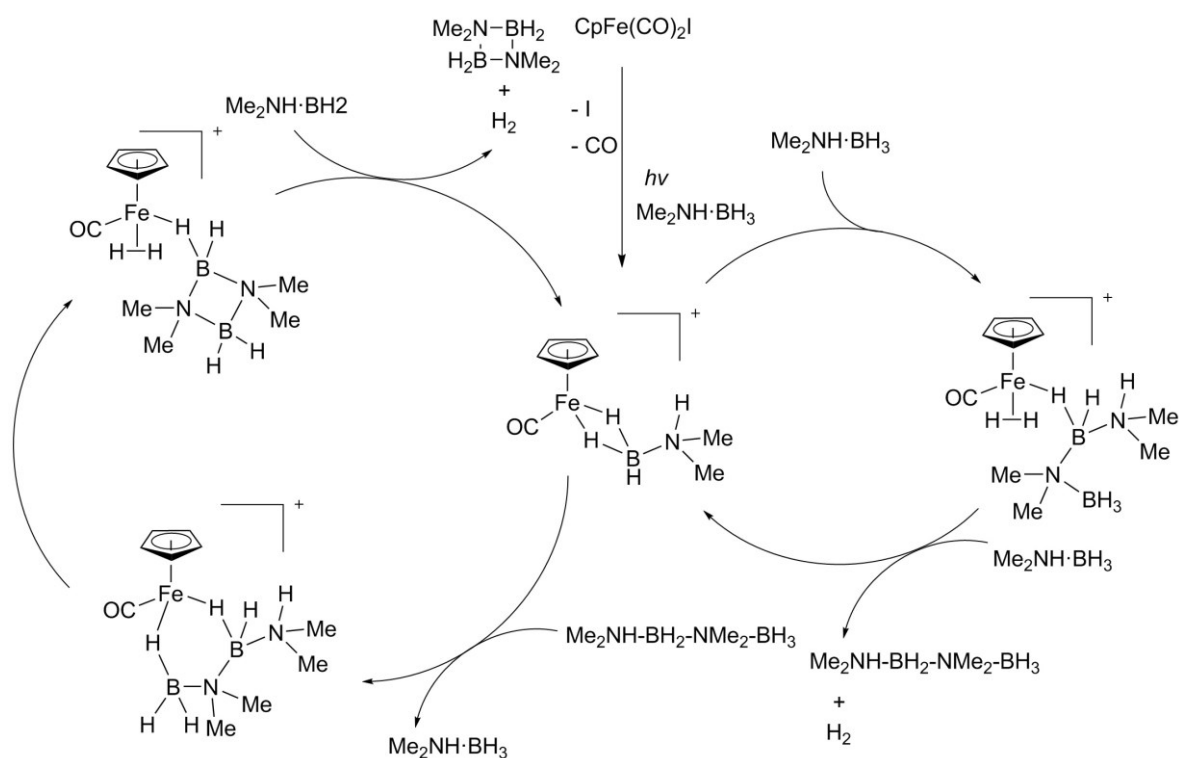


Figure 10. Fe catalysts employed by Manners and co-workers.



Scheme 13. Possible catalytic cycle of two-stage DMAB dehydrocoupling using complex **70**.

In 2013, Morris and Sonnenberg first reported on a Fe NP heterogeneous catalytic system for dehydrogenation of AB,^[72] (the aforementioned Fe heterogeneous catalytic system reported by Manners et al. was described earlier, however the authors did not identify the active form of the catalyst at that time^[57]) inspired by their earlier hydrogenation and transfer hydrogenation work on a catalytic systems originating from $[\text{Fe}(\text{MeCN})(\text{L})(\text{PNNP})][\text{BF}_4]_2$ ($\text{L} = \text{MeCN}$ or CO and $\text{PNNP} = (\text{PPh}_2\text{C}_6\text{H}_4\text{CH}=\text{NCHR}-)_2$ and $\text{Ru}(\text{PN})$).^[73] It turned out that using complex **75** (Figure 11) release of one equivalent of hydrogen needs less than a minute and up to 1.83 equivalents of hydrogen can be formed within one hour under the optimized conditions (i.e. THF, 22 °C, KO^tBu as base). First generation Fe complexes are converted to Fe NPs ($d \approx 4$ nm) at the beginning and are coated in and stabilized by the PNNP ligand. They also found that reactive B-N intermediates may bind to the active sites of Fe NPs during dehydrogenation of AB which leads to catalyst deactivation. This could explain the phenomenon that hydrogen evolution starts with a high initial rate (maximum TOF is up to 3.66 s^{-1}) and apparently slows down over time. Steric and electronic changes at the Fe catalyst had little effect on the catalytic activity of the system. Different from the first generation, the second generation Morris' catalyst is much less active than the complexes **72-75** and acts as a homogenous catalyst. Experimental results indicated that Fe NPs probably generated during catalysis, but they did not explain why the dehydrogenation mechanisms of first and second generation catalysts are different.^[72, 74]

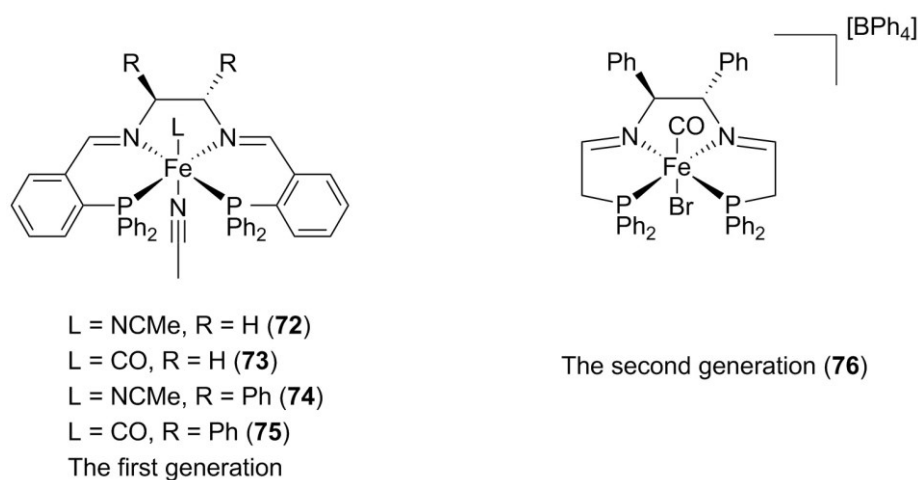
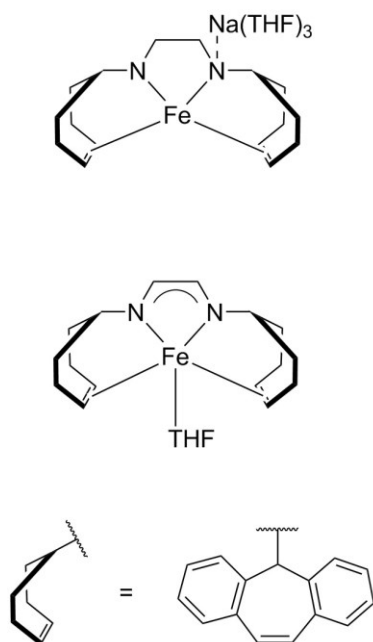


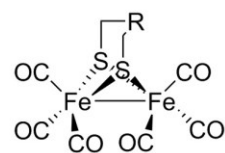
Figure 11. Morris' precatalyst for AB dehydrogenation.

Apart from these complexes, other Fe complexes were reported by different groups as candidates for the dehydrogenation and dehydrocoupling of amine boranes in recent years, a selection is shown in Figure 12.^[75]

Grützmacher 2015

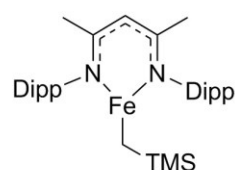


Darensbourg 2016



R = CH₂, CMe₂, CEt₂
 R = NMe, NtBu, NPh

Webster 2017

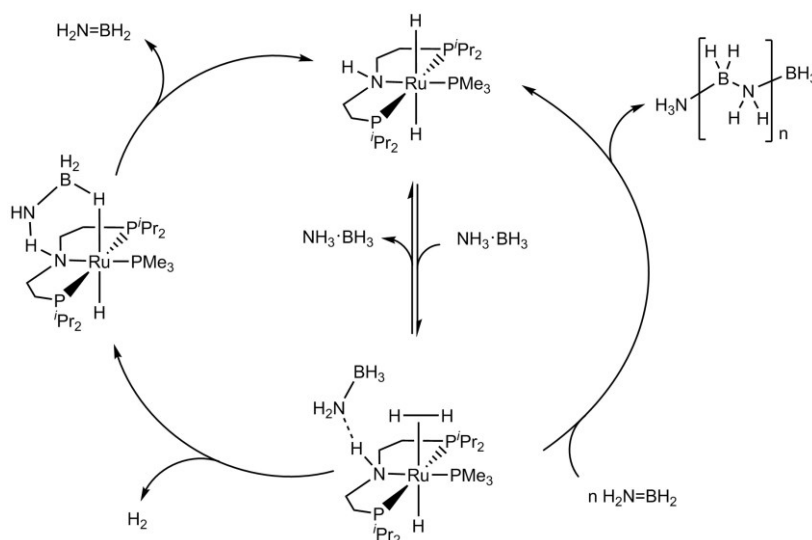


Dipp = 2,6 - diisopropylphenyl
 TMS = trimethylsilyl

Figure 12. Iron catalysts for dehydrogenation and dehydrocoupling published in recent years.

In 2009, Schneider and co-workers presented a Ru(II)pincer amido complex (PNP)Ru(H)(PMe₃) (**77**) (PNP = N(CH₂CH₂PiPr₂)₂) which could reversibly bind and release hydrogen and thus be transformed between amino, amido and enamido forms via heterolytic H₂ activation reactions (Scheme 14).^[67] The authors found that the Ru catalyst had an extraordinary performance on dehydrogenating AB in THF at 25 °C, catalyst loading of 0.1 mol% and 0.01 mol% producing slightly more than one equivalent and 0.83 equivalent of hydrogen, respectively. The data of dehydrogenated AB characterized by powder X-ray diffraction, IR, ¹¹B NMR-MAS showed the presence of linear oligomer (BH₂-NH₂)_n. In addition to that, trace amounts of borazine were formed in solution which explains the H₂ yield being slightly above one equivalent. The mechanism of dehydrogenation was deeper analyzed by determination of KIEs. The KIE values using a catalyst loading of 0.1 mol% were 2.1 (H₃N·BD₃), 5.2 (D₃N·BH₃) and 8.1 (D₃N·BD₃). These results indicated that a concerted N-H and B-H bond activation at metal center and ligand was the rate-determining step. Later, the same authors reported on DMAB dehydrocoupling using the same Ru amido complex **77** and Ru amino complex (PNHP)Ru(H)₂(PMe₃) (**78**) (PNHP = HN(CH₂CH₂PiPr₂)₂).^[76] Aminoborane cyclodimerization (i.e. the dehydrogenation and B-N coupling process) was found to be on-metal. Additionally, a stable deactivated PNP Ru complex showing a four-membered Ru-N-B-H metallacycle was found which gave valuable suggestions for further catalyst design. In 2013, Schneider and co-workers presented a mechanistic study of amine borane dehydrogenation using **78** which involves metal-ligand cooperation.^[77] For drawing the conclusion, experimental KIE (H₃N·BD₃, D₃N·BH₃ and D₃N·BD₃) were determined and computational studies of the Ru amido complex and Ru amine complex (PNMeP)Ru(H)₂(PMe₃) (**79**) (PNMeP =

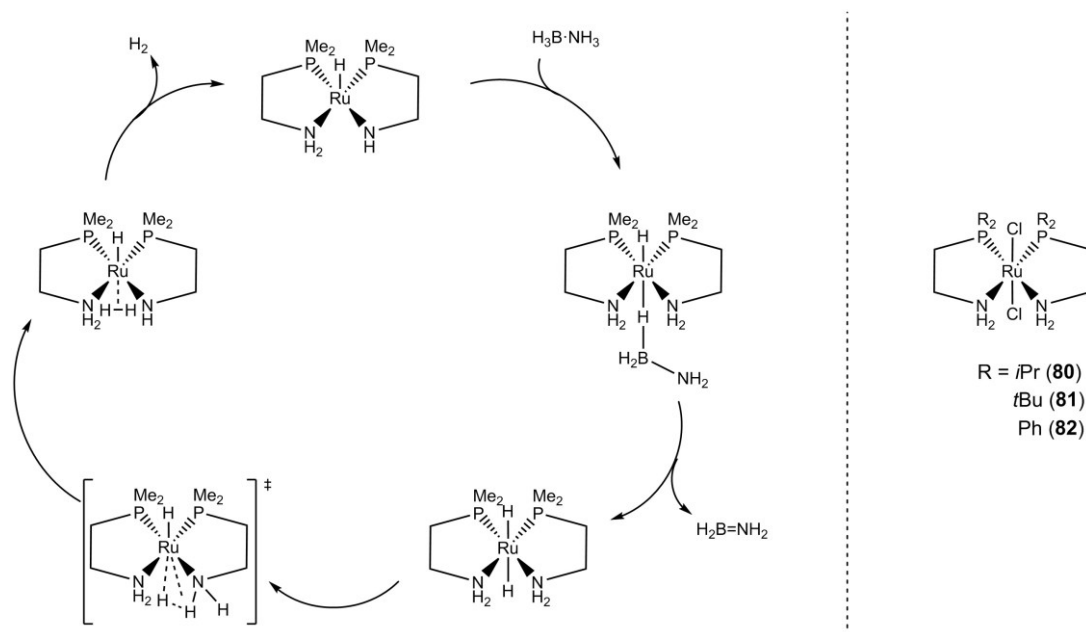
$\text{MeN}(\text{CH}_2\text{CH}_2\text{P}^i\text{Pr}_2)_2$) were performed. NMR spectroscopy was also employed to analyze the mechanism of dehydrogenation by complex **78** by reacting with amine boranes that do not possess hydrogen at the B or N terminus (i.e. $\text{R}_3\text{B}\cdot\text{NH}_3$ or $\text{H}_3\text{B}\cdot\text{NR}_3$). Cyclohexene was employed to trap the intermediate aminoborane $[\text{NH}_2=\text{BH}_2]$ probably existing during dehydrogenation. Through experiment and computation, it was found that if hydroboration or borazine formation are not kinetically competitive with metal-promoted B–N coupling, then $\text{Cy}_2\text{B}\cdot\text{NH}_2$ will not be observed, even if free amino borane is formed transiently. Polymers formed by B–N coupling were filtered and characterized by ^{11}B solid-state NMR. Compared to a previously published model differences between their experimental and computational results and theoretical studies were shown and it was pointed out that the two subcycles of release of $[\text{NH}_2=\text{BH}_2]$ and subsequent polymerization of it were facilitated by N–H activation of substrate which made the B–N coupling process different from that of Brookhart’s Ir catalyst and Baker’s $\text{Ni}(\text{NHC})_2$ catalyst.^[78]



Scheme 14. Proposed mechanistic cycle for AB dehydrocoupling using complex **78**.

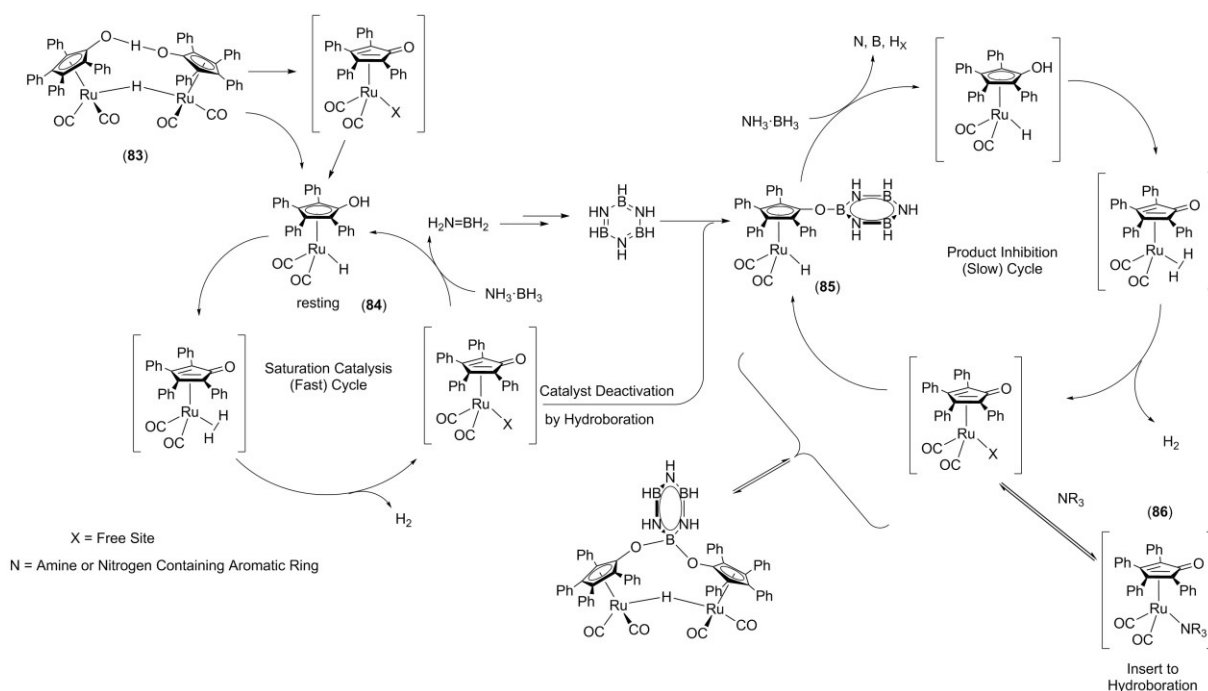
Similarly, as Schneider and his group, Fagnou and co-workers, followed the strategy of cooperative amino ligands which was introduced by Noyori et al. for the hydrogenation and transfer hydrogenation of polar double bonds.^[79] In this context, Fagnou also presented an extraordinary Ru catalyst.^[73c] AB, MAB and mixtures thereof were dehydrogenated by Ru(II) complexes $(\text{PN})_2\text{RuCl}_2$ ($\text{PN} = \text{R}_2\text{PCH}_2\text{CH}_2\text{NH}_2$, $\text{R} = i\text{Pr}$ (**80**), $t\text{Bu}$ (**81**), Ph (**82**)) (Scheme 15) which were bifunctional undergoing reversible chemical transformation in the catalytic cycle. It was interesting that when catalyzed by 0.03 mol% loading of Ru complex containing isopropyl backbone, one equivalent of hydrogen was evolved from AB within only five minutes at room temperature, two equivalents of hydrogen were evolved from MAB by 0.5 mol% loading in less than ten minutes at 22 °C, and it only took ten seconds to release the first equivalent of hydrogen. After blended, as much as 3.6 system wt% hydrogen was produced from a mixture of AB and MAB within one hour with 0.1 mol% Ru loading. The Ru complex which had good dehydrogenation capability was also found to shuttle hydrogen and transfer it

to ketones and imines very well with a relatively high yield. A DFT supported mechanism of the AB dehydrogenation process is shown in Scheme 15 and involves cooperation between an amino and a Ru hydride moiety. Information about the structure of dehydrogenated AB, MAB and of mixtures thereof was not given. This is noteworthy, as most likely in the case of AB, a linear polymer was formed (release of one equivalent of H_2) whereas for MAB borazines must be present (release of up to two equivalents of H_2).



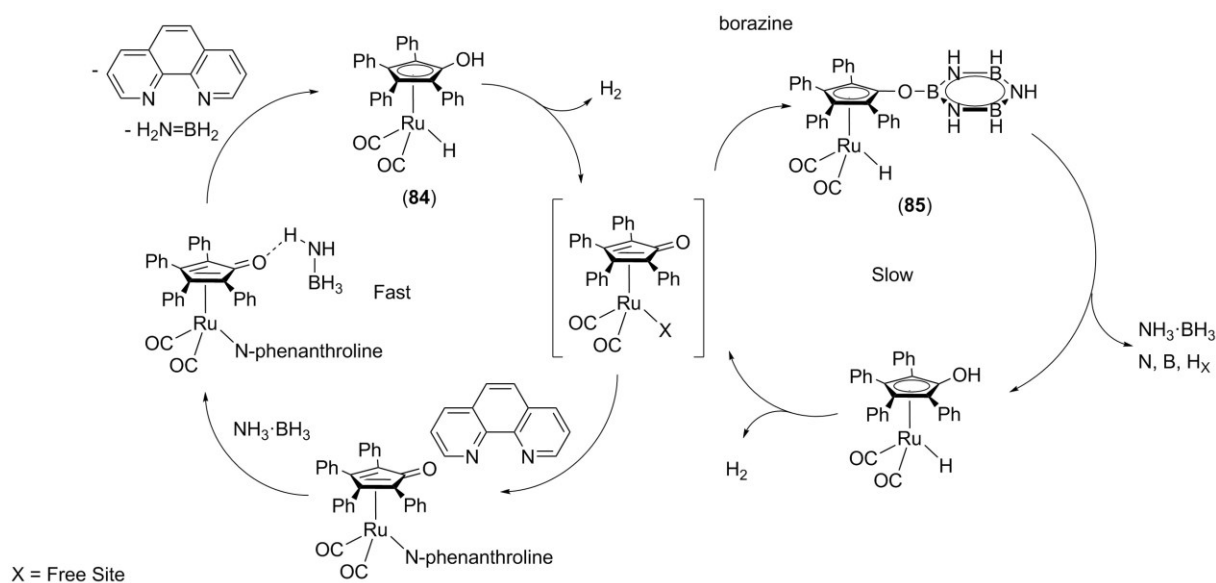
Scheme 15. Presumed steps for AB dehydrogenation part of transfer hydrogenation from DFT calculation (left). Precatalysts for dehydrogenation (right).

In 2010, Shvo's complex **83** was presented as catalyst in the field of AB dehydrogenation by Conley and Williams.^[80] It was highlighted that the reaction system consisting of diglyme, benzene and a catalytic amount of ethanol at 70 °C with 2.5 to 10 mol% catalyst loading was productive for dehydrogenation of AB and promoted release of two equivalents of hydrogen from the substrate which made it the second example of a homogeneous transition metal catalyst that can liberate over one equivalent of hydrogen from AB. The authors assumed a metal-ligand cooperative dehydrogenation cycle, based on ^1H and ^{11}B NMR spectroscopy (Scheme 16, left cycle), and classified the cycle into three regimes, all of which were explained particularly. The only product that remained after hydrogen release was borazine.



Scheme 16. Proposed mechanism of AB dehydrogenation catalyzed by Shvo's complex.

Two years later, Williams and co-workers further discussed the reaction mechanism and provided evidence for catalyst deactivation (Scheme 16, right cycle).^[81] When investigating the details of catalytic rate change from fast to slow, they figured out that the highly dehydrogenated product borazine had negative impact on the catalytic rate by hydroborating intermediate **84** to give the deactivated complex **85** which represents an O-borylated form of the precatalyst. In addition to that, the authors confirmed that free ammonia which is known to modulate the reactivity of Shvo's reaction system originating from ammonia borane dissociation could also deactivate the catalyst by NH_3 ligation to it. However, a much more interesting phenomenon was observed during finding the effect the NH_3 had on the catalyst. Although complex **86** catalyzed (with NH_3) dehydrogenation of AB was slower than that of **83**, the reaction of **86** maintained its fast kinetic regime longer than that of **83**. The phenomenon appeared as well when adding 1,10-phenanthroline to a complex **84** catalyzed dehydrogenation system. The authors presumed that the ligand should reversibly associate and dissociate to the open site of **84**, which made the fast cycle of catalysis much more competitive compared to the cycle involving hydroboration that deactivates complex **84** (Scheme 17).^[82]



Scheme 17. Catalysis involving competition between phenanthroline and borazine.

According to these experimental results, Williams and co-workers later presented another study on accelerating dehydrogenation of AB by nitrogen containing ligands.^[83] They compared the dehydrogenation performance of monomeric Ru complexes which are similar to Shvo's catalyst with two nitrogen containing ligands, 1,10-phenanthroline and *p*-substituted pyridine (Figure 13, **87-89**). It turned out that monodentate *p*-substituted pyridine, especially CF₃ substituted, ligating to Ru center can accelerate AB dehydrogenation compared to Shvo's complex. This phenomenon was termed as "semi-site" protection strategy by the authors.^[84] For bidentate nitrogen ligands like 1,10-phenanthroline, 2,2'-dipyridine and tetramethylethylenediamine, the same result corresponded to a totally different reason, namely replacement of the tetraphenylcyclopentadienone by the bidentate N-donor ligand and formation of a comparably more reactive ruthenium species.

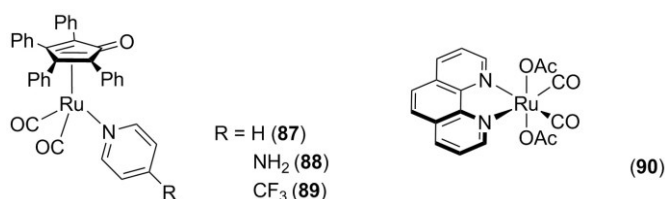


Figure 13. Shvo-type dehydrogenation catalyst (left). A Ru catalyst with bidentate N-donor ligand that almost fully dehydrogenates AB (right).

As another improvement of these Ru systems for AB dehydrogenation, Williams and co-workers later presented the catalyst (phen)Ru(OAc)₂(CO)₂ (phen = 1,10-phenanthroline) (Figure 13, **90**)^[85] based on the aforementioned "semi-site" protection strategy. When 1 mol% complex was used for dehydrogenation at 70 °C in diglyme, 2.7 equivalents of hydrogen could be liberated from AB. To date, only a handful of catalysts can reach a similar level, but not all of them like this complex **90** are water

and air stable. It was also demonstrated that the Ru complex not only can form H_2 from AB, but also release H_2 from the substrate that already evolved one equivalent of hydrogen.

A different approach was used by the Williams group for designing a highly robust Ru catalyst for AB dehydrogenation.^[86] The catalyst showed an extraordinary performance with release of more than two equivalents of hydrogen (two equivalents in the first four hours, in total 2.2 equivalents) from AB with 0.1 mol% catalyst loading at 70 °C under air and in the presence of water. Additionally, the system was remarkably reusable and long-lived (TON > 5000). According to experimental data, it at least successively reacted with AB and recharging it three times in a single reactor gave similar rates for hydrogen evolution and release of 2.2, 2.1, 2.3 and 2.2 equivalents of hydrogen, respectively, was observed. Additionally, the authors showed that the linking group of ruthenium bis(pyridyl)borate complexes between Ru and the pendant boron atom has an influence on the rate of AB consumption as dehydrogenation with a complex possessing a trifluoroacetate group showed only half the rate of a similar OH bridged catalyst (Figure 14). The dehydrogenation products other than H_2 were borazine and polyborazylene. The mechanism was later theoretically analyzed by Paul and co-workers.^[87]

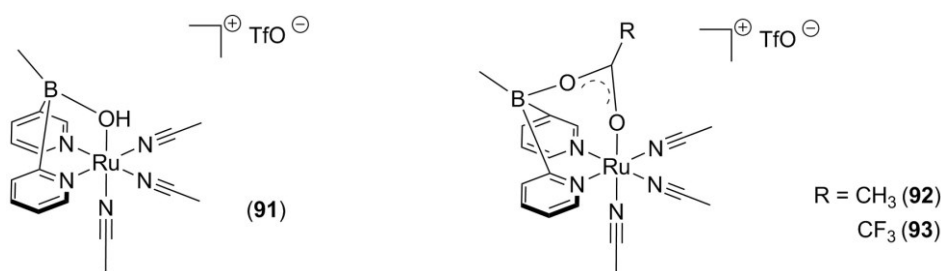
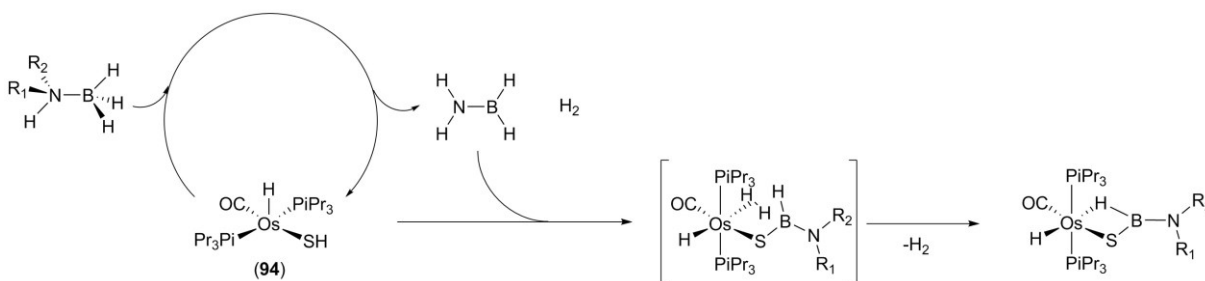


Figure 14. Ru bis(pyridyl)borate complex with different linker groups.

Based on previous observations that the Os complex $OsH(CO)(SH)(P^iPr_3)_2$ (**94**) could promote heterolytic B-H activation of pinacolborane, catecholborane and diborane 9-borabicyclo[3.5.1]nonane (9-BBN) dimer to afford dihydrogen borylthiolate complexes,^[88] Fernández, Oñate and co-workers reported dehydrogenation of amine boranes using this five-coordinate Os complex (Scheme 18).^[89]

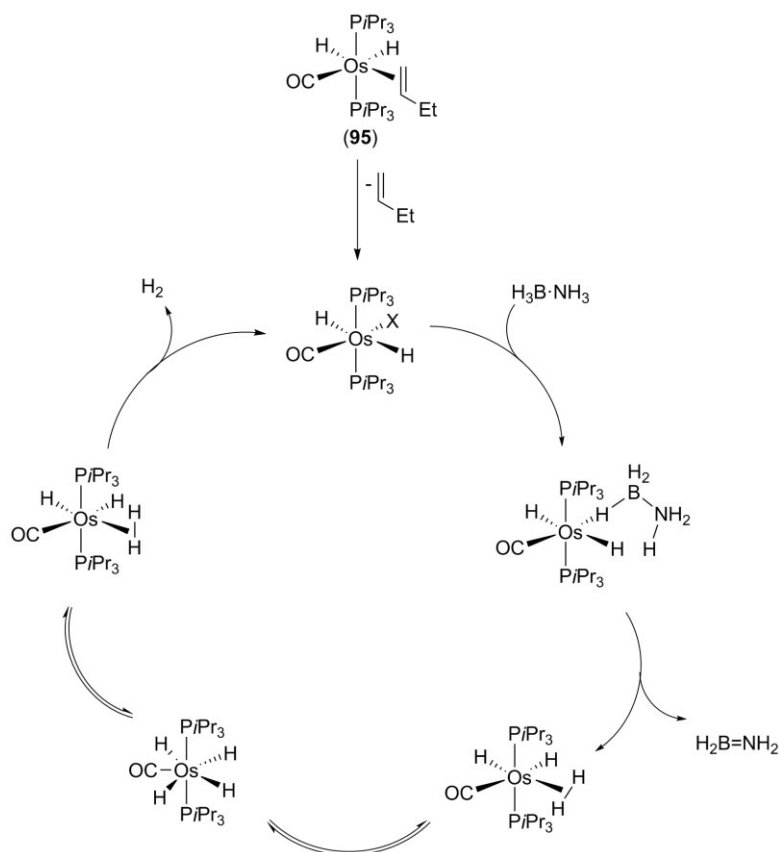


Scheme 18. Formation of Os aminoborane complexes during AB dehydrogenation.

The first Os amine borane dehydrogenation catalyst has a relatively good activity as it can promote release of one equivalent of hydrogen from AB and DMAB with TOF values at 50% conversion (TOF_{50%}) of 43 and 7 h⁻¹, respectively, in THF at 31 °C. Interestingly, except for hydrogen releasing,

the complex was able to capture aminoborane dehydrogenation products as well, forming a hydrogenaminothioborate complex. The complex is stable enough to persist in the amine borane solution without hydrogen evolution. The phenomenon that catalysis works and does not halt during reaction was interpreted by the authors as a consequence of a fast reaction between the metal center and the amine borane substrates. Compared to that, coordination of amine borane dehydrogenation products should be much slower.

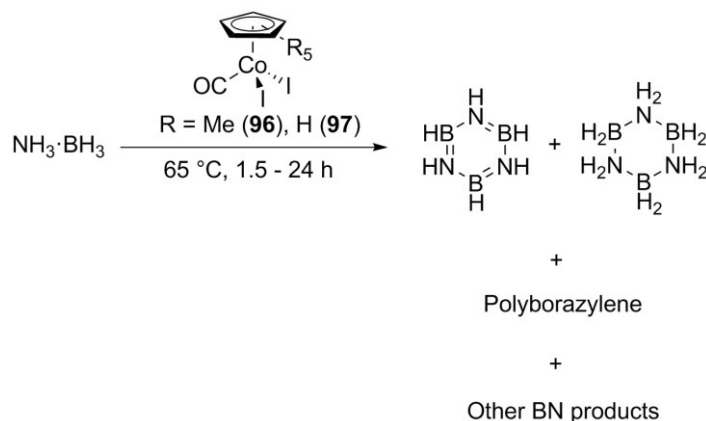
Esteruelas and co-workers described dehydrogenation of AB using an osmium dihydride complex **95** and analyzed the kinetics and the mechanism of the dehydrogenation process.^[90] This Os complex afforded one equivalent of hydrogen from AB with a TOF of 46 h^{-1} at 50% conversion in THF under a constant atmospheric pressure at 31°C . After variation of reaction conditions in terms of temperature, concentration of substrate and Os complex, the authors postulated that the catalytic cycle starts with formation of a vacant site at Os via dissociation of the alkene ligand from complex **95**. AB coordinates to the free site of the metal center via the B-H bond and hydrogen is liberated through concerted N-H and B-H activation (Scheme 19). Distinct from outer and inner sphere pathway, the catalytic reaction experiences a hydride pathway without any change in the metal oxidation state or ligand assistance.



Scheme 19. Catalytic cycle for AB dehydrogenation promoted by Os catalyst.

2.3.6. Group 9 complexes

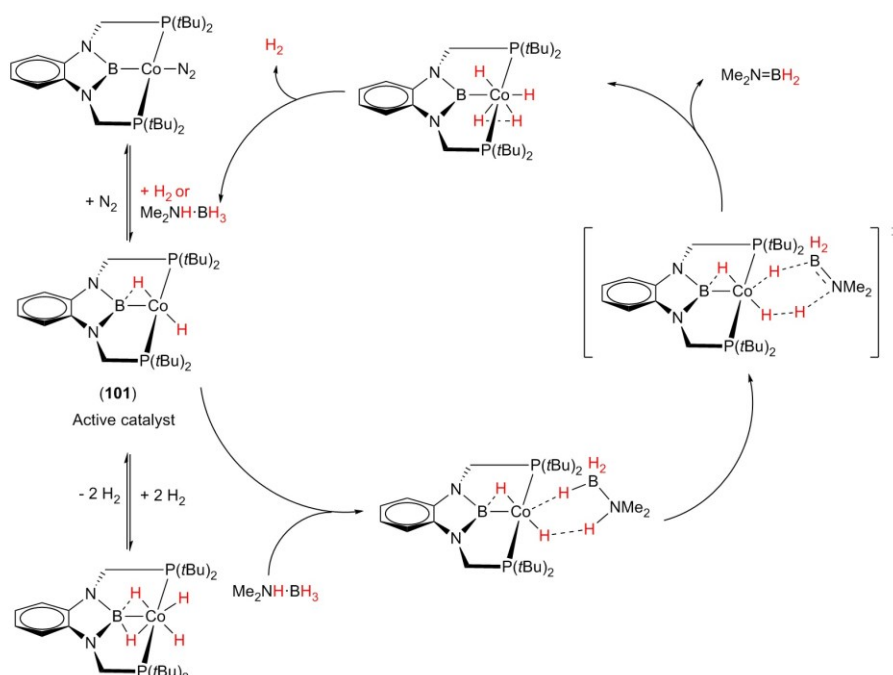
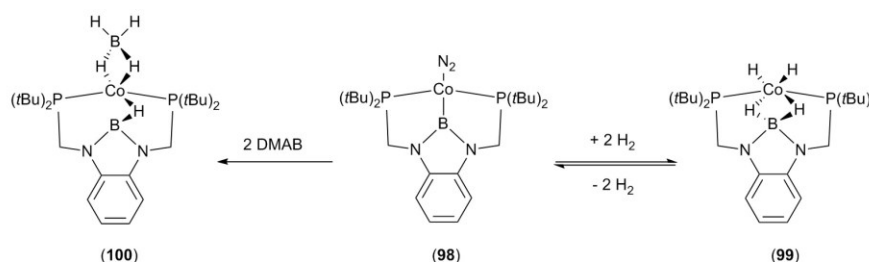
The research group of Waterman reported two Co complexes that can dehydrogenate AB and directly transfer hydrogen from AB to alkynes and alkenes without hydrogen gas release.^[91] In their contribution, they selected two Co complexes as catalysts, $\text{Cp}'\text{Co}(\text{CO})\text{I}_2$ ($\text{Cp}' = \text{Cp}$ (**96**), $\text{Cp}' = \text{Cp}^*$ (**97**)). Both catalysts fully convert all AB substrate at 65 °C in THF. Even when reactions were carried out under aerobic condition, the volume of H_2 evolved during catalysis was close to two equivalents per equivalent of AB, giving an average TON of 1924 and a TOF of 496 h^{-1} . Upon addition of an excess of water, dehydrogenation of AB stopped. The authors also found that if hydrogen is released in an open vessel (air or N_2), polyborazylene was much favored over borazine and the time needed for full conversion of AB was significantly shorter than that in a sealed tube under reducing atmosphere. This demonstrates inhibition of catalysis by hydrogen. The entire process was found to be homogenous, and the catalyst is stable even with low catalyst loading (0.1 mol%). NMR spectroscopy showed no evidence for loss of a Cp ligand.



Scheme 20. AB dehydrogenation using a Co(III) catalyst.

Peters and Lin reported a Co complex (**98**),^[92] ligated to a PBP pincer system synthesized by Nozaki,^[93] and employed this for dehydrogenation of DMAB. To further understand what structures the (PBP)Co complex may have during hydrogen activation reaction, compound **98** was exposed to one atmosphere of hydrogen in toluene- d_8 at 25 °C and the mixture was analyzed by multinuclear NMR spectroscopy, giving characteristic resonances, including ^{31}P (138.2 ppm), ^{11}B (47.1 ppm) and ^1H (-6.5 ppm, broad hydridic resonance). The Co dinitrogen complex could quantitatively convert to a Co dihydridoborato dihydride (**99**). Formation of alternative possible Co hydride species was excluded by the authors. Apart from that, reversible uptake and release of two equivalents of hydrogen to a single Co center is an attractive unique characteristic, also shown by Heinekey, Goldberg and co-workers.^[94] Upon reaction with DMAB in a 1:2 stoichiometry, the Co complex **98** quantitatively transforms to a tetrahydridoborate Co complex (**100**), both species could promote hydrogen liberation in six hours in benzene at room temperature under N_2 atmosphere. It was pointed out that the unusual character of the

presented system contributed to the ability of the cobalt-boryl fragment to bind and release hydrogen atoms by forming cobalt-boryl (**98**), -dihydridoborate (**99**), and -hydridoborane (**100**) species (Scheme 21, above).

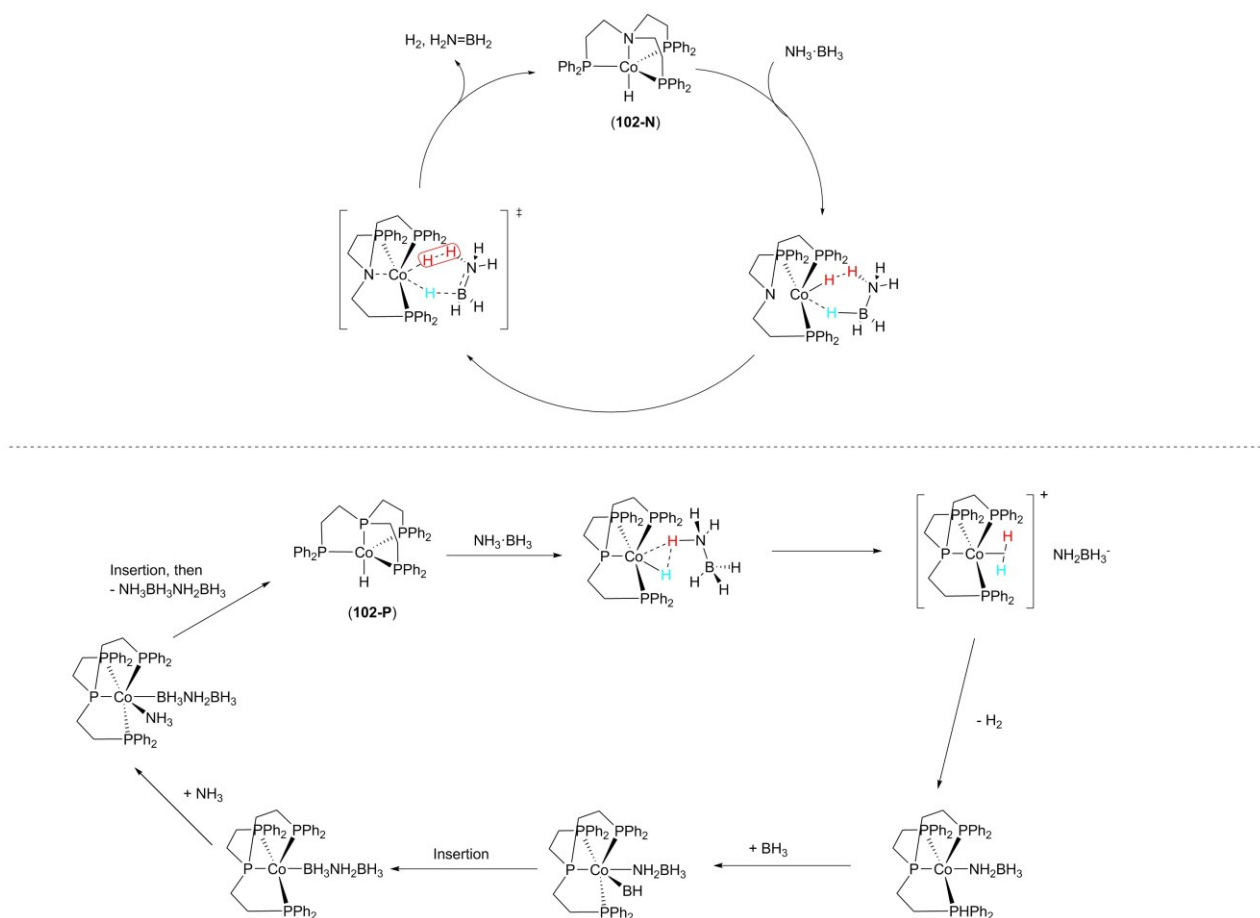


Scheme 21. (PBP)Co complexes react with hydrogen and DMAB (above). DFT calculation elucidated DMAB dehydrogenation with a (PBP)Co complex (below).

Full computational analysis of the process was performed by Paul and co-workers.^[95] They conclude that the active intermediate existing during catalysis is the (PBP)Co dihydride complex (**101**) shown in Scheme 21, below.

In 2017, two Co complexes bearing a tetradentate P_3E ($E = N$ (**102-N**), P (**102-P**)) ligand were reported for AB dehydrogenation by Rossin, Shubina and co-workers.^[96] Both ligands containing nitrogen and phosphorus are more flexible than that of carbon and can enhance the basicity of the metal center at the same time. The reaction catalyzed by complex **102-N** requires 48 hours for release of two equivalents of hydrogen at 55 °C in THF; borazine is the residue of dehydrogenation. In contrast, reacting under the same conditions, one equivalent of hydrogen was released with complex **102-P** as the catalyst and long chain poly(aminoboranes) were detected after reaction. Due to its better

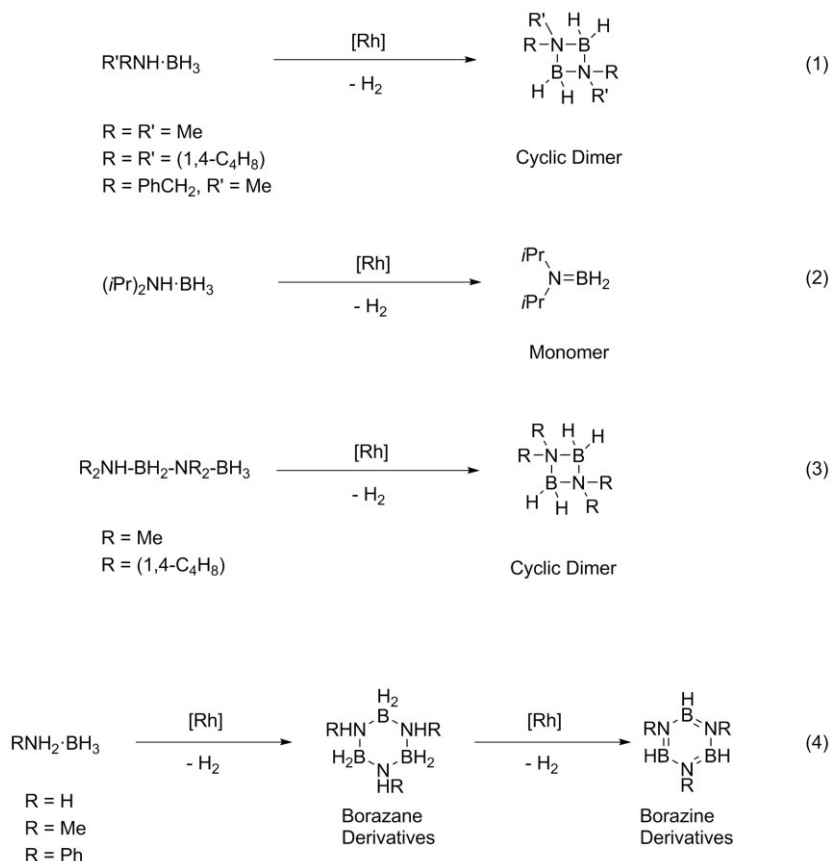
catalytic capability, KIE values were determined using complex **102-P**. The parameters of $\text{H}_3\text{N}\cdot\text{BD}_3$, $\text{D}_3\text{N}\cdot\text{BH}_3$ and $\text{D}_3\text{N}\cdot\text{BD}_3$ were 2.2, 2.2 and 4.5, respectively, which inferred that both B-H and N-H activation take place simultaneously as part of the rate-determining step after preliminary AB coordination to the Co center. The authors also demonstrated that $[\text{H}_2\text{B}=\text{NH}_2]$ is the intermediate by adding cyclohexene to the system to form $\text{Cy}_2\text{B}\cdot\text{NH}_2$, which was detected by $^{11}\text{B}\{^1\text{H}\}$ spectroscopy. In contrast, when performing the same trapping experiment with complex **102-P**, the intermediate was not observed, because no $[\text{H}_2\text{N}=\text{BH}_2]$ formation takes place, and the process is better described as a sequential BH_3/NH_3 group insertion into the initially formed $[\text{Co}]\text{-NH}_2\text{BH}_3$ amidoborane complex (Scheme 22).



Scheme 22. Postulated catalytic AB dehydrogenation cycle of complex **102-N** (above) and **102-P** (below).

In 2003, inspired by formation of B-P bonds by dehydrocoupling of primary and secondary phosphine borane adducts using late transition metal catalysts,^[97] Manners and co-workers for the first time presented a series of dehydrocoupling reactions of amine borane adducts with different transition metal catalysts.^[98] Products of dehydrocoupling reactions were characterized in detail. $[\text{Rh}(1,5\text{-COD})(\mu\text{-Cl})]_2$ (COD = 1,5-cyclooctadiene) was employed as the precatalyst for dehydrocoupling of various primary and secondary amine boranes as well as linear dimer aminoboranes. In a later paper, Manners *et al.* investigated the nature of the catalytically active species and found that heterogeneous

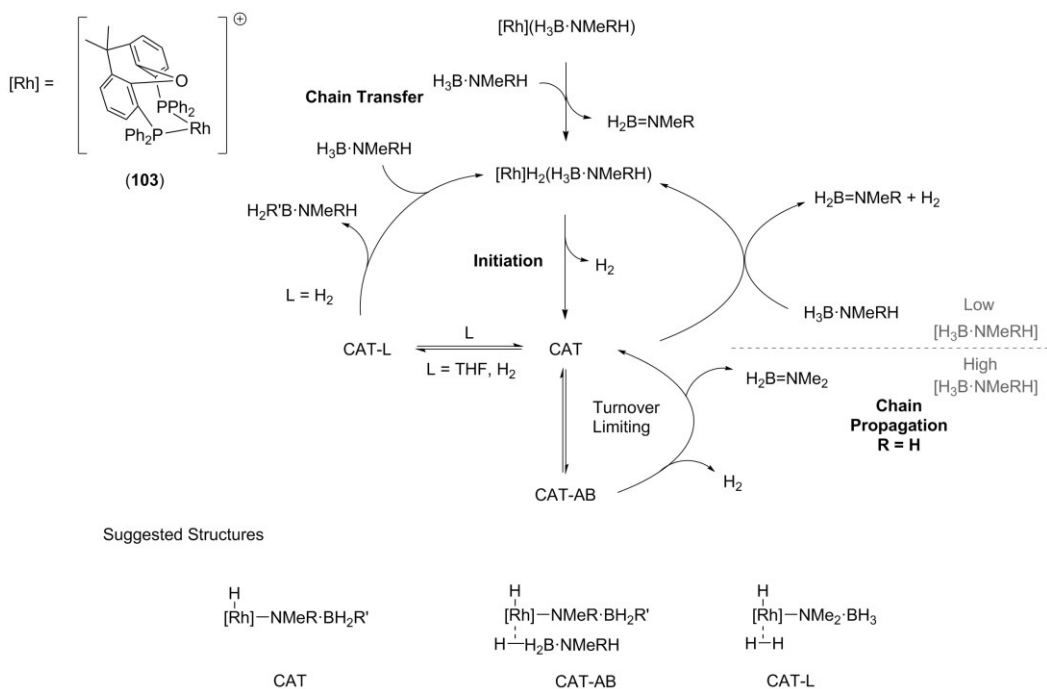
Ru NPs are responsible for catalytic activity.^[99] The authors point out that the use of transition metal catalysts could allow for dehydrocoupling of amine boranes under milder conditions and overcome the disadvantage of thermal routines that require heating to 100 °C or higher. The structure of final BN products differed with the amine borane used [Scheme 23 (1 - 4)]. These results paved the way for the entire area of research concerning transition metal catalyzed dehydrogenation and dehydrocoupling of amine boranes.



Scheme 23. Catalytic dehydrocoupling of secondary amine boranes (1), secondary amine boranes with bulky substituents (2), linear amine borane dimers (3) and primary amine boranes using heterogeneous Rh catalysts (4)

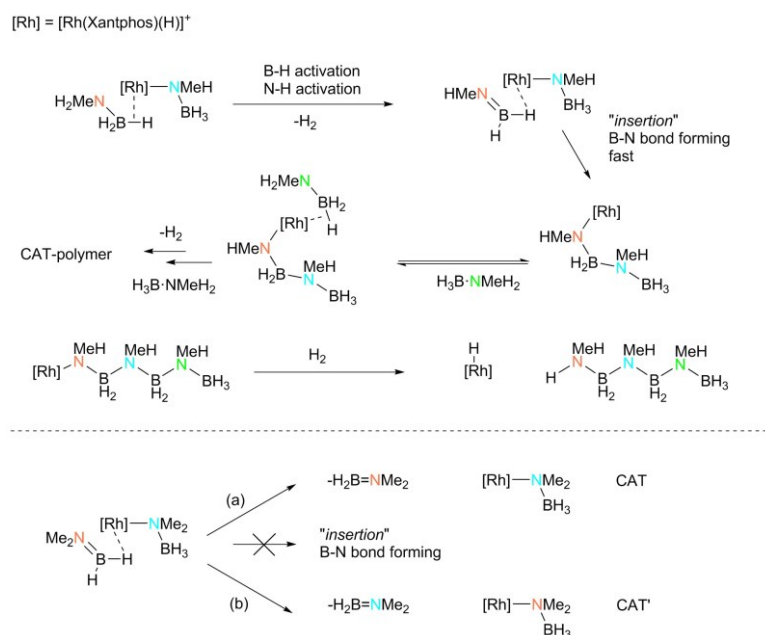
Enlightened by an example that the $\text{Rh}(\text{Xantphos})^+$ fragment (**103**) (Xantphos = 4,5-bis(diphenylphosphino)-9,9-dimethylxanthene) can perform homocoupling of $\text{Me}_3\text{N}\cdot\text{BH}_3$ to form B-B bonds,^[100] Weller, Manners and co-workers studied the dehydropolymerization process of MAB with respect to stoichiometric and catalytic reactivity using the same Rh fragment (Scheme 24). More information about the catalytic cycle and interactions between the metal center Rh and substrate were collected by reacting with DMAB, $\text{Me}_3\text{N}\cdot\text{BH}_3$ and $\text{iPr}_2\text{N}=\text{BH}_2$.^[101] When using 0.2 mol% Rh catalyst, the dehydrogenated products from substrates DMAB and MAB were dimeric $[\text{H}_2\text{B}=\text{NMe}_2]_2$ and polymethylaminoborane ($M_n = 22700$ g/mol, PDI = 2.1), respectively. The authors showed that all the catalytic, stoichiometric and kinetic data point to the presence of similar mechanisms for both substrates, in which a key step was the generation of the active catalyst, postulated to be a Rh

amidoborane complex that reversibly binds the amine borane substrate. The mechanism is only divergent in that the B-N bond formation, resulting in chain growth is more favored for MAB compared to DMAB, thus giving a polymer for MAB.



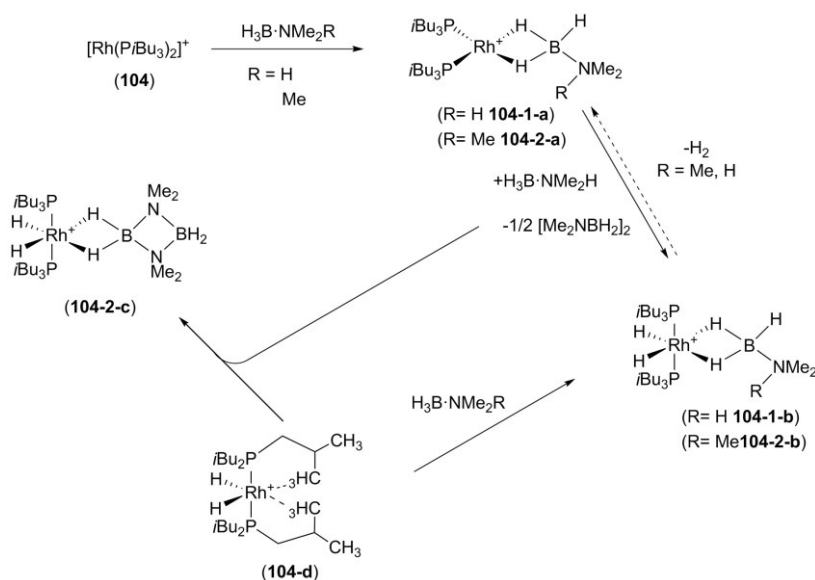
Scheme 24. Suggested mechanistic cycle and intermediates for the dehydrocoupling of DMAB and the dehydropolymerization of MAB.

Baker, Dixon and co-workers discussed earlier whether the free transient aminoboranes such as $\text{MeHN}=\text{BH}_2$ and $\text{Me}_2\text{N}=\text{BH}_2$ which form by dehydrogenation and may be the most important intermediate could still strongly bind to a metal center and then rapidly insert aminoboranes into the growing polymer chain. Otherwise, if the intermediate does not coordinate to the metal center borazine would form via trimerization (Scheme 25).^[102] These free aminoboranes can be trapped by hydroboration of cyclohexene and thus form $\text{Cy}_2\text{B}-\text{NH}_2$. According to Weller, it should however be noted that if the formation of hydroborated product or borazine were not kinetically competitive with metal-promoted B-N coupling, even if free aminoboranes appeared transiently, $\text{Cy}_2\text{B}-\text{NH}_2$ would not be observed. The trapping experiment using cyclohexene is in this case not suitable to verify the presence of a free aminoborane. They also figured out how to control the molecular weight of the polymer. Hydrogen was presumed to act as a chain-transfer reagent and low-molecular-weight polymers were formed in closed systems. On the contrary, THF retarded chain transfer, so that, longer polymer chains were obtained.



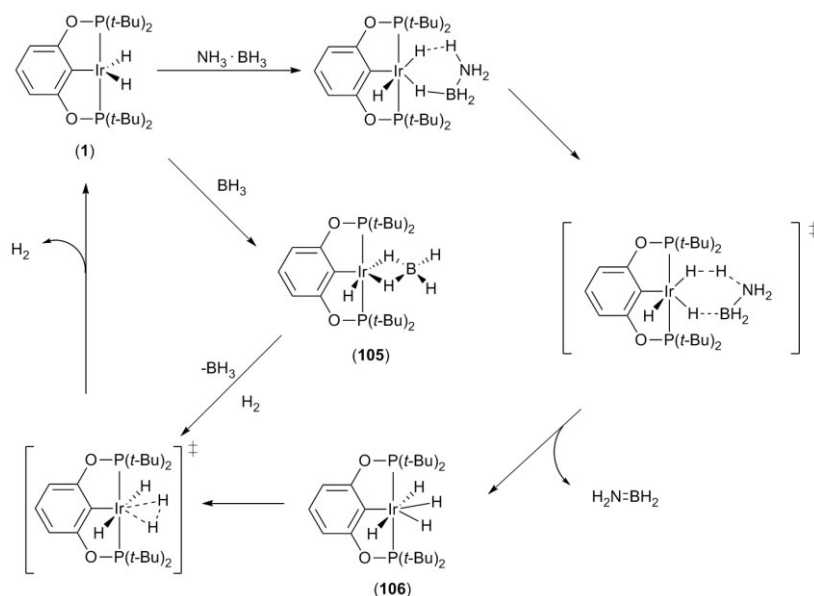
Scheme 25. Proposed ways for dehydropolymerizaion of MAB (top) and dehydrocoupling of DMAB (bottom).

In 2008, Weller and co-workers discussed previously published studies and pointed out that sigma complexes of amine boranes should be present in the reactions with transition metal complexes.^[103] However, such intermediates involved are elusive at that time.^[103a, 104] They presented a rhodium complex that can be applied for both dehydrocoupling and dehydrogenation. DMAB could be dehydrogenated in moderate rate in an open system under argon (TON = 34 h⁻¹, 5 mol% loading, 298 K, 100% conversion) and produced cyclic dimer [H₂BNMe₂]₂. Most importantly, two Rh(I) and Rh(III) σ amine borane complexes of H₃B·NMe₂R (**104-2-a** and **104-1-b**), and a σ -complex of a cyclic aminoborane [Rh(PiBu₃)₂{ η^2 -(H₂BNMe₂)₂}] [BAR^F₄] (**104-2-c**) were observed by means of NMR spectroscopy and X-ray analysis (Scheme 26).



Scheme 26. Synthesis of new amine borane σ -complexes ([BAR^F₄] not show).

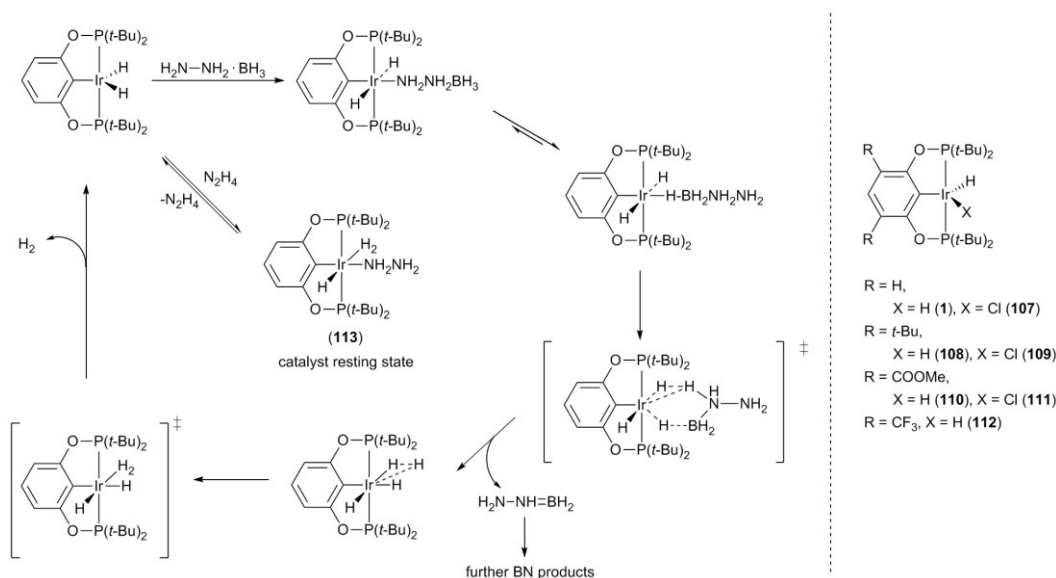
In 2006, Goldberg, Heinekey and co-workers reported on the dehydrogenation reaction of AB mediated by (POCOP)Ir(H)₂ (**1**) (POCOP = [κ^3 -2,6-(OPtBu₂)₂C₆H₃]) which was developed before by Brookhart's group for alkane dehydrogenation (Scheme 27).^[103b, 105] One equivalent of hydrogen was found to evolve with different rates depending on the catalyst loading (it took roughly four minutes to release one equivalent of hydrogen with 1 mol% loading and 30 minutes using 0.25 mol% loading, respectively). The IR spectrum and X-ray powder diffraction data of the precipitated B-N product was found to be in good agreement with a known cyclic pentamer [H₂NBH₂]₅.^[106] Later, Manners *et al.* discussed the B-N product of AB dehydrogenation as the linear polymer [H₂NBH₂]_n.^[107] The resting state complex, [(POCOP)Ir(H)₂(BH₃)] (**105**) was isolated after reaction and can be activated by reaction with hydrogen to form POCOPIr(H)₄ (**106**) which eliminates hydrogen to give the dihydride catalyst again. Paul and Musgrave, in order to address questions about the iridium complex catalyzed AB dehydrogenation, calculated the process via density functional theory (DFT) and proposed a catalytic cycle.^[108] They suggest that the dehydrogenation of AB takes place by a concerted proton and hydride transfer from AB to the metal catalyst with the hydride of the B-H bond binding to iridium and the NH proton approaching the metal hydride. This results in the formation of **106** and an aminoborane. The dehydrogenation cycle is closed by H₂ release from **106** and formation of the active catalyst **1**.



Scheme 27. AB dehydrogenation proposed by Paul and Musgrave.

Our group also utilized Brookhart's (POCOP)Ir(H)₂ complex when looking for proper catalysts for HB dehydrogenation.^[11b] In order to further explore the influence of substituents at the aryl backbone of the iridium complex on the catalytic capability, we synthesized a series of 3,5-disubstituted cyclometalated iridium(III) hydrido complexes [3,5-R₂(POCOP)IrHX] ((POCOP) = κ³-2,6-(OP*t*Bu₂)₂C₆H₃ with R = *t*-Bu, COOMe; X = Cl, H) (Scheme 28, right) and applied them for dehydrogenation of HB and compared with the original iridium catalyst. It turned out that iridium catalyst with an electron-withdrawing group (**110**), surprisingly, shows a significantly higher activity

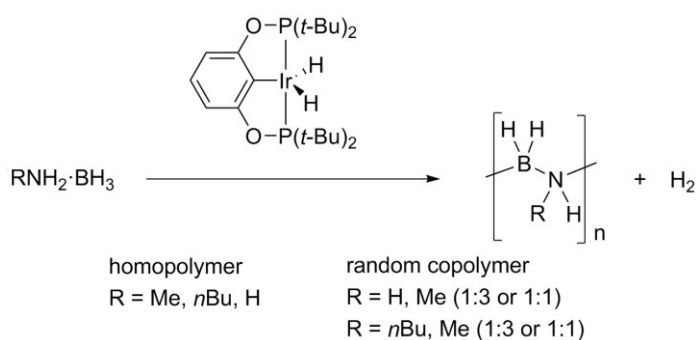
as this complex took only about 60 seconds (1 mol% loading) for evolution of one equivalent of hydrogen from HB. This trend is in line with a report on dehydrogenation of alkanes with $[3,5-(\text{CF}_3)_2\text{POCOPIr}(\text{H})_2]$ (**112**). These complexes show slightly better activity.^[109] In addition to that, the resting state of catalyst could be identified based on a species that was separated from reaction solutions after reaction. Compound **113** is a Ir(III) dihydrido hydrazine complex that still is significantly active as it can be used to dehydrogenate HB at least four times with only minor loss of activity. We deeper analyzed the mechanism of the reaction by *in situ* NMR and found that even at low temperature (198 K) formation of the tetrahydrido complex **106** takes place.^[110] This Ir complex fully converted into $(\text{POCOP})\text{Ir}(\text{H})_2(\text{N}_2\text{H}_4)$ (**113**), the resting state of catalyst. Formation of complex **105** as it was discussed by Heinekey and Goldberg was not observed (Scheme 28, left). As for the dehydrogenated material, ^{11}B solid state NMR indicates the presence of four-coordinate B centers with different B–H and B–N–H proton environments, thus suggesting a three-dimensional, most likely polymeric structure.



Scheme 28. Catalytic cycle of HB dehydrogenation proposed by our group (left). The catalysts used by our group (**1**, **107** - **111**) and literature (**112**) (right).

Motivated by Heinekey's and Goldberg's study, Manners and co-workers showed that this iridium system can catalyze the dehydrocoupling of other primary amine boranes.^[107] MAB was found to react with 0.1 mol% loading of complex **1** in THF at 0 °C, followed by stirring for 20 minutes at 20 °C. The resulting product was isolated and purified, then characterized by NMR, elemental analysis (EA), IR spectroscopy, gel permeation chromatography (GPC) and dynamic light scattering (DLS). The results showed that they obtained a high molecular weight polymer ($M_w = 160000$) with a polydispersity index (PDI) of 2.9. Furthermore, AB, *n*-butylamine borane and MAB were tested in homopolymerization and copolymerization reactions (Scheme 29). All products, like dehydrogenated MAB, were characterized by GPC, DLS, NMR, EA, IR and thermogravimetric analysis (TGA). These

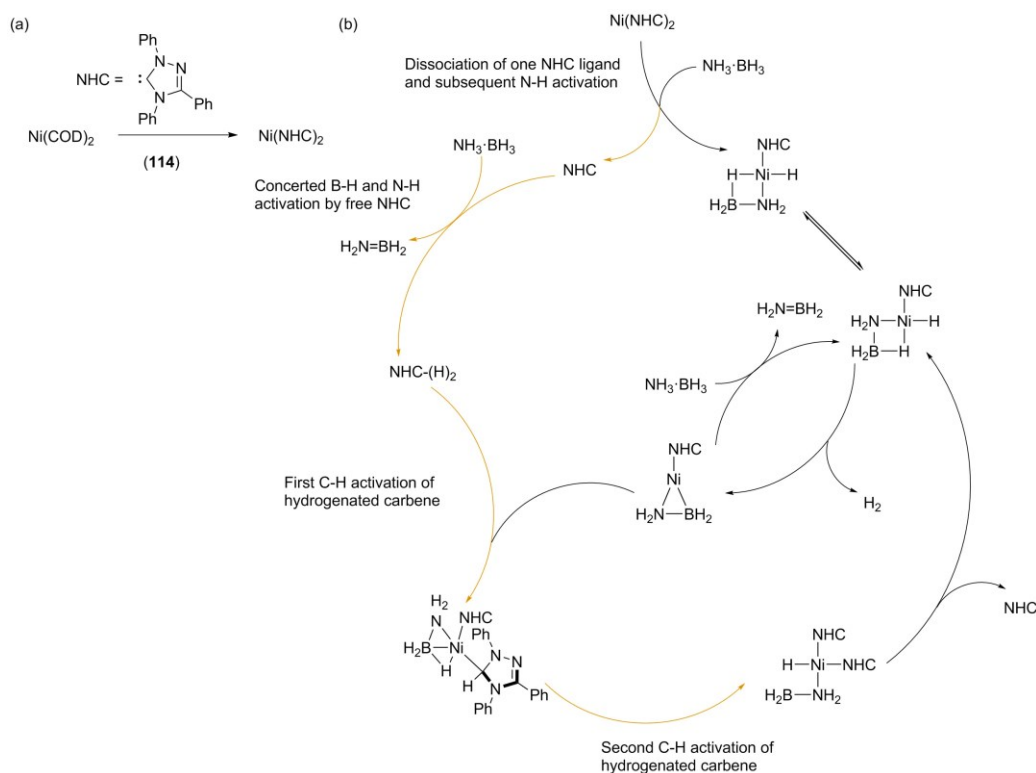
characterization results resembled those of polymethylaminoborane, but the NMR data was much more complicated. Later, Manners and co-workers revealed in another paper that temperature, solvent, substrate concentration, catalyst loading and nature of the catalyst could affect the molecular weight of the polymer as well. Moreover, details on the polymer characterization were given.^[31] However, in neither of these studies, it was mentioned how much hydrogen evolved during reactions, an information that is very valuable for the interpretation of the reaction mechanism. Recently, the Ir complex was also employed by the Manners group for a dehydrocoupling reaction of $\text{NH}_3 \cdot \text{BH}_2\text{Ph}$, a boron substituted amine borane.^[111] Two high molecular weight polyaminoboranes were thus prepared for the first time.



Scheme 29. Brookhart's Iridium system for catalytic dehydrocoupling of primary amine boranes.

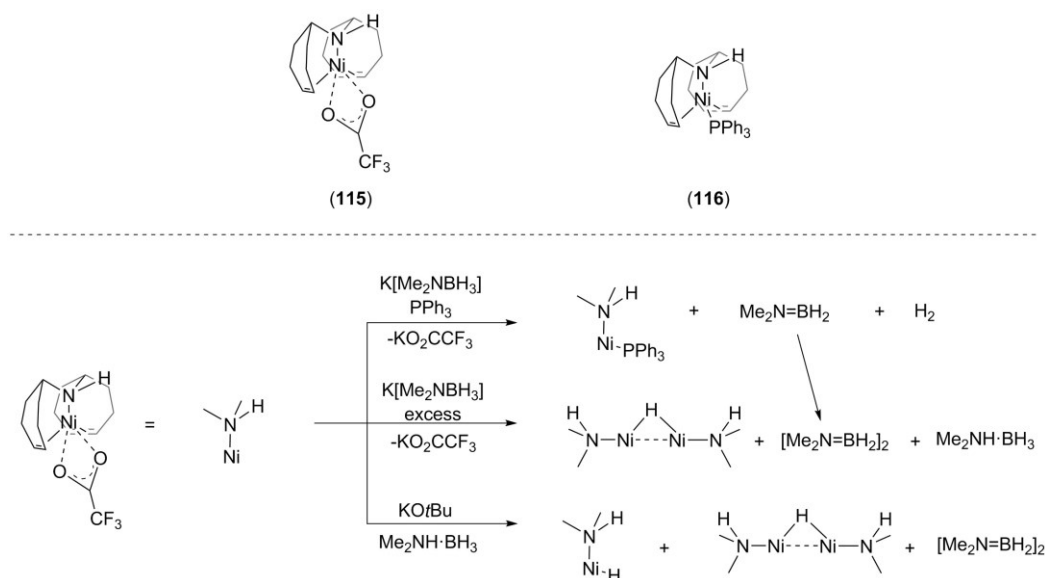
2.3.7. Group 10 complexes

In 2007, Baker reported the first Ni complex for dehydrogenation of AB. After being generated *in situ* from $\text{Ni}(\text{COD})_2$ and a carbene ligand, the complex has a high catalytic ability and can release more than two equivalents of hydrogen from AB at 60 °C in a benzene/diglyme mixture within four hours.^[64] It should be emphasized that the NHC (NHC = 1,3,4-triphenyl-4,5-dihydro-1H-1,2,4-triazol-5-ylidene) ligated Ni complex has the best performance, and exceeds the activity of noble transition metals catalysts based on Rh and Ru. The authors measured KIE values and NMR spectra, however, as information from KIE were limited, they only proposed that the initial step was B-H activation and β N-H elimination. Later, Hall and co-workers also investigated this reaction though DFT calculations.^[112] Nevertheless, they only reasonably explained how the first equivalent of hydrogen is released. The research team of Paul also computed the reaction and presented a catalytic pathway according to their results (Scheme 30).^[113] In spite of the fact that several important species were presented during catalytic dehydrogenation such as $\text{Ni}(\text{NHC})(\text{H}_2\text{N}=\text{BH}_2)$ and non-innocent free NHC ligand, in view of the complexity of the catalytic process, far more studies need to be done.



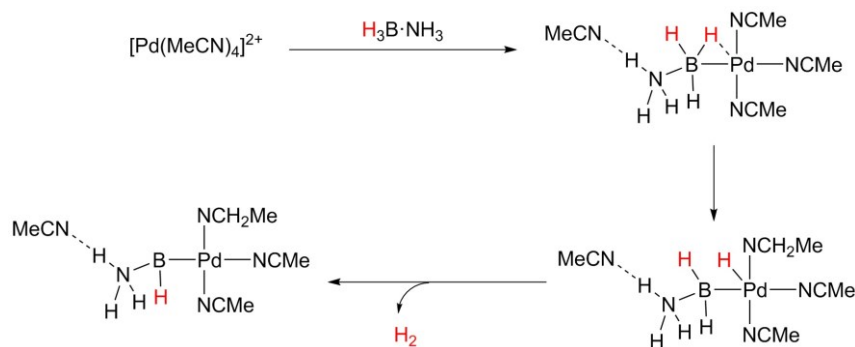
Scheme 30. *In situ* generated catalyst (a). Mechanism proposed by Paul and co-workers (b).

In 2011, a rare paramagnetic organometallic Ni(I) olefin complex (**115**) was presented by Trincado, Grützmacher and co-workers.^[114] The Ni complex was isolated and fully characterized by the authors. Dehydrogenation of DMAB catalyzed by this species was compared with its derivative $[\text{Ni}^0(\text{trop}_2\text{NH})(\text{PPh}_3)]$ (trop_2NH = bistropylidenylamine) (**116**). It turned out that **115** was an extremely active precatalyst. Even at a very low loading (0.3 mol%) with base activation (1 mol% to 3 mol%), one equivalent of hydrogen could be released from DMAB within one minute in THF at room temperature. Ni(0) complex **116** was significantly slower and in the first reaction step the linear chain dimer $\text{BH}_3\text{-NMe}_2\text{-BH}_2\text{-NMe}_2\text{H}$ was the kinetically favored dehydrogenation product and would gradually be converted to the cyclic dimer $[\text{Me}_2\text{NBH}_2]_2$ which could directly be obtained by **115** catalyzed DMAB dehydrogenation. It is noteworthy that the catalytic capability of **115** and even of **116** for dehydrogenation of DMAB was much better than that of a similar Ru complex reported by the same authors.^[115] When discussing the individual steps of the catalytic cycle, the authors suggested that radical pathways took part in the reaction. Nevertheless, since ^1H NMR signals showed Ni(0) hydrido complexes, these may also be involved in DMAB dehydrogenation (Scheme 31). Different from the Ru analogue where the olefinic binding sites served only as placeholders for ‘vacant’ coordination sites, the ligand coordinating to the Ni center proved suitable as steering ligands in the catalytic reaction.



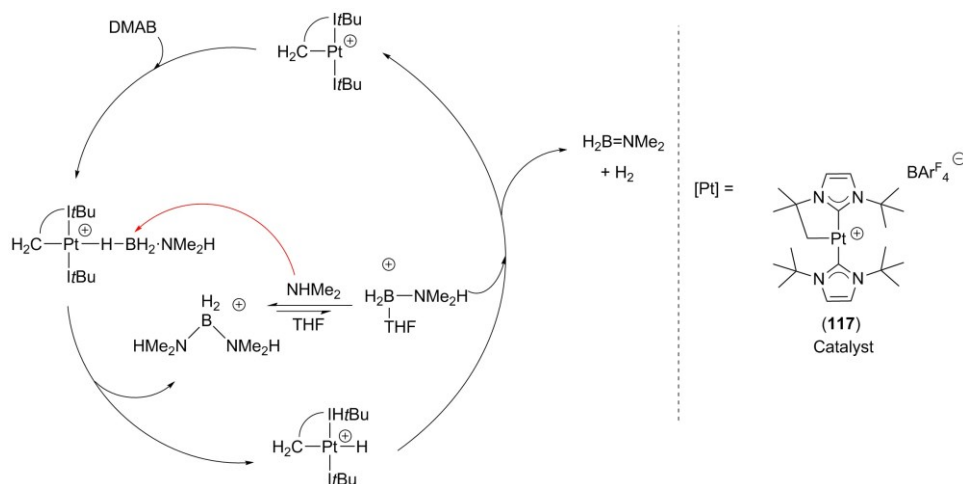
Scheme 31. Ni catalysts used for DMAB dehydrogenation (above). different pathways for **115** to hydrido Ni(0) complexes (below).

In 2010, Kang, Michalak and co-workers synthesized three cationic palladium complexes for dehydrogenation of AB (Scheme 32).^[116] All three complexes showed outstanding performance for dehydrogenation of AB. Even the slowest one, $[\text{Pd}(\text{MeCN})_4][\text{BF}_4]$ can release two equivalents of hydrogen in 60 seconds at 25 °C. For the fastest, it took only 20 seconds. The authors thoroughly studied the reaction and optimized it for the catalyst $[\text{Pd}(\text{MeCN})_4][\text{BF}_4]$. The KIE values of $\text{ND}_3\cdot\text{BH}_3$, $\text{H}_3\text{N}\cdot\text{BD}_3$ and $\text{D}_3\text{N}\cdot\text{BD}_3$ were measured (2.5, 8.2 and 9.5, respectively) for probing interaction between substrate and Pd center which indicated that B-H and B-D bonds weakened markedly. Amine boranes with alkyl and aryl groups binding to B or N end were also employed for investigation of the interaction. The authors discovered that every two equivalents of hydrogen releasing from AB result in the formation of two B-B bonds and one B-N bond and the first equivalent of hydrogen actually completely originated from the borane moiety of AB. As a consequence, the structural features were different from the linear B-N polymer that the Manners group synthesized via metal-catalyzed dehydropolymerization.^[107] No more information was given about how the second equivalent of hydrogen is liberated.



Scheme 32. Proposed process for the first equivalent of hydrogen generation.

In 2013, the first platinum dehydrocoupling catalyst was published by Conejero, López-Serrano and Roselló-Merino (Scheme 33).^[117] Generally, for main group and early transition metals employed in amine borane dehydrogenation and dehydrocoupling reactions, the first step is always the activation of N-H bond of amine borane. For late transition metal catalysts, on the contrary, the activation commonly starts from the opposite terminus, i.e. the B-H bond. Different from the literature knowledge, the authors found a new mechanistic scenario that involved the initial formation of boronium cations $(\text{NMe}_2\text{H})_2\text{BH}_2^+$ through hydride abstraction from DMAB by highly electrophilic Pt(II) complexes with concomitant formation of a Pt(II) hydride. The $[\text{Pt}(\text{ItBu})(\text{ItBu})][\text{BAR}^{\text{F}}_4]$ ($\text{ItBu} = 1,3\text{-di-tert-butylimidazol-2-ylidene}$) catalyzed reaction was monitored by $^{11}\text{B}\{^1\text{H}\}$ NMR and pressure change in a sealed system. The states of Pt catalyst during dehydrocoupling of DMAB were supported by a series of stoichiometric reactions and monitoring with multinuclear NMR spectroscopy. The authors suggested that the mechanism involving the highly electrophilic Pt complex dehydrogenating DMAB is related to that of Frustrated Lewis Pairs. It includes several steps: First, hydride transfers from the BH_3 fragment to the platinum center, followed by nucleophilic attack of free HNMe_2 to the coordinated B atom to afford the boronium ion $[(\text{HMe}_2\text{N})_2\text{BH}_2]^+$. After that, Pt(II) hydride complex is formed and next protonated by the acidic NH of the boronium cation $[(\text{HMe}_2\text{N})(\text{THF})\text{BH}_2]^+$ (one NHMe_2 of $[(\text{HMe}_2\text{N})_2\text{BH}_2]^+$ is replaced by THF). In the meantime, $\text{NMe}_2=\text{BH}_2$ and hydrogen release with regeneration of the Pt catalyst.

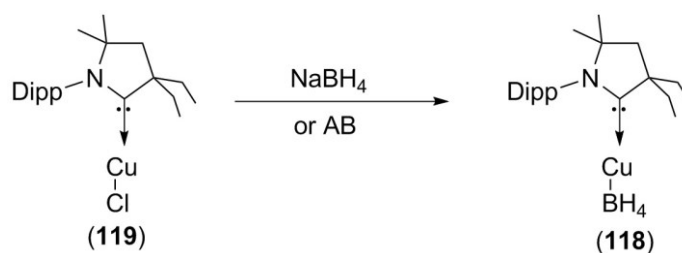


Scheme 33. Catalytic dehydrogenation of DMAB by Pt catalyst **117**, $[\text{BAR}^{\text{F}}_4]$ not shown (left). Pt catalyst (right).

2.3.8. Group 11 complexes

In 2015, the first air stable copper borohydride complex $[(\text{CAAC})\text{CuBH}_4]$ (**118**) and its parent complex $[(\text{CAAC})\text{CuCl}]$ (**119**) [$\text{CAAC} = \text{cyclic(alkyl)(amino)carbene}$] were reported as catalysts for the hydrolytic dehydrogenation of AB by Hu, Bertrand and co-workers.^[118] The general procedure for dehydrogenation experiments was that 1 mol% Cu catalysts in acetone/ H_2O solution (20 wt% of H_2O) was added to AB at 25 °C. When complex **119** was employed, 2.6 equivalents of H_2 were released

over five minutes with a TOF of 3100 h^{-1} . Meanwhile, when adding complex **118**, 2.8 equivalents of H_2 evolved within two minutes, giving a TOF of 8400 h^{-1} . Efforts for augmenting reactivity of complex **119** were made as well by using potassium tetrakis(pentafluorophenyl)borate (KBAr^{F}_4) as additive in the reaction of complex **119**. The amount of H_2 released increased to 2.8 equivalents with a TOF of 3360 h^{-1} . This approach also works for the recycling processes: complex **119** and KBAr^{F}_4 (1:1) were reused 15 times without noticeable loss of catalytic activity. For each cycle, the dehydrogenation reaction was finished within five minutes with around 2.8 equivalents of H_2 released.

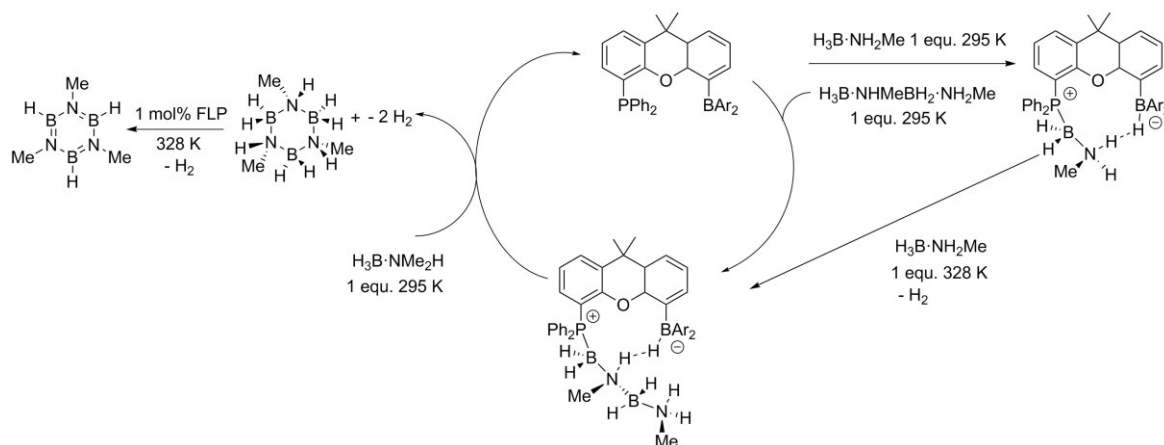


Scheme 34. Cu complexes for hydrolytic dehydrogenation of AB.

2.4. Metal-free catalytic dehydrogenation of amine boranes

2.4.1. Frustrated lewis pairs (FLP)

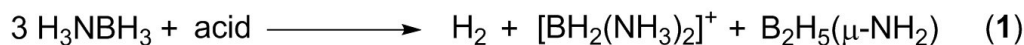
Based on the result of theoretical calculation of $\text{Ni}(\text{NHC})_2$ promoted AB dehydrogenation that the NHC may be involved in the dehydrogenation process and the comparison of its reactivity to FLP which can split H_2 ,^[64, 119] Miller and Bercaw first proposed that FLP may be suitable for amine boranes dehydrogenation. The FLP $t\text{Bu}_3\text{P}/\text{B}(\text{C}_6\text{F}_5)_3$ acts as a mediator for DMAB dehydrogenation in $\text{C}_6\text{D}_5\text{Cl}$ at 25°C , producing approximately 97% of $[\text{NMe}_2\text{BH}_2]_2$, trace amounts of $(\text{BH}_2)_2\text{NMe}_2(\mu\text{-H})$ and the linear dimer $\text{H}_3\text{B}\cdot\text{NMe}_2\text{BH}_2\cdot\text{NMe}_2\text{H}$ alone with $[\text{H}/t\text{Bu}_3\text{P}][\text{HB}(\text{C}_6\text{F}_5)_3]$.^[120] H_2 was released by heating the phosphonium and borohydride salt between 90°C to 130°C . However, it is a stoichiometric dehydrogenation process. More recently, catalytic dehydrogenation of amine boranes by a FLP bearing a dimethylxanthene backbone was reported by Aldridge's group (Scheme 35).^[121] The postulated mechanism involves initial B-H bond activation at the phosphorous moiety to give the zwitterionic phosphonium-boronate species. Subsequent reaction with substrate MAB results in reaction of the B terminus of the substrate with the amine group of the zwitterion and release of H_2 . As a consequence, the linear MAB dimer is formed. Finally, a third equivalent of amine borane would react with the two coordinated BN units, dissociating a cyclic borazane which can be further dehydrogenated to borazine by the FLP catalyst.



Scheme 35. Dehydrogenation process proposed by Aldridge's group.

2.4.2. Acid-catalyzed dehydrogenation

In 2007, Baker, Dixon and co-workers observed that H_2 is released from mixtures of the Lewis acid $\text{B}(\text{C}_6\text{F}_5)_3$ and AB. During the course of the reaction a prominent NMR resonance corresponding to the anion $[\text{HB}(\text{C}_6\text{F}_5)_3]^-$ was detected.^[122] Based on this result, various acids were added to AB and reaction conditions were modified for optimizing dehydrogenation and obtaining insight into the mode of action. The authors found that the concentration of acid has a significant effect on the extent of dehydrogenation, higher acid loading promoted. Considering this experimental observation, they suggested that during the reaction, due to rate mismatch of the initiation and propagation steps, a linear dimer $\text{H}_3\text{BNH}_2\text{BH}_2\text{NH}_3$ transformed a NH_3 to boronium $[\text{NH}_2\text{BH}_3]^+$, which originated from AB deprotonation. As in the chain-transfer mechanism, the equilibrium Eq. (1) elucidates that adding acid to AB will not liberate the equimolecular amount of H_2 . While, it was confirmed that by reducing the concentration of acid ($\text{B}(\text{C}_6\text{F}_5)_3$) from 25 mol% to 0.5 mol%, up to 1.1 equivalents H_2 produced in 20 hours instead of 0.6 equivalent in 24 hours. The same behavior was formed when using HOSO_2CF_3 as well.



2.4.3. Based-catalyzed dehydrogenation

Opposite to acid-catalyzed dehydrogenation, theoretically, a base is able to dehydrogenate amine borane as well. In 2009, a strongly non-nucleophilic base bis(dimethylamino)naphthalene (Proton Sponge, PS) was announced that can promote the release of H_2 from AB either in the solid state or in ionic-liquid and tetraglyme solutions.^[123] The dehydrogenation starts with PS initiating the deprotonation of AB to give the anion $[\text{NH}_2\text{BH}_3]^-$ in solid state or ionic liquids through an anionic dehydropolymerization pathway, in which the *in situ* generated anion activates AB to form initially branched-chain polyaminoborane and cross link to polyborazylene. More than two equivalents of H_2 were evolved with just 1 mol% of PS.

3. Objectives of this work

H₂ as an energy carrier is a good option for realization of an environmentally benign sustainable energy supply. To overcome the disadvantages it has, a large number of H₂ storage methods have been developed and amine boranes are one of the most promising candidates with a lot of advantages. In addition to that, dehydrogenation of amine boranes allows for synthesizing BN polymers, which are interesting compounds for main group and material chemistry due to the isoelectronic analogy to carbon based polymers. Thus, categories of catalysts, including those described above have been employed for catalytic dehydrogenation of ammonia borane, primary amine boranes and secondary amine boranes for extracting H₂ or synthesizing BN materials. Transition metal complexes were found to be suitable for hydrogen release, transfer hydrogenations and construction of BN materials. In the future, the latter application should become more interesting in terms of applications as the development of main group polymers can give valuable inspirations for the implementation of new materials. Also, despite the promising characteristics of amine boranes such as the high gravimetric H₂ capacity, these compounds are of limited applicability on a larger scale due to the problem of regeneration of spent amine borane fuels. As a derivative of ammonia borane, to our best knowledge, only one example for transition metal complex catalyzed dehydrogenation of hydrazine borane under homogenous conditions was described before. Therefore, the main objective of this work was to further study suitable transition metal complexes for efficiently dehydrogenating HB under mild conditions. Also, insights into the mechanism of HB dehydrogenation for improving the catalytic capability of metal complexes and reaction conditions were needed. For this noble metal and base metal complexes were used. The influence of the ligand backbone was investigated by tuning the ligand by introducing groups with different electronic and steric properties, or ligands coordinating to the metal are altered. Apart from investigating the hydrogen release, the focus of this work will be on the formation of BN materials from amine borane substrates.

A significant number of catalysts described before show the pincer ligand motif. As part of this thesis we aimed to synthesize PNP ligands for dehydrogenation catalysts. When preparing these, special attention is required with respect to reaction conditions as otherwise, a number of isomers, including PN and PPN ligands are formed. As a part of this thesis, the coordination chemistry of PN and PPN ligands to 3d metal is described.

4. References

- [1] S. Chu, A. Majumdar, *Nature* **2012**, *488*, 294-303.
- [2] (a) C. Bailleux, *Int. J. Hydrogen Energy* **1981**, *6*, 461-471. (b) K. Mazloomi, C. Gomes, *Renewable and Sustainable Energy Reviews* **2012**, *16*, 3024-3033.
- [3] (a) T. B. Marder, *Angew. Chem., Int. Ed.* **2007**, *46*, 8116-8118. (b) N. L. Garland, D. C. Papageorgopoulos, J. M. Stanford, *Energy Procedia* **2012**, *28*, 2-11.
- [4] (a) H.-F. Klein, S. Camadanli, R. Beck, U. Florke, *Chem. Commun.* **2005**, 381-382. (b) J. Yang, A. Sudik, C. Wolverton, D. J. Siegel, *Chem. Soc. Rev.* **2010**, *39*, 656-675. (c) A. F. Dalebrook, W. Gan, M. Grasemann, S. Moret, G. Laurenczy, *Chem. Commun.* **2013**, *49*, 8735-8751.
- [5] (a) G. G. Tibbetts, G. P. Meisner, C. H. Olk, *Carbon* **2001**, *39*, 2291-2301. (b) J. Dong, X. Wang, H. Xu, Q. Zhao, J. Li, *Int. J. Hydrogen Energy* **2007**, *32*, 4998-5004. (c) P. M. Budd, A. Butler, J. Selbie, K. Mahmood, N. B. McKeown, B. Ghanem, A. Walton, *Phys. Chem. Chem. Phys.* **2007**, *9*, 1802-1808. (d) N. B. McKeown, P. M. Budd, *Chem. Soc. Rev.* **2006**, *35*, 675-683. (e) J. L. C. Rowsell, O. M. Yaghi, *Angew. Chem., Int. Ed.* **2005**, *44*, 4670-4679. (f) D. J. Collins, H.-C. Zhou, *J. Mater. Chem.* **2007**, *17*, 3154-3160.
- [6] S. Satyapal, J. Petrovic, C. Read, G. Thomas, G. Ordaz, *Catal. Today* **2007**, *120*, 246-256.
- [7] (a) G. P. Pez, A. R. Scott, A. C. Cooper, H. Cheng, *US Pat.* 7 101 530, 2006. (b) K. M. Eblagon, D. Rentsch, O. Friedrichs, A. Remhof, A. Zuettel, A. J. Ramirez-Cuesta, S. C. Tsang, *Int. J. Hydrogen Energy* **2010**, *35*, 11609-11621.
- [8] (a) A. Moores, M. Poyatos, Y. Luo, R. H. Crabtree, *New J. Chem.* **2006**, *30*, 1675-1678. (b) D. Lacina, J. Wegrzyn, J. Reilly, Y. Celebi, J. Graetz, *Energy & Environ. Sci.* **2010**, *3*, 1099-1105. (c) E. R. Abbey, L. N. Zakharov, S.-Y. Liu, *J. Am. Chem. Soc.* **2008**, *130*, 7250-7252.
- [9] (a) T. Zell, B. Butschke, Y. Ben-David, D. Milstein, *Chem.–Eur. J.* **2013**, *19*, 8068-8072. (b) I. Mellone, N. Gorgas, F. Bertini, M. Peruzzini, K. Kirchner, L. Gonsalvi, *Organometallics* **2016**, *35*, 3344-3349.
- [10] (a) U. B. Demirci, *Int. J. Hydrogen Energy* **2017**, *42*, 9978-10013. (b) J.-F. Petit, P. Miele, U. B. Demirci, *Int. J. Hydrogen Energy* **2016**, *41*, 15462-15470. (c) A. Al-Kukhun, H. T. Hwang, A. Varma, *Int. J. Hydrogen Energy* **2013**, *38*, 169-179. (d) R. Benzouaa, U. B. Demirci, R. Chiriac, F. Toche, P. Miele, *Thermochim. Acta* **2010**, *509*, 81-86. (e) M. Rakap, S. Özkar, *Int. J. Hydrogen Energy* **2010**, *35*, 3341-3346. (f) A. Brockman, Y. Zheng, J. Gore, *Int. J. Hydrogen Energy* **2010**, *35*, 7350-7356. (g) M. Chandra, Q. Xu, *J. Power Sources* **2006**, *156*, 190-194. (h) A. Gutowska, L. Li, Y. Shin, C. M. Wang, X. S. Li, J. C. Linehan, T. Autrey, *Angew. Chem., Int. Ed.* **2005**, *44*, 3578-3582. (i) S. B. Kalidindi, A. A. Vernekar, B. R. Jagirdar, *Phys. Chem. Chem. Phys.* **2009**, *11*, 770-775. (j) Ö. Metin, V. Mazumder, S. Özkar, S. Sun, *J. Am. Chem. Soc.* **2010**, *132*, 1468-1469. (k) Q.-L. Zhu, D.-C. Zhong, U. B. Demirci, Q. Xu, *ACS Catal.* **2014**, *4*, 4261-4268. (l) J. Hannauer, U. B. Demirci, C. Geantet, J.-M. Herrmann, P. Miele, *Int. J. Hydrogen Energy* **2012**, *37*, 10758-10767.
- [11] (a) J. Thomas, M. Klahn, A. Spannenberg, T. Beweries, *Dalton Trans.* **2013**, *42*, 14668-14672. (b) D. Han, M. Joks, M. Klahn, A. Spannenberg, H. J. Drexler, W. Baumann, T. Beweries, *Dalton Trans.* **2016**, *45*, 17697-17704.
- [12] https://availabletechnologies.pnnl.gov/media/87_723200830003.pdf.
- [13] (a) M. Albrecht, G. van Koten, *Angew. Chem., Int. Ed.* **2001**, *40*, 3750-3781. (b) M. E. van der Boom, D. Milstein, *Chem. Rev.* **2003**, *103*, 1759-1792. (c) J. Choi, A. H. R. MacArthur, M. Brookhart, A. S. Goldman, *Chem. Rev.* **2011**, *111*, 1761-1779.

- [14] (a) C. J. Moulton, B. L. Shaw, *J. Chem. Soc., Dalton Trans.* **1976**, 1020-1024. (b) G. van Koten, K. Timmer, J. G. Noltes, A. L. Spek, *J. Chem. Soc., Chem. Commun.* **1978**, 250-252.
- [15] (a) K. Arashiba, Y. Miyake, Y. Nishibayashi, *Nat. Chem.* **2011**, *3*, 120-125. (b) R. Ghosh, M. Kanzelberger, T. J. Emge, G. S. Hall, A. S. Goldman, *Organometallics* **2006**, *25*, 5668-5671.
- [16] (a) R. Tanaka, M. Yamashita, K. Nozaki, *J. Am. Chem. Soc.* **2009**, *131*, 14168-14169. (b) K. Rohmann, J. Kothe, M. W. Haenel, U. Englert, M. Hölscher, W. Leitner, *Angew. Chem., Int. Ed.* **2016**, *55*, 8966-8969. (c) P. Daw, S. Chakraborty, G. Leitus, Y. Diskin-Posner, Y. Ben-David, D. Milstein, *ACS Catal.* **2017**, 2500-2504.
- [17] (a) G. Zhang, B. L. Scott, S. K. Hanson, *Angew. Chem.* **2012**, *124*, 12268-12272. (b) S. Monfette, Z. R. Turner, S. P. Semproni, P. J. Chirik, *J. Am. Chem. Soc.* **2012**, *134*, 4561-4564. (c) K. V. Vasudevan, B. L. Scott, S. K. Hanson, *Eur. J. Inorg. Chem.* **2012**, *2012*, 4898-4906.
- [18] (a) S. Rösler, J. Obenauf, R. Kempe, *J. Am. Chem. Soc.* **2015**, *137*, 7998-8001. (b) N. Gorgas, B. Stöger, L. F. Veiros, K. Kirchner, *ACS Catal.* **2016**, *6*, 2664-2672. (c) R. Langer, M. A. Iron, L. Konstantinovski, Y. Diskin-Posner, G. Leitus, Y. Ben-David, D. Milstein, *Chem.–Eur. J.* **2012**, *18*, 7196-7209. (d) F. Kallmeier, T. Irrgang, T. Dietel, R. Kempe, *Angew. Chem., Int. Ed.* **2016**, *55*, 11806-11809.
- [19] (a) S. Elangovan, M. Garbe, H. Jiao, A. Spannenberg, K. Junge, M. Beller, *Angew. Chem., Int. Ed.* **2016**, *55*, 15364-15368. (b) J. Zhang, G. Leitus, Y. Ben-David, D. Milstein, *Angew. Chem., Int. Ed.* **2006**, *45*, 1113-1115.
- [20] (a) C. Prichatz, E. Alberico, W. Baumann, H. Junge, M. Beller, *ChemCatChem* **2017**, *9*, 1891-1896. (b) M. Nielsen, E. Alberico, W. Baumann, H.-J. Drexler, H. Junge, S. Gladiali, M. Beller, *Nature* **2013**, *495*, 85-89. (c) E. Alberico, P. Sponholz, C. Cordes, M. Nielsen, H.-J. Drexler, W. Baumann, M. Beller, *Angew. Chem., Int. Ed.* **2013**, *52*, 14162-14166. (d) S. Chakraborty, P. O. Lagaditis, M. Förster, E. A. Bielinski, N. Hazari, M. C. Holthausen, S. Schneider, *ACS Catal.* **2014**, *4*, 3994-4003.
- [21] R. Xu, S. Chakraborty, H. Yuan, W. D. Jones, *ACS Catal.* **2015**, *5*, 6350-6354.
- [22] A. Kumar, T. M. Bhatti, A. S. Goldman, *Chem. Rev.* **2017**, *117*, 12357-12384.
- [23] (a) W.-P. Leung, Q. W.-Y. Ip, S.-Y. Wong, T. C. W. Mak, *Organometallics* **2003**, *22*, 4604-4609. (b) A. Jansen, S. Pitter, *Monatshefte für Chemie / Chemical Monthly* **1999**, *130*, 783-794. (c) M. Kawatsura, J. F. Hartwig, *Organometallics* **2001**, *20*, 1960-1964.
- [24] S. Zhang, R. Pattacini, P. Braunstein, *Inorg. Chem.* **2011**, *50*, 3511-3522.
- [25] (a) R. Langer, A. Gese, D. Gesevičius, M. Jost, B. R. Langer, F. Schneck, W. Xu, *Eur. J. Inorg. Chem.* **2015**, *2015*, 696-705. (b) W. Zuo, D. E. Prokopchuk, A. J. Lough, R. H. Morris, *ACS Catal.* **2016**, *6*, 301-314. (c) P. E. Sues, K. Z. Demmans, R. H. Morris, *Dalton Trans.* **2014**, *43*, 7650-7667. (d) R. Noyori, C. A. Sandoval, K. Muñiz, T. Ohkuma, *Philosophical Transactions of the Royal Society A: Mathematical, Physical and Engineering Sciences* **2005**, *363*, 901-912.
- [26] (a) Z. Shao, S. Fu, M. Wei, S. Zhou, Q. Liu, *Angew. Chem., Int. Ed.* **2016**, *55*, 14653-14657. (b) S. Fu, N.-Y. Chen, X. Liu, Z. Shao, S.-P. Luo, Q. Liu, *J. Am. Chem. Soc.* **2016**, *138*, 8588-8594. (c) C. A. Jaska, I. Manners, *J. Am. Chem. Soc.* **2004**, *126*, 2698-2699.
- [27] Z. Liu, T. B. Marder, *Angew. Chem., Int. Ed.* **2008**, *47*, 242-244.
- [28] (a) C. Dou, J. Liu, L. Wang, *Sci. China Chem.* **2017**, *60*, 450-459. (b) X. Long, N. Wang, Z. Ding, C. Dou, J. Liu, L. Wang, *J. Mater. Chem. C* **2016**, *4*, 9961-9967. (c) Z. Ding, X. Long, C. Dou, J. Liu, L. Wang, *Chem. Sci.* **2016**, *7*, 6197-6202. (d) S. Iyer, A. Detwiler, S. Patel, D. A. Schiraldi, *J. Appl. Polym. Sci.* **2006**, *102*, 5153-5161. (e) A. M. Diez-Pascual, A. L. Diez-Vicente, *RSC Adv.* **2016**, *6*, 79507-79519.

- [29] (a) C. Pan, Y. Ji, N. Xiao, F. Hui, K. Tang, Y. Guo, E. Miranda, *Adv. Funct. Mater.* **2017**, *27*. (b) K. A. Schwetz, *Ullmann's encyclopedia of industrial chemistry* **1985**. (c) R. F. Davis, *Proceedings of the IEEE* **1991**, *79*, 702-712.
- [30] (a) A. P. M. Robertson, E. M. Leitao, I. Manners, *J. Am. Chem. Soc.* **2011**, *133*, 19322-19325. (b) H. Helten, A. P. M. Robertson, A. Staubitz, J. R. Vance, M. F. Haddow, I. Manners, *Chem.–Eur. J.* **2012**, *18*, 4665-4680. (c) A. P. M. Robertson, E. M. Leitao, T. Jurca, M. F. Haddow, H. Helten, G. C. Lloyd-Jones, I. Manners, *J. Am. Chem. Soc.* **2013**, *135*, 12670-12683.
- [31] A. Staubitz, M. E. Sloan, A. P. Robertson, A. Friedrich, S. Schneider, P. J. Gates, I. Manners, *J. Am. Chem. Soc.* **2010**, *132*, 13332-13345.
- [32] C. J. Stevens, R. Dallanegra, A. B. Chaplin, A. S. Weller, S. A. Macgregor, B. Ward, S. Sabo-Etienne, *Chem.–Eur. J.* **2011**, *17*, 3011-3020.
- [33] F. Anke, D. Han, M. Klahn, A. Spannenberg, T. Beweries, *Dalton Trans.* **2017**, *46*, 6843-6847.
- [34] J. Spielmann, D. Piesik, B. Wittkamp, G. Jansen, S. Harder, *Chem. Commun.* **2009**, 3455-3456.
- [35] M. S. Hill, G. Kociok-Kohn, T. P. Robinson, *Chem. Commun.* **2010**, *46*, 7587-7589.
- [36] (a) S. Harder, J. Spielmann, *Chem. Commun.* **2011**, *47*, 11945-11947. (b) H. J. Cowley, M. S. Holt, R. L. Melen, J. M. Rawson, D. S. Wright, *Chem. Commun.* **2011**, *47*, 2682-2684. (c) D. J. Liptrot, M. S. Hill, M. F. Mahon, D. J. MacDougall, *Chem.–Eur. J.* **2010**, *16*, 8508-8515. (d) J. Spielmann, S. Harder, *J. Am. Chem. Soc.* **2009**, *131*, 5064-5065. (e) M. S. Hill, M. Hodgson, D. J. Liptrot, M. F. Mahon, *Dalton Trans.* **2011**, *40*, 7783-7790. (f) J. Spielmann, M. Bolte, S. Harder, *Chem. Commun.* **2009**, 6934-6936. (g) J. Spielmann, G. Jansen, H. Bandmann, S. Harder, *Angew. Chem.* **2008**, *120*, 6386-6391. (h) M. M. Hansmann, R. L. Melen, D. S. Wright, *Chem. Sci.* **2011**, *2*, 1554-1559.
- [37] J. Spielmann, D. F. J. Piesik, S. Harder, *Chem. Eur. J.* **2010**, *16*, 8307-8318.
- [38] R. J. Less, S. Hanf, R. García-Rodríguez, A. D. Bond, D. S. Wright, *Organometallics* **2017**.
- [39] K. A. Erickson, D. S. Wright, R. Waterman, *J. Organomet. Chem.* **2014**, *751*, 541-545.
- [40] E. Lu, Y. Yuan, Y. Chen, W. Xia, *ACS Catal.* **2013**, *3*, 521-524.
- [41] P. Cui, T. P. Spaniol, L. Maron, J. Okuda, *Chem.–Eur. J.* **2013**, *19*, 13437-13444.
- [42] K. A. Erickson, J. L. Kiplinger, *ACS Catal.* **2017**, *7*, 4276-4280.
- [43] (a) T. J. Clark, C. A. Russell, I. Manners, *J. Am. Chem. Soc.* **2006**, *128*, 9582-9583. (b) J. Y. Corey, J. L. Huhmann, X. H. Zhu, *Organometallics* **1993**, *12*, 1121-1130.
- [44] M. E. Sloan, A. Staubitz, T. J. Clark, C. A. Russell, G. C. Lloyd-Jones, I. Manners, *J. Am. Chem. Soc.* **2010**, *132*, 3831-3841.
- [45] D. Pun, E. Lobkovsky, P. J. Chirik, *Chem. Commun.* **2010**, 3297-3299.
- [46] L. J. Sewell, G. C. Lloyd-Jones, A. S. Weller, *J. Am. Chem. Soc.* **2012**, *134*, 3598-3610.
- [47] U. Rosenthal, V. V. Burlakov, P. Arndt, W. Baumann, A. Spannenberg, *Organometallics* **2003**, *22*, 884-900.
- [48] (a) T. Beweries, S. Hansen, M. Kessler, M. Klahn, U. Rosenthal, *Dalton Trans.* **2011**, *40*, 7689-7692. (b) T. Beweries, J. Thomas, M. Klahn, A. Schulz, D. Heller, U. Rosenthal, *ChemCatChem* **2011**, *3*, 1865-1868.
- [49] Y. Luo, K. Ohno, *Organometallics* **2007**, *26*, 3597-3600.
- [50] A. M. Chapman, M. F. Haddow, D. F. Wass, *J. Am. Chem. Soc.* **2011**, *133*, 8826-8829.
- [51] M. Klahn, D. Hollmann, A. Spannenberg, A. Bruckner, T. Beweries, *Dalton Trans.* **2015**, *44*, 12103-12111.
- [52] J. A. Buss, G. A. Edouard, C. Cheng, J. Shi, T. Agapie, *J. Am. Chem. Soc.* **2014**, *136*, 11272-11275.

- [53] R. T. Baker, J. C. Gordon, C. W. Hamilton, N. J. Henson, P.-H. Lin, S. Maguire, N. C. Smythe, *J. Am. Chem. Soc.* **2012**, *134*, 5598-5609.
- [54] Y. Kawano, M. Uruichi, M. Shimoi, S. Taki, T. Kawaguchi, T. Kakizawa, H. Ogino, *J. Am. Chem. Soc.* **2009**, *131*, 14946-14957.
- [55] M. Gediga, C. M. Feil, S. H. Schlindwein, J. Bender, M. Nieger, D. Gudat, *Chem.–Eur. J.* **2017**, *23*, 11560-11569.
- [56] H. R. Sharpe, A. M. Geer, T. J. Blundell, F. R. Hastings, M. W. Fay, G. A. Rance, D. L. Kays, *Catalysis Science & Technology* **2018**, *8*, 229-235.
- [57] J. R. Vance, A. P. M. Robertson, K. Lee, I. Manners, *Chem.–Eur. J.* **2011**, *17*, 4099-4103.
- [58] K. Taeko, K. Yasuro, N. Kohsuke, S. Mamoru, *Chem. Lett.* **2011**, *40*, 171-173.
- [59] Y. Kuninobu, Y. Tokunaga, A. Kawata, K. Takai, *J. Am. Chem. Soc.* **2006**, *128*, 202-209.
- [60] Y. Jiang, H. Berke, *Chem. Commun.* **2007**, 3571-3573.
- [61] Y. Jiang, O. Blacque, T. Fox, C. M. Frech, H. Berke, *Organometallics* **2009**, *28*, 5493-5504.
- [62] P. Bhattacharya, J. A. Krause, H. Guan, *J. Am. Chem. Soc.* **2014**, *136*, 11153-11161.
- [63] D. Han, T. Beweries, unpublished results.
- [64] R. J. Keaton, J. M. Blacquiere, R. T. Baker, *J. Am. Chem. Soc.* **2007**, *129*, 1844-1845.
- [65] H. A. Kalviri, F. Gartner, G. Ye, I. Korobkov, R. T. Baker, *Chem. Sci.* **2015**, *6*, 618-624.
- [66] A. Glüer, M. Förster, V. R. Celinski, J. Schmedt auf der Günne, M. C. Holthausen, S. Schneider, *ACS Catal.* **2015**, *5*, 7214-7217.
- [67] M. Käß, A. Friedrich, M. Drees, S. Schneider, *Angew. Chem., Int. Ed.* **2009**, *48*, 905-907.
- [68] D. Han, R. Knitsch, F. Anke, H. Jiao, M. R. Hansen, T. Beweries, manuscript in preparation.
- [69] R. Moury, U. B. Demirci, *Energies* **2015**, *8*, 3118-3141.
- [70] S. Chakraborty, H. Dai, P. Bhattacharya, N. T. Fairweather, M. S. Gibson, J. A. Krause, H. Guan, *J. Am. Chem. Soc.* **2014**, *136*, 7869-7872.
- [71] E. W. Abel, F. G. A. Stone, G. Wilkinson, *Comprehensive Organometallic Chemistry II: Heteronuclear metal-metal bonds*. Elsevier: 1995; Vol. 10.
- [72] J. F. Sonnenberg, R. H. Morris, *ACS Catal.* **2013**, *3*, 1092-1102.
- [73] (a) C. Sui-Seng, F. Freutel, A. J. Lough, R. H. Morris, *Angew. Chem.* **2008**, *120*, 954-957. (b) N. Meyer, A. J. Lough, R. H. Morris, *Chem.–Eur. J.* **2009**, *15*, 5605-5610. (c) N. Blacquiere, S. Diallo-Garcia, S. I. Gorelsky, D. A. Black, K. Fagnou, *J. Am. Chem. Soc.* **2008**, *130*, 14034-14035.
- [74] J. F. Sonnenberg, R. H. Morris, *Catalysis Science & Technology* **2014**, *4*, 3426-3438.
- [75] (a) A. M. Lunsford, J. H. Blank, S. Moncho, S. C. Haas, S. Muhammad, E. N. Brothers, A. A. Bengali, *Inorg. Chem.* **2016**, *22*, 964-973. (b) N. T. Coles, M. F. Mahon, R. L. Webster, *Organometallics* **2017**, *36*, 2262-2268. (c) C. Lichtenberg, L. Viciu, M. Adelhardt, J. Sutter, K. Meyer, B. de Bruin, H. Grützmacher, *Angew. Chem., Int. Ed.* **2015**, *54*, 5766-5771. (d) C. Lichtenberg, M. Adelhardt, T. L. Gianetti, K. Meyer, B. de Bruin, H. Grützmacher, *ACS Catal.* **2015**, *5*, 6230-6240.
- [76] A. Friedrich, M. Drees, S. Schneider, *Chem.–Eur. J.* **2009**, *15*, 10339-10342.
- [77] A. N. Marziale, A. Friedrich, I. Klopsch, M. Drees, V. R. Celinski, J. r. Schmedt auf der Günne, S. Schneider, *J. Am. Chem. Soc.* **2013**, *135*, 13342-13355.
- [78] S. Swinnen, V. S. Nguyen, M. T. Nguyen, *Chem. Phys. Lett.* **2011**, *513*, 195-200.

- [79] (a) R. Noyori, T. Ohkuma, *Angew. Chem., Int. Ed.* **2001**, *40*, 40-73. (b) S. E. Clapham, A. Hadzovic, R. H. Morris, *Coord. Chem. Rev.* **2004**, *248*, 2201-2237.
- [80] B. L. Conley, T. J. Williams, *Chem. Commun.* **2010**, *46*, 4815-4817.
- [81] Z. Lu, B. L. Conley, T. J. Williams, *Organometallics* **2012**, *31*, 6705-6714.
- [82] (a) J. S. M. Samec, A. H. Éll, J. B. Åberg, T. Privalov, L. Eriksson, J.-E. Bäckvall, *J. Am. Chem. Soc.* **2006**, *128*, 14293-14305. (b) C. P. Casey, T. B. Clark, I. A. Guzei, *J. Am. Chem. Soc.* **2007**, *129*, 11821-11827.
- [83] X. Zhang, Z. Lu, L. K. Foellmer, T. J. Williams, *Organometallics* **2015**, *34*, 3732-3738.
- [84] X. Zhang, L. Kam, R. Trerise, T. J. Williams, *Acc. Chem. Res.* **2017**, *50*, 86-95.
- [85] X. Zhang, L. Kam, T. J. Williams, *Dalton Trans.* **2016**, *45*, 7672-7677.
- [86] B. L. Conley, D. Guess, T. J. Williams, *J. Am. Chem. Soc.* **2011**, *133*, 14212-14215.
- [87] S. Bhunya, L. Roy, A. Paul, *ACS Catal.* **2016**, *6*, 4068-4080.
- [88] M. A. Esteruelas, A. M. Lopez, M. Mora, E. Onate, *Chem. Commun.* **2013**, *49*, 7543-7545.
- [89] M. A. Esteruelas, I. Fernández, A. M. López, M. Mora, E. Oñate, *Organometallics* **2014**, *33*, 1104-1107.
- [90] M. A. Esteruelas, A. M. López, M. Mora, E. Oñate, *ACS Catal.* **2015**, *5*, 187-191.
- [91] J. K. Pagano, J. P. W. Stelmach, R. Waterman, *Dalton Trans.* **2015**, *44*, 12074-12077.
- [92] T.-P. Lin, J. C. Peters, *J. Am. Chem. Soc.* **2013**, *135*, 15310-15313.
- [93] Y. Segawa, M. Yamashita, K. Nozaki, *J. Am. Chem. Soc.* **2009**, *131*, 9201-9203.
- [94] T. J. Hebden, A. J. St. John, D. G. Gusev, W. Kaminsky, K. I. Goldberg, D. M. Heinekey, *Angew. Chem., Int. Ed.* **2011**, *50*, 1873-1876.
- [95] G. Ganguly, T. Malakar, A. Paul, *ACS Catal.* **2015**, *5*, 2754-2769.
- [96] S. Todisco, L. Luconi, G. Giambastiani, A. Rossin, M. Peruzzini, I. E. Golub, E. S. Shubina, *Inorg. Chem.* **2017**, *56*, 4296-4307.
- [97] H. Dorn, R. A. Singh, J. A. Massey, J. M. Nelson, C. A. Jaska, A. J. Lough, I. Manners, *J. Am. Chem. Soc.* **2000**, *122*, 6669-6678.
- [98] C. A. Jaska, K. Temple, A. J. Lough, I. Manners, *J. Am. Chem. Soc.* **2003**, *125*, 9424-9434.
- [99] C. A. Jaska, I. Manners, *J. Am. Chem. Soc.* **2004**, *126*, 1334-1335.
- [100] H. C. Johnson, C. L. McMullin, S. D. Pike, S. A. Macgregor, A. S. Weller, *Angew. Chem., Int. Ed.* **2013**, *52*, 9776-9780.
- [101] H. C. Johnson, E. M. Leita, G. R. Whittell, I. Manners, G. C. Lloyd-Jones, A. S. Weller, *J. Am. Chem. Soc.* **2014**, *136*, 9078-9093.
- [102] V. Pons, R. T. Baker, N. K. Szymczak, D. J. Heldebrant, J. C. Linehan, M. H. Matus, D. A. Dixon, *Chem. Commun.* **2008**, 6597-6599.
- [103] (a) D. Pun, E. Lobkovsky, P. J. Chirik, *Chem. Commun.* **2007**, 3297-3299. (b) M. C. Denney, V. Pons, T. J. Hebden, D. M. Heinekey, K. I. Goldberg, *J. Am. Chem. Soc.* **2006**, *128*, 12048-12049.
- [104] T. M. Douglas, A. B. Chaplin, A. S. Weller, *J. Am. Chem. Soc.* **2008**, *130*, 14432-14433.
- [105] I. Göttker-Schnetmann, P. S. White, M. Brookhart, *Organometallics* **2004**, *23*, 1766-1776.
- [106] K. W. Böddeker, S. G. Shore, R. K. Bunting, *J. Am. Chem. Soc.* **1966**, *88*, 4396-4401.
- [107] A. Staubitz, A. Presa Soto, I. Manners, *Angew. Chem., Int. Ed.* **2008**, *47*, 6212-6215.
- [108] A. Paul, C. B. Musgrave, *Angew. Chem.* **2007**, *119*, 8301-8304.

- [109] (a) O. O. Kovalenko, O. F. Wendt, *Dalton Trans.* **2016**, 45, 15963-15969. (b) I. Göttker-Schnetmann, P. White, M. Brookhart, *J. Am. Chem. Soc.* **2004**, 126, 1804-1811.
- [110] T. J. Hebden, K. I. Goldberg, D. M. Heinekey, X. Zhang, T. J. Emge, A. S. Goldman, K. Krogh-Jespersen, *Inorg. Chem.* **2010**, 49, 1733-1742.
- [111] D. A. Resendiz-Lara, N. E. Stubbs, M. I. Arz, N. E. Pridmore, H. A. Sparkes, I. Manners, *Chem. Commun.* **2017**, 53, 11701-11704.
- [112] X. Yang, M. B. Hall, *J. Am. Chem. Soc.* **2008**, 130, 1798-1799.
- [113] (a) P. M. Zimmerman, A. Paul, Z. Zhang, C. B. Musgrave, *Angew. Chem., Int. Ed.* **2009**, 48, 2201-2205. (b) P. M. Zimmerman, A. Paul, C. B. Musgrave, *Inorg. Chem.* **2009**, 48, 5418-5433.
- [114] M. Vogt, B. de Bruin, H. Berke, M. Trincado, H. Grützmacher, *Chem. Sci.* **2011**, 2, 723-727.
- [115] T. Zweifel, J.-V. Naubron, T. Büttner, T. Ott, H. Grützmacher, *Angew. Chem., Int. Ed.* **2008**, 47, 3245-3249.
- [116] S.-K. Kim, W.-S. Han, T.-J. Kim, T.-Y. Kim, S. W. Nam, M. Mitoraj, S. O. Kang, *J. Am. Chem. Soc.* **2010**, 132, 9954-9955.
- [117] M. Roselló-Merino, J. López-Serrano, S. Conejero, *J. Am. Chem. Soc.* **2013**, 135, 10910-10913.
- [118] X. Hu, M. Soleilhavoup, M. Melaimi, J. Chu, G. Bertrand, *Angew. Chem., Int. Ed.* **2015**, 54, 6008-6011.
- [119] (a) G. D. Frey, V. Lavallo, B. Donnadieu, W. W. Schoeller, G. Bertrand, *Science* **2007**, 316, 439-441. (b) G. C. Welch, R. R. S. Juan, J. D. Masuda, D. W. Stephan, *Science* **2006**, 314, 1124-1126.
- [120] A. J. M. Miller, J. E. Bercaw, *Chem. Commun.* **2010**, 46, 1709-1711.
- [121] Z. Mo, A. Rit, J. Campos, E. L. Kolychev, S. Aldridge, *J. Am. Chem. Soc.* **2016**, 138, 3306-3309.
- [122] F. H. Stephens, R. T. Baker, M. H. Matus, D. J. Grant, D. A. Dixon, *Angew. Chem.* **2007**, 119, 760-763.
- [123] D. W. Himmelberger, C. W. Yoon, M. E. Bluhm, P. J. Carroll, L. G. Sneddon, *J. Am. Chem. Soc.* **2009**, 131, 14101-14110.

5. List of publications

The following chapter contains the original papers in which the presented results were published. The own contribution of author of the dissertation to each publication is highlighted separately.

In paper 5.1, the work I undertook is carrying out all experiments and taking part in analyzing catalytic system. In addition, the major part of the manuscript corresponding to the paper was written by me.

In paper 5.2, the work I undertook is synthesizing a part of catalysts for co-workers and taking part in analyzing the catalytic system.

In paper 5.3, the work I undertook is carrying out most part of experiments. In addition, the major part of the manuscript corresponding to the paper was written by me.

In paper 5.4, the work I did is carrying out most part of experiments and taking part in analyzing the catalytic system. In addition, the catalysis part of the manuscript corresponding to the paper was written by me.

5.1. Iridium(III) hydrido complexes for the catalytic dehydrogenation of hydrazine borane

D. Han, M. Joksch, M. Klahn, A. Spannenberg, H.-J. Drexler, W. Baumann, H. Jiao, R. Knitsch, M. R. Hansen, H. Eckert and T. Beweries

Dalton transaction, **2016**, 45, 17697.

DOI: 10.1039/c6dt03068h

© 2017 Royal Society of Chemistry 2017

Contribution to this paper is 70%.

PAPER

View Article Online

View Journal | View Issue



Cite this: *Dalton Trans.*, 2016, **45**, 17697

Received 2nd August 2016,
Accepted 11th October 2016

DOI: 10.1039/c6dt03068h

www.rsc.org/dalton

Iridium(III) hydrido complexes for the catalytic dehydrogenation of hydrazine borane†

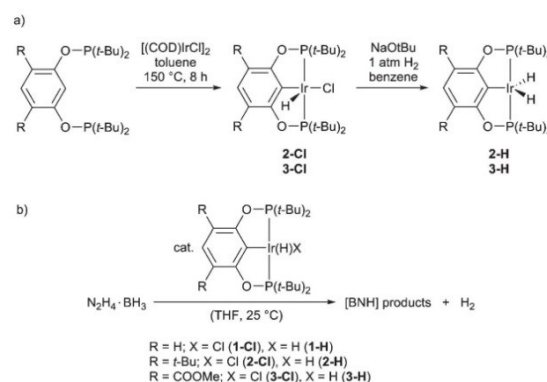
D. Han,^a M. Jokschi,^a M. Klahn,^a A. Spannenberg,^a H.-J. Drexler,^a W. Baumann,^a H. Jiao,^a R. Knitsch,^b M. R. Hansen,^b H. Eckert^{b,c} and T. Beweries^{*a}

The synthesis of 3,5-disubstituted cyclometalated iridium(III) hydrido complexes of the type [3,5-R₂(POCOP)IrHX] (3,5-R₂(POCOP) = κ^3 -C₅HR₂-2,6-(OPtBu₂)₂ with R = *t*-Bu, COOMe; X = Cl, H) is described. All complexes were investigated in the catalytic dehydrogenation of hydrazine borane and compared with the unsubstituted compounds [(POCOP)IrHX] (X = Cl, H). All catalysts are highly active and recyclable, clearly maintaining hydrogen production activity. The dehydrogenation products were structurally characterised by solid state NMR and FTIR spectroscopy. Experimental observations were complemented by a dispersion-corrected DFT study to rationalise the mechanism of hydrazine borane dehydrogenation.

Introduction

One of the most important challenges in order to establish hydrogen as a viable alternative for commonly used fossil fuels in mobile and stationary applications is the storage of the energy carrier itself.¹ Major concerns are related to its physical properties that complicate safe, efficient and economical storage. Of the known H₂ storage methods chemical hydrides show the highest gravimetric storage capacities.² Among these, amine borane adducts such as ammonia borane (AB, 19.6 wt% H₂ capacity) were widely investigated in the past and a plethora of examples of its catalytic dehydrogenation were described.³ One of the most prominent reports was published by Heinekey and Goldberg, who used an Ir pincer complex [(POCOP)IrH₂] (POCOP = κ^3 -C₆H₃-2,6-(OPtBu₂)₂) for the catalytic dehydrogenation of AB.⁴ Later, this complex was also used for the dehydropolymerisation of primary amine boranes.⁵ The structurally similar compound hydrazine borane (HB), also shows a well-balanced ratio of protic and hydridic H atoms, making it a promising candidate for the storage of a substantial amount of H₂ (15.4 wt% H₂ capacity). Compared to the hydrazine (bis)borane, which is reported to be

explosive when being rapidly heated and at *T* > 160 °C,⁶ HB can be conveniently handled in a wide temperature range in solid state and in solution.⁷ As pointed out in a recent review,⁸ apart from several examples for the thermolysis⁶ and hydrolysis,⁹ only one example for the homogeneous catalytic release of H₂ has been reported to date. Based on our previous experiences in dimethylamine borane chemistry,¹⁰ our group has recently demonstrated the full catalytic dehydrogenation of HB using a variety of group 4 metallocene alkyne and hydrido complexes.¹¹ These reactions required several days for completion, however, this was the first example for transition metal complex catalysed dehydrogenation of HB. In this contribution, we present a study of the release of H₂ from HB using Brookhart's well-described catalysts [(POCOP)IrHX] (X = Cl, H)¹² (1-Cl, 1-H) as well as substituted complexes of the type [3,5-R₂(POCOP)IrHX] with R = *t*-Bu (2-Cl, 2-H) and R = COOMe (3-Cl, 3-H) (Scheme 1).



Scheme 1 (a) Synthesis of 3,5-disubstituted [(POCOP)Ir] hydrido complexes. (b) Ir(III) hydrido complex catalysed dehydrogenation of HB.

^aLeibniz-Institut für Katalyse an der Universität Rostock e.V., Albert-Einstein-Str. 29a, 18059 Rostock, Germany. E-mail: torsten.beweries@catalysis.de

^bWestfälische Wilhelms-Universität Münster, Institut für Physikalische Chemie, Corrensstr. 28/30, 48149 Münster, Germany

^cInstitute of Physics Sao Carlos, University of Sao Paulo, Sao Carlos, SP 13560-590, Brazil

†Electronic supplementary information (ESI) available: Experimental and crystallographic details, NMR and MS of Ir complexes, characterization of the dehydrogenated material and full volumetric data. CCDC 1431007–1431009 and 1454019. For ESI and crystallographic data in CIF or other electronic format see DOI: 10.1039/c6dt03068h

Results and discussion

Catalytic dehydrogenation of HB

Upon addition of the catalyst to HB in THF under an atmosphere of Ar at room temperature, vigorous evolution of gas was observed. Simultaneously, the intense red colour of the Ir hydrido complexes slowly faded to pale yellow and a white solid precipitated. The progress of the reaction was monitored by volumetric analysis, indicating that both complexes **1-Cl** and **1-H** catalyse the release of approximately 1 equiv. of H_2 per molecule HB (Fig. 1). This is of special importance as full dehydrogenation of HB would produce a thermodynamically very stable BN species. For a potential application of HB in closed dehydrogenation/hydrogenation cycles this would be of significant disadvantage. For a catalyst loading of 5 mol% and an HB concentration of 0.11 M full conversion was obtained after 200 (**1-H**) and 300 min (**1-Cl**), respectively. Notably, in runs with lower catalyst concentrations, full conversion could not be reached (Fig. S14 and S15†). This is in contrast to our previous study of group 4 metallocene catalysed decomposition of HB, where full dehydrogenation and N_2 release was observed. In the present case H_2 was the only gaseous product formed as evidenced by TCD-GC (Fig. S28†). To investigate the possibility of catalyst recycling, we separated the catalyst solution from the insoluble white residue and subsequently transferred this to a freshly prepared solution of HB. Monitoring the gas evolution revealed that both catalysts remain active after removal from the reaction mixture (Fig. 2).

NMR spectra recorded from the filtrate after every catalytic run indicated the presence of a single Ir species (Fig. S7†) which did not undergo any changes during recycling. The exact nature of this compound could not be identified unequivocally at this stage, however, irrespective of using **1-Cl** or **1-H** the same 1H and ^{31}P NMR resonances were observed, whereas no signals were found in ^{11}B NMR spectra. The most prominent feature of 1H NMR spectra is the hydride resonance which is found as a triplet at -9.28 ppm ($^2J_{PH} = 16.1$ Hz), indicating the presence of a symmetric $[(POCOP)Ir]$ hydrido environment. Also, two characteristic isolated resonances at

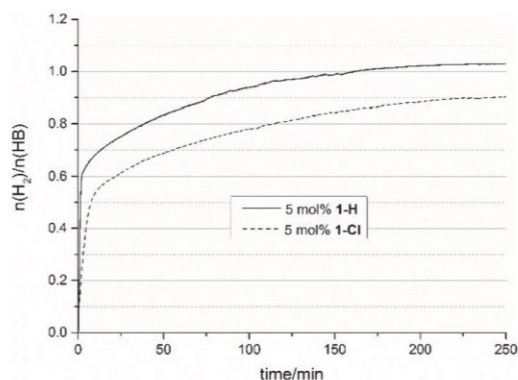


Fig. 1 Volumetric curves for HB dehydrogenation with complexes **1-Cl** and **1-H**.

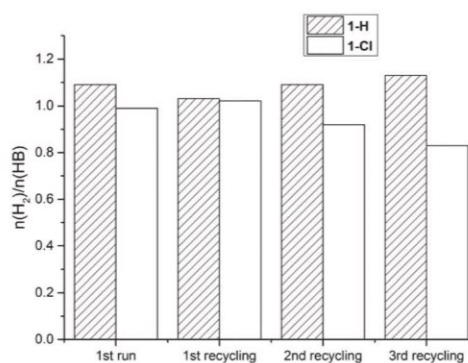


Fig. 2 Summary of volumetric data obtained from HB dehydrogenation recycling experiments with **1-Cl** and **1-H**. Note that for each run, a fresh 50 mg portion of HB was added (THF, $T = 25$ °C, initial Ir concentration $c = 5$ mol%).

3.90 and 5.07 ppm with an intensity ratio of 2 : 2 referring to two hydrides could correspond to a coordinated N_2H_4 unit. CI-MS analysis of the Ir containing residue gave a peak at m/z 591 with the expected isotopic pattern for the species $[(POCOP)IrH]$ as well as a signal at m/z 626 which could correspond to the fragment $[(POCOP)Ir(N_2H_4)_2 + 2H]$ (Fig. S10†). Reaction monitoring by NMR spectroscopy at reaction conditions (*i.e.* at $T = 298$ K) using **1-H** or **1-Cl** showed the presence of the aforementioned Ir hydrido species (1H : $\delta = -9.28$, ^{31}P : 169.2 ppm) throughout the HB dehydrogenation reaction. Intermediates for the formation of this species from the starting complexes **1-Cl** and **1-H** were not observed, indicating that this conversion is too fast to be observable on the NMR time-scale at room temperature. The formation of an Ir dihydrido BH_3 adduct, which should correspond to the inactive form of the catalyst, as it was reported before for the dehydrogenation of AB, was not observed.⁴ This is in line with the found recyclability of the catalysts. We thus repeated the *in situ* experiment starting at $T = 194$ K with slow warming to room temperature and found that immediately upon mixing complex **1-H** and HB formation of the formal tetrahydrido complex $[(POCOP)IrH_4]$ ($\delta = -8.71$ ppm)¹³ takes place (Fig. 3).

This species is directly converted into the aforementioned new hydrido complex that resonates at -9.28 ppm. Also in this case, no further intermediates pointing towards HB activation by BH coordination were observed. In line with this, $^{11}B\{^1H\}$ NMR spectra show solely the decay of the HB resonance. Formation of free hydrazine is observed ($\delta = 2.96$ ppm), thus suggesting a more complex dehydrogenation pathway as seen before for other amine borane adducts.

Synthesis and application of 3,5-disubstituted (POCOP)Ir hydrido complexes

In order to further explore the scope of this reaction and to shed light on the role of the substitution pattern at the POCOP ligand, we aimed at the synthesis of different compounds having ligands with either electron donating or withdrawing character. The electronic and steric influence of modifications

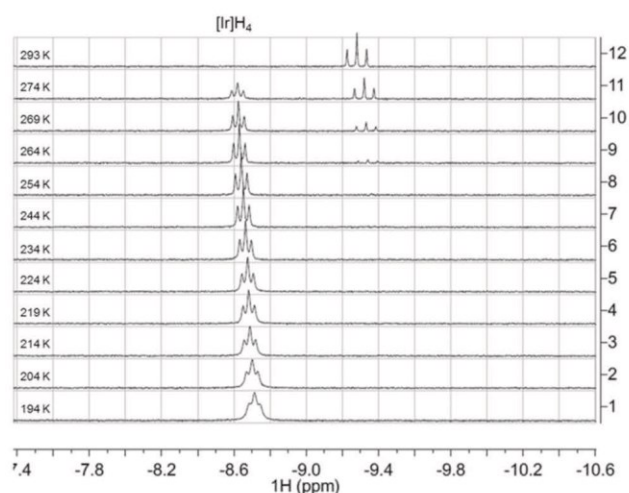


Fig. 3 Hydride region of the VT-*in situ* ^1H NMR spectra of HB dehydrogenation with complex **1-H** in $\text{THF-}d_8$ (300 MHz, $c(\text{1-H}) = 1.4 \times 10^{-6} \text{ mol l}^{-1}$, $c(\text{HB}) = 2.7 \times 10^{-5} \text{ mol l}^{-1}$).

at the POCOP ligand framework was discussed before¹⁴ and Ir complexes of this type were described on various occasions as common tools in dehydrogenation chemistry.¹⁵ Waterman reported on the influence of introduction of COOMe and NMe_2 groups in the 4-position of the POCOP ligand on the catalytic performance of Ir chloro-hydrido compounds in silane dehydrocoupling and redistribution.¹⁶ Examples for Ir hydrido complexes with 3,5-substituted POCOP ligands were published before by Driess and Hartwig, who also prepared compound **2-Cl**.¹⁷

The preparation of 3,5-disubstituted Ir hydrido complexes was possible using a procedure established by Brookhart and co-workers (Scheme 1).¹² Starting from the resorcinol, the substituted POCOP ligands were obtained after deprotonation and reaction with $t\text{-Bu}_2\text{P-Cl}$ in good yields.¹⁸ Addition of $[(\text{COD})\text{IrCl}]_2$ and heating in toluene at 150 °C furnished the corresponding chloro-hydrido complexes **2-Cl** and **3-Cl**. Typical spectroscopic features include the upfield hydride resonance at -41.60 (**2-Cl**) and -40.59 ppm (**3-Cl**) as well as the ^{31}P NMR signal at 176.6 (**2-Cl**) and 181.5 ppm (**3-Cl**) and are in line with data for the unsubstituted complex **1-Cl**.^{12b} Reaction of these complexes with H_2 in the presence of NaOtBu yields dihydrido complexes which show well-precedented resonances for the hydrido ligands (^1H : **2-H**: -18.1 ; **3-H**: -17.3 ppm) and for the P donor atoms (^{31}P : **2-H**: 206.5; **3-H**: 210.6 ppm). Single crystals suitable for an X-ray analysis were obtained from **3-Cl** and **2-H** by slow evaporation of THF and pentane, respectively. The molecular structure of **3-Cl** (Fig. 6) shows the five-coordinate Ir centre with the hydrido ligand in the apical position of a square-pyramidal arrangement. Notably, the hydrido ligand is slightly tilted towards the POCOP ligand (C1-Ir1-H1 $79.3(18)^\circ$), a phenomenon that is also observed in structurally similar Rh(III) and Ir(III) hydrido chlorido pincer complexes.¹⁹ In **2-H** (Fig. 4), the metal centre adopts a distorted trigonal

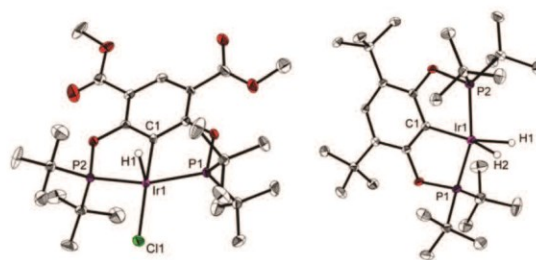


Fig. 4 Left: Molecular structure of complex **3-Cl**. Thermal ellipsoids correspond to 30% probability at 150 K. Hydrogen atoms except H1 and the second position of the methyl carbon atom of the disordered COOMe group are omitted for clarity. Right: Molecular structure of complex **2-H**. Thermal ellipsoids correspond to 30% probability at 150 K. Hydrogen atoms except H1 and H2 are omitted for clarity.

bipyramidal coordination geometry with Ir–H bond distances of 1.59 Å.

Dehydrogenation of HB under similar conditions as before using complexes **1-Cl** and **1-H** showed that **2-Cl** and **2-H** display similar activities for H_2 release. To our surprise, COOMe substituted complexes **3-Cl** and **3-H** significantly outperformed all other complexes, giving approximately 1 equiv. of H_2 after very short reaction times of (e.g. full conversion after 28 s (**3-Cl**) and 18 s (**3-H**) using 2 mol% catalyst). A comparison of volumetric data is shown in Fig. 5.²⁰

An explanation of the higher activity of COOMe substituted complexes based on spectroscopic features is difficult as reactions are much too fast for NMR observation. Also, binding

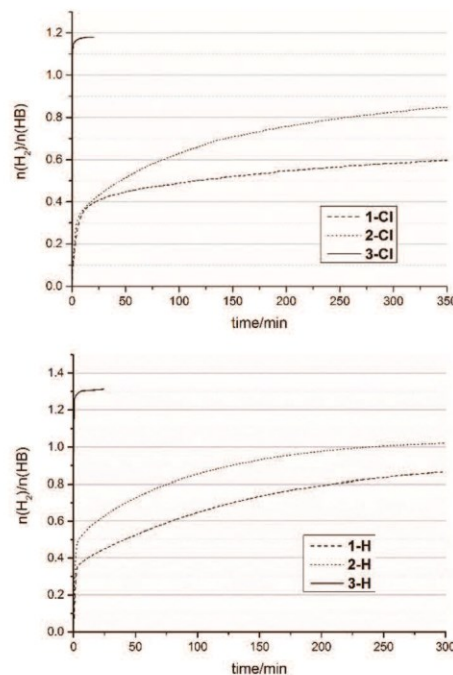


Fig. 5 Volumetric data of HB dehydrogenation using complexes **1-Cl**, **2-Cl**, and **3-Cl** (top) as well as **1-H**, **2-H**, and **3-H** (bottom) (THF , $T = 25^\circ\text{C}$, $c = 2 \text{ mol}\%$).

parameters of the dihydrido moiety determined by deuterium labelling^{21,22} do not point towards significant differences in the nature of the hydrido ligands in the series **1-H**/**2-H**/**3-H**. However, some NMR properties of dihydrido and chlorohydrido complexes differ considerably (see ESI†).

Recycling experiments showed that also *t*Bu and COOMe substituted catalysts are reusable without loss of overall H₂ production activity (Fig. S24 and S25†). However, similarly as observed for compounds **1-Cl** and **1-H**, initial activities are lower, thus giving longer reaction times for the release of 1 equiv. of H₂. To rationalise this behaviour, we investigated the soluble fraction of the reaction mixture. ¹H and ³¹P NMR analysis of the filtered solution after every HB dehydrogenation experiment showed that all spectra show identical spectroscopic features, *i.e.* similar values for δ_{hydride} and J_{PH} as well as the aforementioned characteristic resonances of equal intensity that could be assigned to a N₂H₄ fragment (Fig. S8 and S9†). Fortunately, we were able to isolate single crystals suitable for an X-ray analysis from the THF mother liquor of the dehydrogenation reaction using **3-H**. The molecular structure of the isolated Ir complex **4** shows the metal coordinated by the POCOP ligand, two hydrido ligands and N₂H₄ in an octahedral geometry (Fig. 6). NMR analysis of these crystals shows the aforementioned spectroscopic features, which clearly point to the presence of complex **4** and its analogues as the catalyst's resting state after each dehydrogenation experiment (*cf.* Fig. 3).

The Ir1–N1 bond length of 2.169(3) Å indicates the presence of a dative amine ligand and is slightly shorter than the values found in the only mononuclear Ir–N₂H₄ complex [Ir(pyb)₂(N₂H₄)₂] (2.192(6) and 2.213(5) Å).²³ Additionally, the presence of coordinated N₂H₄ is corroborated by the N1–N2 bond length of 1.447(5) Å, which is slightly longer than the sum of the covalent radii ($\sum r_{\text{cov}} = 1.42$ Å²⁴) but well in line with distances found in the above mentioned complex.²³

Analysis of the dehydrogenation residue

A catalytic dehydrogenation with hydrogen abstraction from NH and BH would theoretically yield a B/N atomic ratio of 1:2. However, elemental analysis of the insoluble white residue formed upon HB dehydrogenation with **1-Cl** and **1-H**

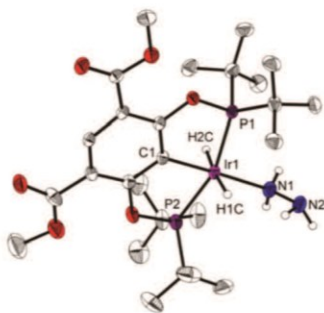


Fig. 6 Molecular structure of complex **4**. Thermal ellipsoids correspond to 30% probability at 150 K. Hydrogen atoms except H1C, H2C and hydrazine-bound are omitted for clarity.

revealed B/N atomic ratios of approximately 1:1.3, which indicates the presence of more than one dehydrogenation pathway. The ¹¹B magic angle spinning (MAS) NMR spectra of these materials are essentially identical and show three intense resonances at isotropic chemical shifts of +18, +1 and –7 ppm vs. BF₃·Et₂O solution (see Fig. 7b). By comparison with analogous experiments based on different catalyst to substrate ratios (see ESI†) a fourth resonance with a chemical shift near to –3 ppm was identified. As shown in Fig. 7a significantly enhanced resolution is available in the 2D ¹¹B triple-quantum (TQ)-MAS NMR spectrum from which the relevant NMR interaction parameters have been extracted (see Table S2†).

The signal at an isotropic chemical shift of +18 ppm shows the characteristic line shape for three-coordinated B compounds. This line shape is caused by second-order quadrupolar perturbations arising from the interaction of the ¹¹B nuclear electric quadrupole moment and the substantial electric field gradient generated by the electronic charge distribution around the three-coordinated B atoms. Furthermore, the line shape indicates that this quadrupole coupling tensor has axial symmetry, consistent with a trigonal-planar BN₃ environment. The ¹¹B chemical shifts for the signals at +1, –3 and –7 ppm are consistent with four-coordinate B centres. For

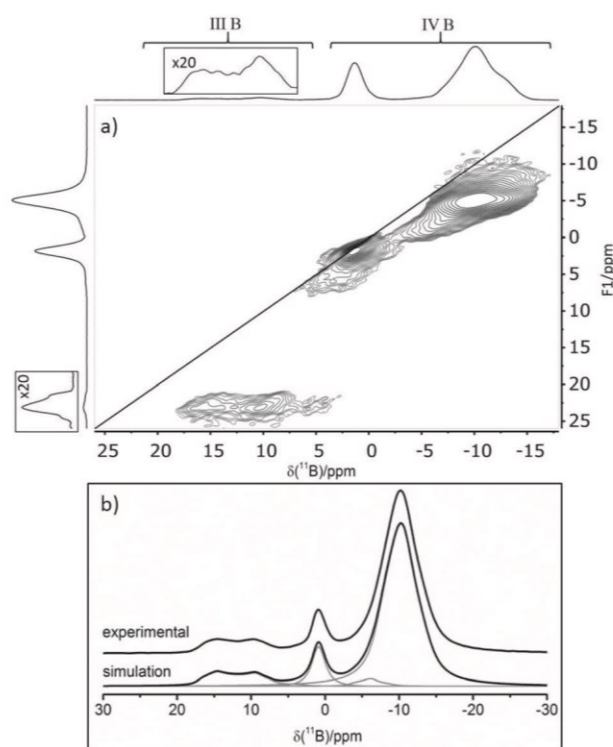


Fig. 7 Solid-state NMR spectra of the dehydrogenation reaction product obtained with **1-H** as the catalyst (*c* = 2 mol%) recorded at a field strength of 11.7 T under ¹H high power decoupling. (a) 2D ¹¹B TQ-MAS NMR spectrum recorded at a spinning speed of 29 762 Hz, showing the different ¹¹B species as indicated. (b) Experimental ¹¹B MAS NMR spectrum recorded at a spinning speed of 10 000 Hz and the corresponding simulation based on the NMR interaction parameters obtained from the 2D ¹¹B TQ-MAS experiment in (a), see Table S2.†

the 1 ppm resonance, no second-order quadrupolar induced line shape is observed because the local electronic environments of this four-fold B species are more symmetrical. In contrast, the -7 ppm peak shows clear evidence of a second-order quadrupolar effect, causing a signal displacement towards lower frequencies. This indicates a four-coordinated boron species in a less symmetric environment. Solid-state ^{11}B MAS NMR spectra similar to those shown in Fig. 7 have been observed for various BN pre-ceramics²⁵ and for thermal dehydrogenation products of HB.²⁶ On the other hand, the spectrum in Fig. 7b differs substantially from that of the BH_3N local environment observed in the molecular HB adduct.²⁶ Therefore, we can confidently exclude the presence of such species in our samples.

^1H - ^{11}B cross polarization experiments and $^{11}\text{B}\{^1\text{H}\}$ rotational echo double resonance (REDOR) experiments (Fig. 8) show that the four-coordinate B species interact strongly with ^1H nuclei, whereas the three-coordinated BN_3 units show relatively little interaction with protons. For the B species at the chemical shifts of -7 and -3 ppm the extremely strong REDOR effect signifies B species with B-H bonds. In

comparison with reference data on AB systems, we tentatively assign the isotropic shifts of -7 ppm and -3 ppm to a BH_2N_2 and a BHN_3 species, respectively.²⁷ Moreover, the much smaller magnitude of the REDOR effect observed for the ^{11}B resonance at 1 ppm is consistent with a four-coordinated B-N-H motif. Simulations of the observed REDOR curves suggest a minimum B-H internuclear distance of 2.0 \AA for this particular species, whereas the estimated minimum B-H distance for the trigonal B species at 18 ppm is 2.5 \AA .

^1H MAS NMR studies (Fig. S11†) reveal two sharp resonances at 1.5 and 4.0 ppm. Furthermore, a shoulder that corresponds to a significantly broader ^1H signal at 3.5 ppm can be observed. $^1\text{H}\{^{11}\text{B}\}$ REAPDOR experiments show a pronounced signal decrease for the latter resonance, consistent with a H-B bonding motif. In contrast, the ^1H signals at 1.5 and 4.0 ppm reveal a much weaker dipolar coupling with ^{11}B nuclei. This observation is also manifested in a 2D $^{11}\text{B}\{^1\text{H}\}$ cross-polarisation heteronuclear correlation (CP-HETCOR) experiment (Fig. S12†), where the ^{11}B signal at 18 ppm includes no correlation with any of the protons. However, the ^1H signal at 4.0 ppm does show a selective correlation with the ^{11}B species at 1 ppm, consistent with its assignment to a B-N-H environment. We note that, in this experiment, the proton resonance at 3.5 ppm shows a strong correlation to the overlapping ^{11}B signals at -3 and -7 ppm. All of the solid state NMR studies discussed above are fully consistent and indicate the presence of four-coordinate B-H and B-N-H species as well as three-coordinated BN_3 units in the dehydrogenated material. Further information on the structure of the dehydrogenated material might be accessible using ^{15}N labelled HB, the synthesis of this starting material is however more challenging. The results of further studies will be presented in due course.

The IR spectrum of the dehydrogenated material (Fig. S16†) shows an isolated sharp band at 3220 cm^{-1} , indicating the presence of NH fragments in a most likely polymeric environment.²⁵ This was observed before by Sneddon for poly(borazylene) structures.²⁸ In addition, a weak band is found for the asymmetric NH bend (1605 cm^{-1}). A band for the NN stretch could not be observed unequivocally. A broad band with a shoulder was observed at $2300\text{--}2450 \text{ cm}^{-1}$, thus pointing towards a material containing BH and most likely BH_2 groups. Note that the IR spectrum, especially the NH stretch region, is slightly different than seen before for similar material obtained from group 4 metallocene catalysed dehydrogenation, thus corroborating the different nature of H_2 release from these systems.

Computational analysis and mechanistic considerations

To get insight into the dehydrogenation reaction and the coordination chemistry of catalyst **1-H** we carried out detailed B3PW91 density functional theory computations including van der Waals dispersion correction (D3) as well as solvation effect of THF. In our discussion we used the computed Gibbs free energy at 298 K and one atmosphere including both effects. For comparison we also discussed the results without dis-

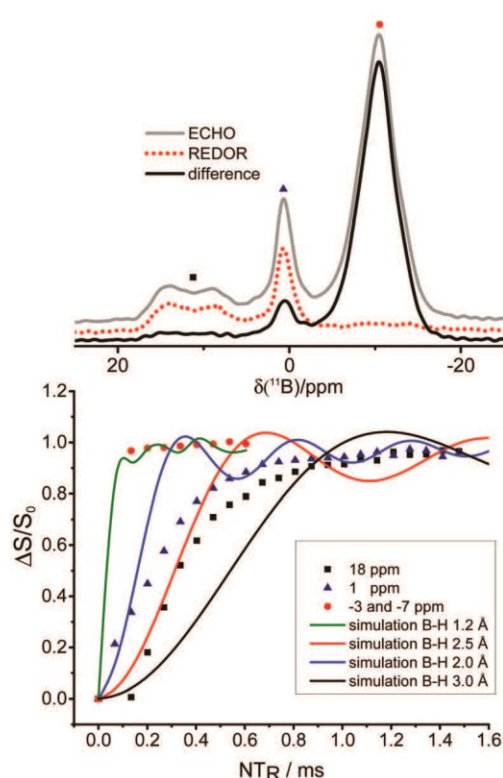
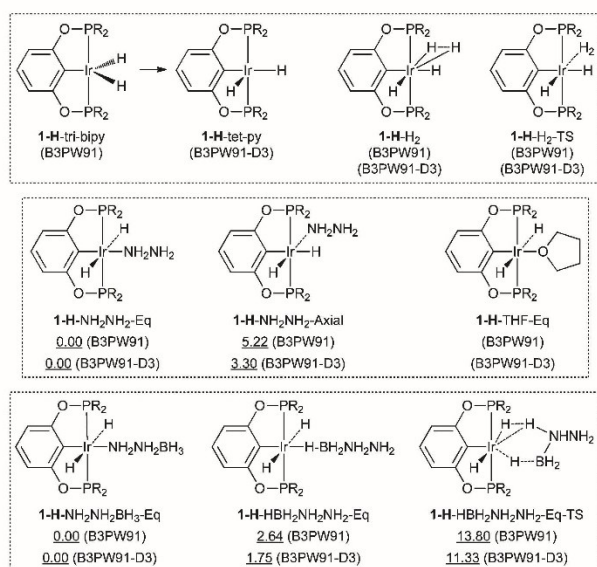


Fig. 8 $^{11}\text{B}\{^1\text{H}\}$ REDOR data recorded at 11.7 T ($\nu_{\text{L}}(^{11}\text{B}) = 160.4 \text{ MHz}$) on the dehydrogenated reaction product obtained with **1-H** as the catalyst ($c = 2 \text{ mol\%}$). Top: Stack plot of the rotor-synchronised spin echo spectrum (dotted red) and the ^1H recoupled spectrum (grey) at a dipolar evolution time of $134.4 \mu\text{s}$. The difference spectrum (black) only includes B species with spatial proximity to ^1H . Bottom: Plot of the REDOR difference signal $\Delta S/S_0$ against the dipolar evolution time $N\tau_{\text{R}}$ for the three intense B species (see Fig. 4b). Two-spin simulations with selected B-H distances as listed in the inset are included.



Scheme 2 Coordination geometries and energies (kcal mol⁻¹) of H₂, N₂H₄, THF and N₂H₄BH₃ with 1-H as well as the transition states for H₂ dissociation and HB dehydrogenation.

persion correction. All computational details are given in the ESI.†

At first we computed the electronic structure of 1-H. Without dispersion correction (B3PW91), 1-H has a trigonal bipyramidal geometry with both P-ligands in the axial positions as well as the hydrido and phenyl ligands in the equatorial plane (1-H-tri-bipy; Scheme 2). The H–H distance is 1.580 Å; and the H–Ir–C angles are 152.5 and 148.1° and the H–Ir–H angle is 59.4°.

Including dispersion correction (B3PW91-D3), however, the geometry of 1-H becomes tetragonal pyramidal with one H ligand in the axial direction (1-H-tet-py) and the H–H distance is 2.100 Å and the H–Ir–H angle is 82.2°. For checking their energy difference, we computed the energy of the B3PW91 optimized 1-H using B3PW91-D3. It is found that 1-H-tet-py is more stable than the 1-H-tri-bipy by 1.16 kcal mol⁻¹ in enthalpy (ΔH), while the latter becomes more stable than the former by 0.49 kcal mol⁻¹ in Gibbs free energy (ΔG); indicating the contribution of the entropy effect. Such very small energy differences might indicate their dynamic exchange between two geometries.

Having both geometries in hand, we computed the coordination of H₂ and hydrazine. For the H₂ complex, we obtained only one stable minimum structure 1-H-H₂; where the H–H distance of the H₂ ligand is 0.911 Å at B3PW91 and 0.904 Å at B3PW91-D3; and both show a H₂ molecular coordination; since they are only slightly longer than in free H₂ (0.745 and 0.746 Å, respectively); and this is in agreement with the experimental and computational studies for a dihydrido–dihydrogen complex [Ir(H₂)(H)₂]. Despite very similar geometries, B3PW91 shows that H₂ coordination is endergonic by 4.55 kcal mol⁻¹, indicating that 1-H-H₂ formation would be thermodynamically

not possible. While B3PW91-D3 shows that H₂ coordination is exergonic by 0.88 kcal mol⁻¹; indicating that 1-H-H₂ formation should be feasible thermodynamically. Compared with the experiment, B3PW91-D3 gives the reasonable results, *i.e.*; 1-H-H₂ is a stable complex; and under H₂ atmosphere 1-H and 1-H-H₂ can form a temperature dependent equilibrium in favour of 1-H-H₂ at lower temperature or 1-H at higher temperature. In addition, we computed the barrier of H₂ addition to 1-H or H₂ elimination for 1-H-H₂. The barrier heights of 13.49 and 14.37 kcal mol⁻¹ are in line with experiment carried out in toluene-*d*₈ in the temperature range from 23–100 °C. All of these calculations reveal the rapid interconversion of 1-H and 1-H-H₂ under H₂ atmosphere.

For hydrazine coordination, hydrazine can be either in the equatorial position *trans* to the phenyl ligand (1-H-N₂H₄-Eq) or axial position (1-H-N₂H₄-Axial). Without dispersion correction (B3PW91), the formation of 1-H-N₂H₄-Eq and 1-H-N₂H₄-Axial is endergonic by 6.20 and 11.43 kcal mol⁻¹, respectively, which shows that it would be not possible to form hydrazine complexes. Including dispersion correction (B3PW91-D3), however, the formation of 1-H-N₂H₄-Eq and 1-H-N₂H₄-Axial becomes exergonic by 4.71 and 1.41 kcal mol⁻¹, respectively, indicating that the formation of hydrazine complexes is thermodynamically possible. Furthermore, it also shows that 1-H-N₂H₄-Eq is more stable and favourable than 1-H-N₂H₄-Axial by 5.22 or 3.30 kcal mol⁻¹, without or with dispersion correction, respectively. The enhanced stability of 1-H-N₂H₄-Eq is in agreement with our experiment. In addition, we computed THF coordination, which is endergonic by 24.10 or 9.55 kcal mol⁻¹, without or with dispersion correction, respectively. This shows that THF does not affect the coordination and plays only the role of a solvent; and this is also in agreement with our experimental observation. All these results demonstrate that it is absolutely necessary to include dispersion correction for such iridium pincer complexes.

On the basis of these results we computed the energies and geometries of other intermediates involved in the catalytic dehydrogenation cycle of HB (NH₂NH₂BH₃), where we used only the more stable isomers with equatorial coordination and the less stable axial coordinated isomers are given in the ESI.†

As shown in Fig. 9, the equatorial coordination of hydrazine borane *via* the terminal nitrogen atom (1-H-N₂H₄BH₃-Eq) is

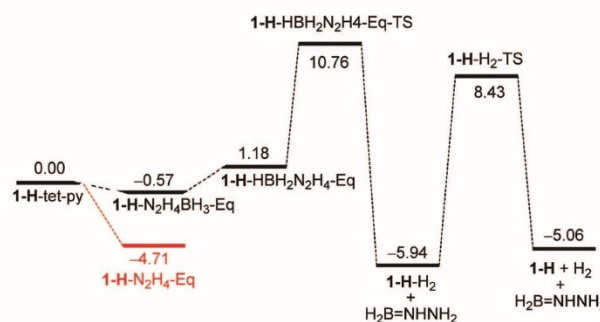
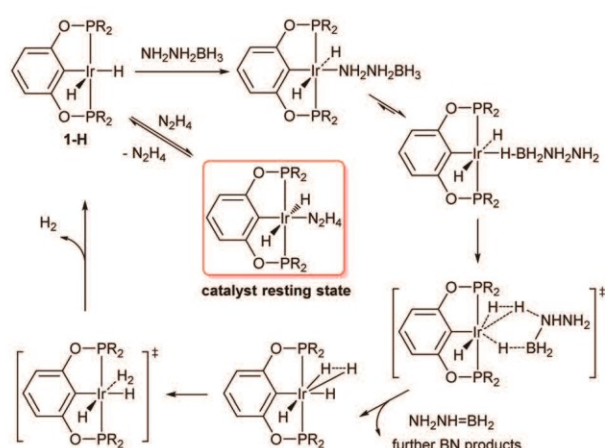


Fig. 9 Potential energy surface (kcal mol⁻¹) of 1-H catalysed N₂H₄BH₃ dehydrogenation.



Scheme 3 Proposed catalytic cycle for **1-H** catalysed HB dehydrogenation.

exergonic by $0.57 \text{ kcal mol}^{-1}$, while the coordination of the B–H bond (**1-H**– $\text{HBH}_2\text{N}_2\text{H}_4$ -Eq) is endergonic by $1.18 \text{ kcal mol}^{-1}$; and the former is more stable than the latter by $1.75 \text{ kcal mol}^{-1}$. On the basis of **1-H**– $\text{N}_2\text{H}_4\text{BH}_3$ -Eq, the dehydrogenation step has a barrier of $11.33 \text{ kcal mol}^{-1}$ and is exergonic by $5.37 \text{ kcal mol}^{-1}$. The second step is the dissociation of the coordinated H_2 ; which has a barrier of $14.37 \text{ kcal mol}^{-1}$, and is slightly endergonic by $0.88 \text{ kcal mol}^{-1}$.

On the basis of the potential energy surface, one can propose the cycle of **1-H** catalysed $\text{N}_2\text{H}_4\text{BH}_3$ dehydrogenation (Scheme 3). Starting from the active catalyst **1-H**-tet-py, the first step is HB complexation *via* either NH_2 or H-BH_2 coordination; and both coordination modes separated by $1.75 \text{ kcal mol}^{-1}$ can form an equilibrium. The second step is the dehydrogenation of HB resulting in the formation of the dihydrogen complex **1-H**– H_2 and $\text{H}_2\text{B=NHNH}_2$. The last step is H_2 dissociation and the regeneration of the active catalyst **1-H**-tet-py.

Without considering the coordination of hydrazine (Fig. 9), the H_2 dissociation step having higher barrier than the dehydrogenation step (14.37 vs. $11.33 \text{ kcal mol}^{-1}$) should be rate-determining. However, this situation can be changed by considering hydrazine coordination ($-4.71 \text{ kcal mol}^{-1}$), which is stronger than that of H_2 ($-0.88 \text{ kcal mol}^{-1}$) and HB ($-0.57 \text{ kcal mol}^{-1}$). Starting from the hydrazine complex, **1-H**– N_2H_4 -Eq, the effective barrier of the dehydrogenation becomes $15.41 \text{ kcal mol}^{-1}$, which is higher than that of the H_2 dissociation step ($14.37 \text{ kcal mol}^{-1}$). This indicates that hydrazine dissociation imposes an additional off-cycle pre-equilibrium. Such pre-equilibrium could shift the turn-over limiting step from H_2 dissociation to substrate dehydrogenation, as well as shift the rate law from zero order to first order in substrate. That might actually explain the abrupt slowing of the rate during catalysis as being associated with buildup of free hydrazine during the reaction. To verify this, we have added free hydrazine to the reaction mixture and found that dehydrogenation proceeds significantly slower (Fig. S27†).

In a recent mechanistic study of AB dehydrogenation using complex **1-H**, Paul and Musgrave have shown that dehydrogenation proceeds through a concerted proton/hydride abstraction from the substrate after initial B–H coordination to the Ir centre with the tetrahydrido complex being the most stable intermediate.²⁹ This is well in line with the experimental observation of this species as the major intermediate. However, our computations show different intermediates in structures and energies from those of Paul and Musgrave; in their study neither van der Waals dispersion correction (D3) nor solvation effect of THF were included. On the basis of the agreement between theory and experiment, it is very important to include dispersion correction for the interpretation of such dehydrogenation mechanisms.

Formation of the hydrazine complex and free hydrazine as well as the fact that in some cases slightly more than one equivalent of hydrogen are obtained suggests that a second, more complex dehydrogenation mechanism is operating. Also, (metal free) dehydrogenative coupling of the transient $[\text{H}_2\text{N-NH=BH}_2]$ as it was observed before by Manners and co-workers for amine borane dehydrocoupling³⁰ might explain the amount of hydrogen formed. Further studies to rationalise these observations are ongoing in our group, details will be published in due course.

Conclusions

We have reported the first highly active homogeneous catalysts for the dehydrogenation of the hydrogen storage material HB. The activity of the Ir hydrido complexes varies with the substitution pattern of the POCOP ligand with the COOMe substituted complexes **3-Cl** and **3-H** outperforming other complexes significantly. The dehydrogenated material contains four-coordinate B centres with different B–H and B–N–H proton environments, thus suggesting a three-dimensional, most likely polymeric structure. The presented system shows potential for the realisation of a closed HB based cycle for H_2 storage. Investigations on the regeneration of the spent fuel either by addition of hydrazine or by re-hydrogenation as well as on the dehydrogenation mechanism are ongoing in our group.

Acknowledgements

We thank our technical and analytical staff for support as well as Dr Kathleen Grabow (LIKAT) for acquisition of the vibrational spectra. D. H. thanks the China Scholarship Council (file No. 20150808083) for funding. T. B. thanks Prof. Uwe Rosenthal (LIKAT) for support. R. K. and H. E. acknowledge support by the Deutsche Forschungsgemeinschaft *via* programme SFB858.

Notes and references

- 1 J. Yang, A. Sudik, C. Wolverton and D. J. Siegel, *Chem. Soc. Rev.*, 2010, **39**, 656.

- 2 (a) C. W. Hamilton, R. T. Baker, A. Staubitz and I. Manners, *Chem. Soc. Rev.*, 2009, **38**, 279; (b) T. Hügler, M. Hartl and D. Lentz, *Chem. – Eur. J.*, 2011, **17**, 10184.
- 3 (a) A. Staubitz, A. P. M. Robertson and I. Manners, *Chem. Rev.*, 2010, **110**, 4079; (b) A. Staubitz, A. P. M. Robertson, M. E. Sloan and I. Manners, *Chem. Rev.*, 2010, **110**, 4023; (c) A. Rossin and M. Peruzzini, *Chem. Rev.*, 2016, **116**, 8848.
- 4 M. C. Denney, V. Pons, T. J. Hebdén, D. M. Heinekey and K. I. Goldberg, *J. Am. Chem. Soc.*, 2006, **128**, 12048.
- 5 (a) B. L. Dietrich, K. I. Goldberg, D. M. Heinekey, T. Autrey and J. C. Linehan, *Inorg. Chem.*, 2008, **47**, 8583; (b) A. Staubitz, A. Presa Soto and I. Manners, *Angew. Chem., Int. Ed.*, 2008, **47**, 6212; (c) A. Staubitz, M. E. Sloan, A. P. M. Robertson, A. Friedrich, S. Schneider, P. J. Gates, J. Schmedt auf der Günne and I. Manners, *J. Am. Chem. Soc.*, 2010, **132**, 13332.
- 6 T. Hügler, M. F. Kühnel and D. Lentz, *J. Am. Chem. Soc.*, 2009, **131**, 7444.
- 7 In previous reports, the decomposition products of HB were reported to be explosive: J. Goubeau and E. Ricker, *Z. Anorg. Allg. Chem.*, 1961, **310**, 123. We did not observe such a behavior in our studies.
- 8 R. Moury and U. B. Demirci, *Energies*, 2015, **8**, 3118.
- 9 (a) S. Karahan, M. Zahmakiran and S. Özkaz, *Int. J. Hydrogen Energy*, 2011, **36**, 4958; (b) J. Hannauer, O. Akdim, U. B. Demirci, C. Geantet, J.-M. Herrmann, P. Miele and Q. Xu, *Energy Environ. Sci.*, 2011, **4**, 3355; (c) D. Çelik, S. Karahan, M. Zahmakiran and S. Özkaz, *Int. J. Hydrogen Energy*, 2012, **37**, 5143; (d) Ç. Çakanyıldırım, U. B. Demirci, T. Şener, Q. Xu and P. Miele, *Int. J. Hydrogen Energy*, 2012, **37**, 9722; (e) D.-C. Zhong, K. Aranishi, A. K. Singh, U. B. Demirci and Q. Xu, *Chem. Commun.*, 2012, **48**, 11945; (f) S. Şencanlı, S. Karahan and S. Özkaz, *Int. J. Hydrogen Energy*, 2013, **38**, 14693; (g) Q.-L. Zhu, D.-C. Zhong, U. B. Demirci and Q. Xu, *ACS Catal.*, 2014, **4**, 4261; (h) D. Cléménçon, J. F. Petit, U. B. Demirci, Q. Xu and P. Miele, *J. Power Sources*, 2014, **260**, 77; (i) Z. Zhang, Z.-H. Lu, H. Tan, X. Chen and Q. Yao, *J. Mater. Chem. A*, 2015, **3**, 23520; (j) Z. Zhang, Z.-H. Lu and X. Chen, *ACS Sustainable Chem. Eng.*, 2015, **3**, 1255.
- 10 (a) T. Beweries, S. Hansen, M. Kessler, M. Klahn and U. Rosenthal, *Dalton Trans.*, 2011, **40**, 7689; (b) T. Beweries, J. Thomas, M. Klahn, A. Schulz, D. Heller and U. Rosenthal, *ChemCatChem*, 2011, **3**, 1865; (c) M. Klahn, D. Hollmann, A. Spannenberg, A. Brückner and T. Beweries, *Dalton Trans.*, 2015, **44**, 12103.
- 11 J. Thomas, M. Klahn, A. Spannenberg and T. Beweries, *Dalton Trans.*, 2013, **42**, 14668.
- 12 (a) I. Göttker-Schnetmann, P. White and M. Brookhart, *Organometallics*, 2004, **23**, 1766; (b) I. Göttker-Schnetmann, P. White and M. Brookhart, *J. Am. Chem. Soc.*, 2004, **126**, 1804.
- 13 T. J. Hebdén, K. I. Goldberg, D. M. Heinekey, X. Zhang, T. J. Emge, A. S. Goldman and K. Krogh-Jespersen, *Inorg. Chem.*, 2010, **49**, 1733.
- 14 J. M. Goldberg, G. W. Wong, K. E. Brastow, W. Kaminsky, K. I. Goldberg and D. M. Heinekey, *Organometallics*, 2015, **34**, 753.
- 15 J. Choi, A. H. R. MacArthur, M. Brookhart and A. S. Goldman, *Chem. Rev.*, 2011, **111**, 1761.
- 16 N. T. Mucha and R. Waterman, *Organometallics*, 2015, **34**, 3865.
- 17 A. Brück, D. Gallego, W. Wang, E. Irran, M. Driess and J. F. Hartwig, *Angew. Chem., Int. Ed.*, 2012, **51**, 11478.
- 18 Single crystals of the COOMe substituted ligand could be obtained by slow evaporation of an *n*-hexane solution. Crystallographic details can be found in the ESI.†
- 19 (a) H. Salem, L. J. W. Shimon, G. Leitius, L. Weiner and D. Milstein, *Organometallics*, 2008, **27**, 2293; (b) B. Punji, T. J. Emge and A. S. Goldman, *Organometallics*, 2010, **29**, 2702; (c) S. D. Timpa, C. M. Fafard, D. E. Herbert and O. V. Ozerov, *Dalton Trans.*, 2011, **40**, 5426.
- 20 For a detailed overview of all volumetric data, please see the ESI.†
- 21 I. Göttker-Schnetmann, D. M. Heinekey and M. Brookhart, *J. Am. Chem. Soc.*, 2006, **128**, 17114.
- 22 D. M. Heinekey, A. Lledos and J. M. Lluch, *Chem. Soc. Rev.*, 2004, **33**, 175.
- 23 K. R. Schwartz and K. R. Mann, *Inorg. Chem.*, 2011, **50**, 12477.
- 24 P. Pykkö and M. Atsumi, *Chem. – Eur. J.*, 2009, **15**, 12770.
- 25 (a) C. Gervais, E. Framery, D. Duriez, J. Maquet, M. Vaultier and F. Babonneau, *J. Eur. Ceram. Soc.*, 2005, **25**, 129; (b) C. Gervais and F. Babonneau, *J. Organomet. Chem.*, 2002, **657**, 75.
- 26 R. Moury, G. Moussa, U. B. Demirci, J. Hannauer, S. Bernard, E. Petit, A. van der Lee and P. Miele, *Phys. Chem. Chem. Phys.*, 2012, **14**, 1768.
- 27 T. Kobayashi, S. Gupta, M. A. Caporini, V. K. Pecharsky and M. Pruski, *J. Phys. Chem. C*, 2014, **118**, 19548.
- 28 P. J. Fazen, E. E. Remsen, J. S. Beck, P. J. Carroll, A. R. McGhie and L. G. Sneddon, *Chem. Mater.*, 1995, **7**, 1942.
- 29 A. Paul and C. B. Musgrave, *Angew. Chem., Int. Ed.*, 2007, **46**, 8153.
- 30 E. M. Leitao, N. E. Stubbs, A. P. M. Robertson, H. Helten, R. J. Cox, G. C. Lloyd-Jones and I. Manners, *J. Am. Chem. Soc.*, 2012, **134**, 16805.

5.2. Formation of high-molecular weight polyaminoborane by Fe hydride catalyzed dehydrocoupling of methylamine borane

F. Anke, D. Han, M. Klahn, A. Spannenberg and T. Beweries

Dalton transaction, **2017**, 46, 6843.

DOI: 10.1039/c7dt01487b

© 2017 Royal Society of Chemistry 2017

Contribution to this paper is 10%.

COMMUNICATION

View Article Online

View Journal | View Issue



Cite this: *Dalton Trans.*, 2017, **46**, 6843

Received 25th April 2017,

Accepted 27th April 2017

DOI: 10.1039/c7dt01487b

rsc.li/dalton

Formation of high-molecular weight polyaminoborane by Fe hydride catalysed dehydrocoupling of methylamine borane†

F. Anke, D. Han, M. Klahn, A. Spannenberg and T. Beweries*

The complex $[(\text{PNHP})\text{Fe}(\text{H})(\text{CO})(\text{HBH}_3)]$ (PNHP = $\text{HN}(\text{CH}_2\text{CH}_2\text{P}(\text{Pr}_2)_2)$) serves as a catalyst precursor for the selective dehydrocoupling of methylamine borane at room temperature, tentatively via an off-metal polymerisation pathway.

In recent years, the dehydrogenation of ammonia borane (AB) and other amine borane adducts has attracted considerable interest due to the ability of such Lewis acid–base complexes to release significant amounts of H_2 under mild conditions.¹ Apart from H_2 , depending on the substitution pattern of the amine borane, a variety of cyclic and linear oligomeric and polymeric BN products can be obtained.² These compounds are very interesting as BN compounds are generally isoelectronic to hydrocarbons and a number of polymeric polarised $\text{B}^{\delta-}\text{N}^{\delta+}$ analogues of non-polar all-carbon structures were presented.³ Particularly borazines and linear polyaminoboranes, formally formed by dehydrogenation with subsequent oligomerisation or polymerisation of the unsaturated BN intermediates, appear to be very attractive as these can be of importance in high-performance polymers.⁴ Also, ammonia borane was discussed as a precursor for boron nitrogen ceramics⁵ and single-layer hexagonal BN.⁶ In this context, the control of polymer stereochemistry and molecular weight as it is possible for polyolefins by means of transition metal catalysed dehydrocoupling is a highly desirable, yet challenging goal. An approach to benefit from the isoelectronic BN/CC analogy in terms of catalysis was reported by Goldberg and Heinekey, who used the alkane dehydrogenation catalyst $[(\text{POCOP})\text{IrH}_2]$ (POCOP = $\kappa^3\text{-C}_6\text{H}_3\text{-2,6-(OP}^i\text{t-Bu)}_2$) (Fig. 1) for the release of H_2 from AB, the inorganic analogue of ethane and observed the formation of an insoluble white BN product, tentatively assigned as the pentamer $[\text{H}_2\text{NBH}_2]_5$.⁷ Manners and co-workers have later reinvestigated this reaction and character-

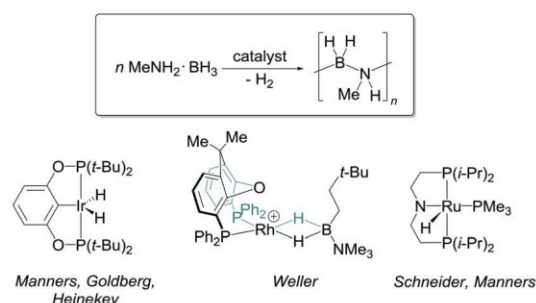


Fig. 1 Selected catalysts for MAB dehydropolymerisation.

ised the BN material as the linear polyaminoborane based on solid state ^{11}B NMR studies.⁸ Additionally, using the same Ir complex as well as a series of other dehydrogenation catalysts the dehydropolymerisation of methylamine borane (MAB) to afford soluble high molecular weight polyaminoboranes was described.⁹ Also, the photoactivation of metal carbonyl complexes was found to form active catalysts for the dehydropolymerisation of MAB¹⁰ and molecular Fe(I) catalysts were reported.¹¹ Detailed catalytic and mechanistic studies on the application of mononuclear and dinuclear $[\text{Rh}(\text{Xantphos})]^+$ catalysts for the generation of polyaminoboranes were presented by Weller and co-workers (Fig. 1).¹² Depending on the catalyst species and the amine borane substrate different mechanisms for the polymer growth were discussed; giving also insights into the pathways for AB dehydrogenation. Whereas dehydrogenative insertion of AB was suggested for Baker's (dcpe)Fe amido complex,¹³ metal-based dehydrogenation of AB followed by insertion of the transient aminoborane $[\text{H}_2\text{N}=\text{BH}_2]$ was reported for $[(\text{POCOP})\text{IrH}_2]$.⁸ Moreover, Schneider and co-workers have presented a study of AB dehydrogenation using $[(\text{PNP})\text{Ru}(\text{H})(\text{PMe}_3)]$ (PNP = $\text{N}(\text{CH}_2\text{CH}_2\text{P}(\text{Pr}_2)_2)$).¹⁴ In this case, metal–ligand cooperation, *i.e.* involvement of the Ru amido moiety, was found to be crucial for effective dehydrogenation. Notably, this complex was also used by Manners *et al.* for MAB dehydropolymerisation (Fig. 1).⁸

Leibniz-Institut für Katalyse an der Universität Rostock e.V., Albert-Einstein-Str. 29a, 18059 Rostock, Germany. E-mail: torsten.beweries@catalysis.de

†Electronic supplementary information (ESI) available: Experimental details, characterisation of the polymer, volumetric data, and NMR data. CCDC 1533415. For ESI and crystallographic data in CIF or other electronic format see DOI: 10.1039/c7dt01487b

In a more recent communication, the group of Schneider has used a Fe pincer complex $[(\text{PNP})\text{FeH}(\text{CO})]$ (**1**, $\text{PNP} = \text{N}(\text{CH}_2\text{CH}_2\text{Pi-Pr}_2)_2$) for the dehydrogenation of AB, also yielding an insoluble polymeric BN material.¹⁵ Fe hydride complexes of this type were described for a series of hydrogenation/dehydrogenation reactions using organic substrates in the past.¹⁶ For example, $[(\text{PNHP})\text{FeH}(\text{CO})(\text{HBH}_3)]$ (**2**) was used for the selective hydrogenation of aromatic and aliphatic nitriles with the amide complex **1** being present in reaction mixtures, thus suggesting this species to be of relevance for catalytic activity.¹⁷ In this contribution, we present a catalytic and mechanistic study of MAB dehydropolymerisation in different solvents using the Fe amine complex **2** as a pre-catalyst to give linear polyaminoborane and/or *N*-methylborazine, respectively.

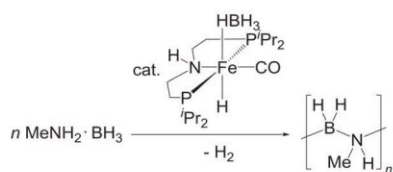
When a solution of MAB in THF was treated with 2 mol% of complex **2**, vigorous gas evolution was observed without previous activation by heating, irradiation or addition of a base (Scheme 1). The addition of elemental Hg does not affect the reaction, thus indicating that the nature of this process is homogeneous with a molecular active species. Also, phosphine poisoning gave no evidence of a heterogeneous active species (Fig. S11 and S12†). GC analysis of the gas phase showed that H_2 is the only gaseous product. Volumetric curves are depicted in Fig. 2.

The release of approximately 1.2 equivalents of H_2 was observed in all cases, indicating the presence of an additional dehydrogenation step, assuming that the formation of poly-*N*-methylaminoborane (p-MAB) requires only the release of one equivalent of H_2 . The addition of a fresh portion of MAB to the filtered bright yellow catalyst solution resulted in immediate further dehydrogenation, suggesting that the Fe catalyst is still intact. Performing the same reaction in toluene gives a slightly

different picture as slightly less H_2 is evolved (Fig. S10†) without the induction period. Reactions in THF were slower than in toluene.

The addition of *n*-hexane to the reaction mixture results in the precipitation of the pale yellow polymeric material that is soluble in organic solvents such as CHCl_3 , THF, and DMF.¹⁸ ^1H and ^{11}B NMR data (Fig. S5†) corroborate the assignment as a linear polymer. The ^{11}B NMR spectrum shows a broad symmetrical signal centred at -6 ppm which is in good agreement with the reports by Manners and co-workers and others.^{8,12a} No further ^{11}B resonances were observed at $+5 < \delta < -5$ ppm, thus suggesting a highly linear structure of the polymer without significant branching.¹⁹ Moreover, the absence of splitting upon proton coupling indicates the presence of a material of high molecular weight as similar coupling products containing short-chain oligomers or the linear dimer $\text{H}_3\text{B-NMeHBH}_2\text{-NMeH}_2$ show significant ^1H - ^{11}B coupling.²⁰ Also, ^1H NMR spectra closely resemble those reported before. The ^1H - ^{15}N HMQC NMR spectrum shows a correlation at -365 ppm, which can be resolved as a doublet with a coupling constant of approximately 65 Hz (Fig. S6†). Further analysis of the isolated material by ATR-IR spectroscopy (Fig. S7†) and comparison with literature data⁸ corroborates the assignment as p-MAB ($\nu_{\text{NH}} = 3265$, $\nu_{\text{CH}} = 2983$, $\nu_{\text{BH}} = 2373$ cm^{-1}). GPC analysis of the polymer obtained from reactions using different conditions showed that in all cases p-MAB of medium- to high-molecular weight was formed (Table 1). GPC data (Fig. S9†) from p-MAB obtained in different solvents show no significant differences that could point to an influence of the coordinating solvent THF for the dehydrogenation and polymerisation process.

NMR spectroscopic reaction monitoring showed that in solution besides the main product p-MAB also *N*-methylborazine is present ($\delta_{\text{HB}} = 33$ ppm), thus explaining the formation of slightly more than one equivalent of H_2 . A signal that points to the presence of free MeNH=BH_2 was not observed.²¹ In previous studies of AB dehydrogenation,²² the formation of *N*-methylborazine and other cyclic oligomers of the transient aminoborane $[\text{H}_2\text{N=BH}_2]$ was assigned to the



Scheme 1 MAB dehydropolymerisation using complex **2**.

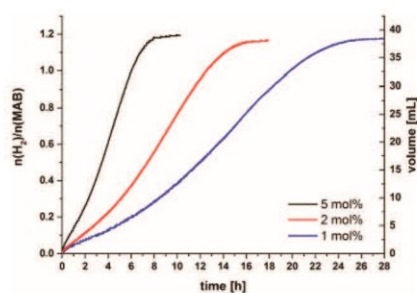


Fig. 2 Volumetric curves of MAB dehydropolymerisation with complex **2** in THF ($[\text{MAB}] = 0.33$ M, $T = 25$ °C).

Table 1 GPC data of p-MAB

Entry	Reaction conditions ^a	Time [h]	M_n [g mol^{-1}]	PDI
1	THF, 1 mol% 2	28	27.000	2.2
2	THF, 2 mol% 2	16	31.000	1.8
3	THF, 5 mol% 2	9	35.000	2.2
4	THF, closed system, 2 mol% 2	24	23.000	2.0
5	THF, 2 mol% 2 , addition of 50 equiv. MAB after reaction	32	38.000	2.1
6	Toluene, 1 mol% 2	23	29.000	1.6
7	Toluene, 2 mol% 2	6	27.000	1.9
8	Toluene, 5 mol% 2	2	24.000	1.6
9	Toluene, closed system, 2 mol% 2	24	31.000	1.9
10	Toluene, 2 mol% 2 , addition of 50 equiv. MAB after reaction	12	26.000	2.2

^a $[\text{MAB}] = 0.33$ M, $T = 25$ °C.

latter species being able to react in a metal-free oligomerisation pathway. In our case, the ^{11}B NMR spectra of MAB dehydropolymerisation in the presence of the trapping agent cyclohexene showed a weak resonance for the aminoborane-cyclohexene adduct at 46 ppm in THF and no resonance in toluene. Also, significant amounts of *N*-methylborazine were formed in THF solvent, whereas in toluene only very little *N*-methylborazine was obtained (Fig. S14 and S15†). This might point to the presence of a so-called off-metal polymerisation pathway for the formation of p-MAB in THF. However, we cannot exclude this mechanism in toluene as the hydroboration of cyclohexene might be too slow in toluene, which would explain the absence of the hydroborated product $\text{Cy}_2\text{B}=\text{NMeH}$ as it was discussed before.^{12a} Monitoring of the dehydropolymerisation reaction by ^{11}B NMR spectroscopy (see the ESI† for details) reveals that the resonance for *N*-methylborazine is only observed after full consumption of the starting material MAB, thus pointing towards the sequential formation of p-MAB and *N*-methylborazine. To further corroborate this, we added 5 mol % of catalyst **2** to analytically pure p-MAB in THF and found that the formation of *N*-methylborazine takes place. We thus conclude that this species is generated by a partial metal-mediated cleavage of the polymer chain at longer reaction times and the formation can be avoided by stopping the dehydropolymerisation reactions after the release of 1.0 equiv. of H_2 . Nucleophilic main chain scission of poly(*N*-methylaminoborane) was reported before.²³ The absence of borazine during polymer formation is an important benefit of the herein described system as further dehydrogenation of the polymer giving thermodynamically stable cyclic borazine species is a general problem with the synthesis of polyaminoboranes.^{9,10,24}

In line with the above assumption of an off-metal pathway, dehydropolymerisation reactions in a closed system, *i.e.* under H_2 pressure gave p-MAB with values for M_n that are in the same range as in reactions with H_2 venting (Table 1, entries 4 and 9). According to this, H_2 does not compete with the coordinated $[\text{MeNH}=\text{BH}_2]$ monomer or the growing polymer chain and does not act as a chain transfer reagent. Also, a comparison of molecular weights and PDIs of polymers made using different concentrations of **2** shows that the values do not deviate substantially. In cases where a metal centred polymerisation is operating, a significant decrease of M_n with increasing catalyst concentration would become evident. A slight increase of M_n in THF (entries 1–3) and a decrease in toluene (entries 6–8) suggest that the metal plays a role in the polymerisation process. We thus conclude that the metal is responsible for the dehydrogenation of MAB and formation of the intermediate aminoborane $[\text{MeNH}=\text{BH}_2]$. Subsequent off-metal polymerisation appears to be dominant; however, the involvement of the Fe centre cannot be excluded.

Analysis of the polymerisation kinetics (*i.e.* M_n vs. conversion/consumption of MAB)²⁵ shows that M_n is not affected significantly by the degree of conversion and high molecular weight polymers are also formed using lower concentrations of the catalyst (Fig. S13†). This points towards a chain growth

mechanism for the formation of p-MAB rather than a step growth pathway.⁸ Also, analysis of M_n after addition of further MAB shows that the catalyst is not living (Table 1, entries 5 and 10).

Monitoring of the dehydrocoupling process by multinuclear NMR spectroscopy was performed in order to shed light on the fate of the Fe catalyst. It should be noted that spectroscopic data of Fe species involved in the catalytic process were reported before.¹⁵ *In situ* ^1H and ^{31}P NMR spectra show the presence of Fe complexes **2** (δ 99.7 ppm), **3** (δ *cis*-3: 113.1, *trans*-3: 116.8 ppm), and **4** (δ 108.7 ppm) in THF solution during MAB dehydrogenation (see the ESI† for details). The highly reactive amide species **1** was not observed which is in line with Schneider's results for AB dehydrogenation.¹⁵ The formation of the amide- BH_3 adduct **4** is likely to take place either by BH_3 addition to **1**, a reaction that we performed independently (*vide infra*), or by H_2 elimination from the catalyst precursor **2**, which was described by Langer for a complex displaying *t*-Bu substituted P donor atoms.²⁶ Based on these observations, we believe that the abstraction of BH_3 from the precatalyst **2** yields the dihydrido complex **3** as it was discussed before by Beller, Langer and Guan (Fig. 3).^{17,26,27}

Complex **3** most likely represents the resting state of the catalyst and is in equilibrium with the pentacoordinate amido complex **1**,²⁷ which could add BH_3 to form **4**. Alternatively, complex **4** might be present due to H_2 abstraction from **2**.²⁶ Cooperative interaction of the metal centre and the amine moiety of the PNP ligand *via* the intermediate **INT** as it was also proposed earlier by Schneider *et al.*¹⁵ is likely to be present in our case as well.

To further corroborate the presence of complex **4** during dehydrogenation reactions we prepared this species by the reaction of **1** with BH_3 . Spectroscopic data resemble those from *in situ* experiments (^1H : -11.28, -14.76 ppm; ^{31}P : 108.7 ppm, Fig. S1–S3†). The IR spectrum shows a distinct BH band at 2340 cm^{-1} (Fig. S4†). The molecular structure of **4** is depicted in Fig. 4 and shows the Fe centre in the expected dis-

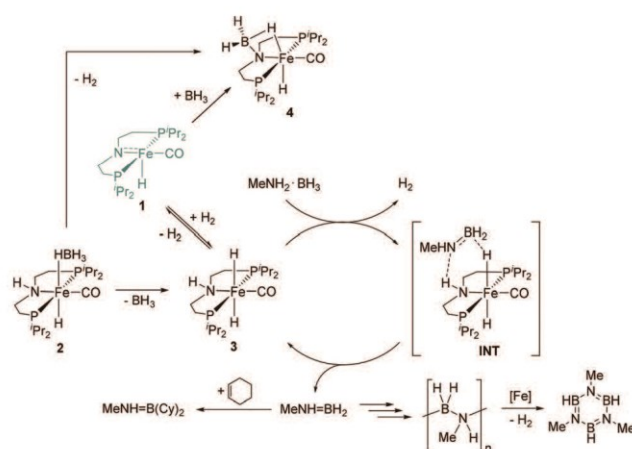


Fig. 3 Proposed mechanism for the dehydrogenation of MAB in THF and the formation of p-MAB.

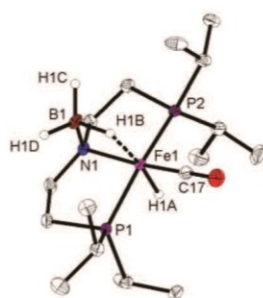


Fig. 4 Molecular structure of complex 4. Thermal ellipsoids correspond to 30% probability at 150 K. For clarity, the second molecule of the asymmetric unit and hydrogen atoms (except B and Fe bound) are omitted.

torted square bipyramidal coordination environment with an agostic interaction to one hydride of the BH_3 fragment (Fe1-H1B 1.62(3), B1-H1B 1.29(3) Å).

We have presented a study of the dehydrogenation of methylamine borane followed by polymerisation to selectively give a high-molecular weight linear polyaminoborane. Analysis of the polymer obtained using different reaction conditions suggests that the Fe catalyst is only involved in the dehydrogenation process and does not participate in the polymer formation itself. This system represents a rare example of a catalyst for the borazine-free dehydropolymerisation of amine boranes. Future studies will aim at the rationalisation of this effect using this and related catalysts.

We thank our technical and analytical staff in particular Susanne Schareina, Dr Christine Fischer (GPC) and Dr Wolfgang Baumann (NMR) for support. We gratefully acknowledge support by Josh Turner and Prof. Ian Manners (University of Bristol).

Notes and references

- (a) C. W. Hamilton, R. T. Baker, A. Staubitz and I. Manners, *Chem. Soc. Rev.*, 2009, **38**, 279; (b) A. Staubitz, A. P. M. Robertson and I. Manners, *Chem. Rev.*, 2010, **110**, 4079; (c) T. Beweries, in *Organometallics and Related Molecules for Energy Conversion*, ed. W.-Y. Wong, Springer-Verlag Berlin Heidelberg, 2015, p. 469.
- (a) E. M. Leitao, T. Jurca and I. Manners, *Nat. Chem.*, 2013, **5**, 817; (b) R. Waterman, *Chem. Soc. Rev.*, 2013, **42**, 5629; (c) R. L. Melen, *Chem. Soc. Rev.*, 2016, **45**, 775; (d) H. Johnson, T. Hooper and A. Weller, in *Synthesis and Application of Organoboron Compounds*, ed. E. Fernández and A. Whiting, Springer International Publishing, 2015, vol. 49, pp. 153.
- Selected recent examples: (a) B. Thiedemann, P. J. Gliese, J. Hoffmann, P. G. Lawrence, F. D. Sonnichsen and A. Staubitz, *Chem. Commun.*, 2017, DOI: 10.1039/C6CC08599G; (b) W.-M. Wan, A. W. Baggett, F. Cheng, H. Lin, S.-Y. Liu and F. Jäkle, *Chem. Commun.*, 2016, **52**, 13616; (c) T. Lorenz, M. Crumbach, T. Eckert, A. Lik and H. Helten, *Angew. Chem., Int. Ed.*, 2017, **56**, 2780.
- S. Bernard, C. Salameh and P. Miele, *Dalton Trans.*, 2016, **45**, 861.
- S. Bernard and P. Miele, *Materials*, 2014, **7**, 7436.
- H. Zeng, C. Zhi, Z. Zhang, X. Wei, X. Wang, W. Guo, Y. Bando and D. Golberg, *Nano Lett.*, 2010, **10**, 5049.
- M. C. Denney, V. Pons, T. J. Hebden, D. M. Heinekey and K. I. Goldberg, *J. Am. Chem. Soc.*, 2006, **128**, 12048.
- A. Staubitz, A. Presa Soto and I. Manners, *Angew. Chem., Int. Ed.*, 2008, **47**, 6212.
- A. Staubitz, M. E. Sloan, A. P. M. Robertson, A. Friedrich, S. Schneider, P. J. Gates, J. S. a. d. Günne and I. Manners, *J. Am. Chem. Soc.*, 2010, **132**, 13332.
- (a) Y. Kawano, M. Uruichi, M. Shimo, S. Taki, T. Kawaguchi, T. Kakizawa and H. Ogino, *J. Am. Chem. Soc.*, 2009, **131**, 14946; (b) T. Kakizawa, Y. Kawano, K. Naganeyama and M. Shimo, *Chem. Lett.*, 2011, **40**, 171; (c) J. R. Vance, A. P. M. Robertson, K. Lee and I. Manners, *Chem. – Eur. J.*, 2011, **17**, 4099.
- C. Lichtenberg, M. Adelhardt, T. L. Gianetti, K. Meyer, B. de Bruin and H. Grützmacher, *ACS Catal.*, 2015, **5**, 6230.
- (a) H. C. Johnson, E. M. Leitao, G. R. Whittell, I. Manners, G. C. Lloyd-Jones and A. S. Weller, *J. Am. Chem. Soc.*, 2014, **136**, 9078; (b) H. C. Johnson and A. S. Weller, *Angew. Chem., Int. Ed.*, 2015, **54**, 10173.
- R. T. Baker, J. C. Gordon, C. W. Hamilton, N. J. Henson, P.-H. Lin, S. Maguire, M. Murugesu, B. L. Scott and N. C. Smythe, *J. Am. Chem. Soc.*, 2012, **134**, 5598.
- M. Käß, A. Friedrich, M. Drees and S. Schneider, *Angew. Chem., Int. Ed.*, 2009, **48**, 905.
- A. Glüer, M. Förster, V. R. Celinski, J. Schmedt auf der Günne, M. C. Holthausen and S. Schneider, *ACS Catal.*, 2015, **5**, 7214.
- Selected examples: (a) E. Alberico, P. Sponholz, C. Cordes, M. Nielsen, H.-J. Drexler, W. Baumann, H. Junge and M. Beller, *Angew. Chem., Int. Ed.*, 2013, **52**, 14162; (b) E. A. Bielinski, P. O. Lagaditis, Y. Zhang, B. Q. Mercado, C. Würtele, W. H. Bernskoetter, N. Hazari and S. Schneider, *J. Am. Chem. Soc.*, 2014, **136**, 10234; (c) S. Chakraborty, W. W. Brennessel and W. D. Jones, *J. Am. Chem. Soc.*, 2014, **136**, 8564; (d) P. O. Lagaditis, P. E. Sues, J. F. Sonnenberg, K. Y. Wan, A. J. Lough and R. H. Morris, *J. Am. Chem. Soc.*, 2014, **136**, 1367.
- C. Bornschein, S. Werkmeister, B. Wendt, H. Jiao, E. Alberico, W. Baumann, H. Junge, K. Junge and M. Beller, *Nat. Commun.*, 2014, **5**, 4111.
- Also, in previous work by Weller and Manners, soluble polymers were obtained. However, Lichtenberg and Grützmacher reported the formation of poorly soluble materials using a Fe(I) catalyst (ref. 10).
- A. N. Marziale, A. Friedrich, I. Klopsch, M. Drees, V. R. Celinski, J. Schmedt auf der Günne and S. Schneider, *J. Am. Chem. Soc.*, 2013, **135**, 13342.
- (a) M. E. Sloan, A. Staubitz, T. J. Clark, C. A. Russell, G. C. Lloyd-Jones and I. Manners, *J. Am. Chem. Soc.*, 2010,

- 132, 3831; (b) C. J. Stevens, R. Dallanegra, A. B. Chaplin, A. S. Weller, S. A. Macgregor, B. Ward, D. McKay, G. Alcaraz and S. Sabo-Etienne, *Chem. – Eur. J.*, 2011, **17**, 3011.
- 21 O. J. Metters, A. M. Chapman, A. P. M. Robertson, C. H. Woodall, P. J. Gates, D. F. Wass and I. Manners, *Chem. Commun.*, 2014, **50**, 12146.
- 22 V. Pons, R. T. Baker, N. K. Szymczak, D. J. Heldebrant, J. C. Linehan, M. H. Matus, D. J. Grant and D. A. Dixon, *Chem. Commun.*, 2008, 6597.
- 23 N. E. Stubbs, T. Jurca, E. M. Leitao, C. H. Woodall and I. Manners, *Chem. Commun.*, 2013, **49**, 9098.
- 24 C. A. Jaska, K. Temple, A. J. Lough and I. Manners, *J. Am. Chem. Soc.*, 2003, **125**, 9424.
- 25 For this purpose, reactions were monitored volumetrically and stopped after 0.05, 0.33, 0.66 and 1.0 equivalents of H₂ were released.
- 26 F. Schneck, M. Assmann, M. Balmer, K. Harms and R. Langer, *Organometallics*, 2016, **35**, 1931.
- 27 S. Chakraborty, H. Dai, P. Bhattacharya, N. T. Fairweather, M. S. Gibson, J. A. Krause and H. Guan, *J. Am. Chem. Soc.*, 2014, **136**, 7869.

5.3. Synthesis and coordination chemistry of the PPN ligand 2-[bis(diisopropylphosphanyl)methyl] 6-methylpyridine

D. Han, B. Andres, A. Spannenberg and T. Beweries

Acta Crystallographica Section C., **2017**, 73, 917.

DOI:10.1107/S205322961701261X

© 2017 WILEY-VCH Verlag GmbH & Co. KGaA, Weinheim

Contribution to this paper is 90%.

**electronic reprint**STRUCTURAL
CHEMISTRY

ISSN: 2053-2296

journals.iucr.org/c

Synthesis and coordination chemistry of the PPN ligand 2-[bis(diisopropylphosphanyl)methyl]-6-methylpyridine

Delong Han, Benjamin Andres, Anke Spannenberg and Torsten Beweries*Acta Cryst.* (2017). **C73**, 917–922**IUCr Journals**

CRYSTALLOGRAPHY JOURNALS ONLINE

Copyright © International Union of Crystallography

Author(s) of this paper may load this reprint on their own web site or institutional repository provided that this cover page is retained. Republication of this article or its storage in electronic databases other than as specified above is not permitted without prior permission in writing from the IUCr.

For further information see <http://journals.iucr.org/services/authorrights.html>

STRUCTURAL
CHEMISTRY

ISSN 2053-2296

Synthesis and coordination chemistry of the PPN ligand 2-[bis(diisopropylphosphanyl)methyl]-6-methylpyridine

Delong Han, Benjamin Andres, Anke Spannenberg and Torsten Beweries*

Leibniz-Institut für Katalyse e. V. an der Universität Rostock, Albert-Einstein-Strasse 29a, 18059 Rostock, Germany.

*Correspondence e-mail: torsten.beweries@catalysis.de

Received 18 July 2017

Accepted 2 September 2017

Edited by A. G. Oliver, University of Notre Dame, USA

Keywords: coordination chemistry; phosphane; crystal structure; pyridine; PPN ligand; iron(II); cobalt(II); manganese(I).

CCDC references: 1550599; 1550598; 1550597; 1550596

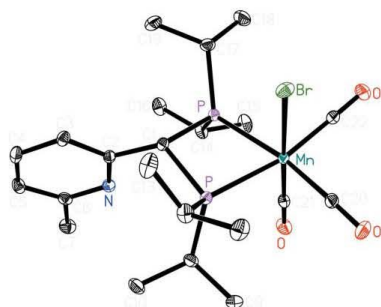
Supporting information: this article has supporting information at journals.iucr.org/c

The synthesis and crystal structure of the multidentate PPN ligand 2-[bis(diisopropylphosphanyl)methyl]-6-methylpyridine (*L*), $C_{19}H_{35}NP_2$, are described. In the isostructural tetrahedral Fe and Co complexes of type $LMCl_2$ ($M = Fe, Co$), namely {2-[bis(diisopropylphosphanyl)methyl]-6-methylpyridine- κ^2P,N }dichloridoiron(II), $[FeCl_2(C_{19}H_{35}NP_2)]$, and {2-[bis(diisopropylphosphanyl)methyl]-6-methylpyridine- κ^2P,N }dichloridocobalt(II), $[CoCl_2(C_{19}H_{35}NP_2)]$, the ligand adopts a bidentate *P,N*-coordination, whereas in the case of the octahedral Mn complex {2-[bis(diisopropylphosphanyl)methyl]-6-methylpyridine- κ^2P,P' }bromidotricarbonylmanganese(I), $[MnBr(C_{19}H_{35}NP_2)(CO)_3]$, the ligand coordinates *via* both P atoms to the metal centre.

1. Introduction

The coordination chemistry of pincer ligands in general is well described, and corresponding transition-metal complexes have been used in a variety of stoichiometric and catalytic applications (Albrecht & van Koten, 2001; van der Boom & Milstein, 2003; Choi *et al.*, 2011). A plethora of complexes with potentially tridentate aromatic PNP pincer ligands, with two P-donor atoms adjacent to the central pyridine fragment, are known, possessing a variety of different backbone and side-arm structures. The most prominent catalytic applications include N_2 activation (Arashiba *et al.*, 2011), CO_2 and ketone hydrogenation (Tanaka *et al.*, 2009; Langer *et al.*, 2011), and dehydrogenation reactions (Montag *et al.*, 2012). In most cases, the synthesis of aromatic PNP ligands is easy, starting from the corresponding pyridine or pyrrole derivatives. However, in cases where 2,6-lutidine and derivatives are used as starting materials, the formation of asymmetric PPN ligands has to be considered as a side reaction, owing to the fact that these compounds are present as intermediates due to partial deprotonation of the methyl groups (see Scheme 1). In a broader context, these PPN ligands can be regarded as hetero-functionality-containing analogues of the well-known short bite angle ligand bis(diphenylphosphanyl)methane (dppm). This concept has been discussed previously by Zhang *et al.* (2011).

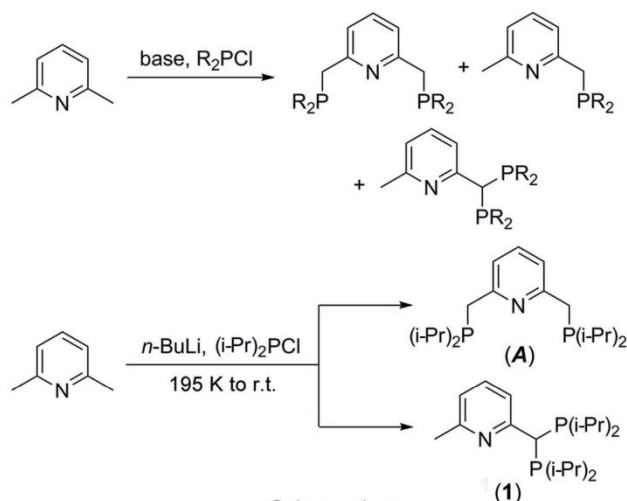
Pyridine-based PPN ligands have been described before. For example, Jansen & Pitter (1999) reported a procedure to access 2-[bis(diisopropylphosphanyl)methyl]pyridine. Mo, Cu and Pd complexes bearing this ligand were mentioned by Lang *et al.* (2002) and point towards a diverse coordination chemistry due to the possibility of adopting various coordination modes. Similar PN ligands based on a 6-methylpyridine backbone with only one PR_2 group [$R = Ph$ (Nelson *et al.*,



© 2017 International Union of Crystallography

research papers

1976), *i*-Pr (Shih & Ozerov, 2015) or *t*-Bu (de Boer *et al.*, 2012; Kinoshita *et al.*, 2012)] have been described on several occasions and the role of an Ru complex in acceptorless alcohol dehydrogenation has been evaluated (Langer *et al.*, 2015). In this article, we describe the synthesis and characterization of the PPN ligand 2-[bis(diisopropylphosphanyl)methyl]-6-methylpyridine, (**1**), along with a study of its coordination chemistry to selected 3d metal centres.



2. Experimental

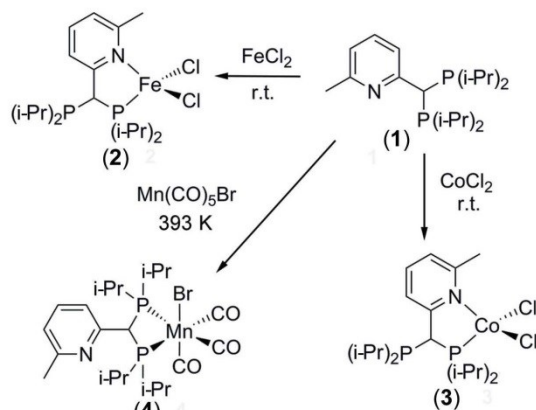
2.1. Synthesis and crystallization

All manipulations were carried out under an oxygen- and moisture-free argon atmosphere using standard Schlenk and glove-box techniques. All solvents were dispensed from a solvent purification system (PureSolv, Innovative Technology) or dried over sodium/benzophenone and freshly distilled prior to use. *i*-Pr₂P-Cl, 2,6-lutidine, *n*-BuLi (2.5 M in hexanes), FeCl₂, CoCl₂ and Mn(CO)₅Br were purchased from Sigma–Aldrich and used as received.

NMR spectra were recorded on a Bruker AV 300 or AV 400 spectrometer. All ¹H NMR spectra are referenced using the chemical shifts of residual protio solvent resonances (CDCl₃: δ_H 7.26, δ_C 77.2). Chemical shifts are reported in ppm (δ) relative to tetramethylsilane. The ³¹P{¹H} NMR spectra were referenced to external H₃PO₄. Mass spectra were recorded on a MAT 95XP Thermo Fisher Mass Spectrometer using electrospray ionization mode. ATR (attenuated total reflectance) IR spectra were recorded on a Bruker Alpha spectrometer.

For the synthesis of (**1**), *n*-BuLi (20.5 ml of a 2.5 M solution in *n*-hexane, 51.3 mmol) was added slowly using a dropping funnel to a solution of 2,6-lutidine (2.5 g, 23.33 mmol) in diethyl ether (10 ml) cooled by an ice bath. The colour of the solution gradually changed from colourless to yellow to red. The temperature of the reaction mixture was raised to 313 K and the mixture was stirred for 15 h. After cooling the reaction mixture to 195 K, chlorodiisopropylphosphane (7.79 g, 48.9 mmol) was added slowly to the reaction flask, and the reaction mixture was warmed to room temperature. The

solution became dark red and a precipitate formed. The reaction was quenched with degassed water and extracted with diethyl ether (3 × 10 ml). The extracts were dried with MgSO₄ and filtered, and the solvent was removed *in vacuo* to furnish a yellow oily residue which contains the PPN ligand (**1**) and the PNP ligand (**A**).



Analytically pure colourless single-crystalline (**1**) was obtained by sublimation of the mixture at 333 K and 1.0×10^{-2} mbar (1.19 g, 15%; 1 bar = 100 000 Pa). PPN ligand (**1**) is pyrophoric in air.

¹H NMR (CDCl₃, 300 MHz, 297 K): δ 7.41 (*t*, *J*_{HH} = 8 Hz, 1H, *m*-CH_{py}), 6.99 (*d*, *J*_{HH} = 8 Hz, 1H, *o*-CH_{py}), 6.89 (*d*, *J*_{HH} = 8 Hz, 1H, *p*-CH_{py}), 3.53 (*s*, 1H, CH), 2.47 (*s*, 3H, py-CH₃), 2.07 [*tsp*, *J*_{PH} = 3 Hz, *J*_{HH} = 7 Hz, 2H, CH(CH₃)₂], 1.95 [*tsp*, *J*_{PH} = 3 Hz, *J*_{HH} = 7 Hz, 2H, CH(CH₃)₂], 1.23 [*m*, 6H, CH(CH₃)₂], 1.14 [*m*, 6H, CH(CH₃)₂], 1.03 [*m*, 6H, CH(CH₃)₂], 0.73 [*m*, 6H, CH(CH₃)₂]; ³¹P{¹H} NMR (C₆D₆, 121 MHz, 297 K): δ 12.9 (*s*); ¹³C NMR (C₆D₆, 75 MHz, 297 K): δ 160.2 (*i*-C), 157.5 [*C*_{Ar}(CH₃)], 135.4 (*m*-CH), 120.6 (*o*-CH), 119.5 (*p*-CH), 38.9 (CH), 32.7 [*C*_{Ar}(CH₃)], 22.5 [CH(CH₃)₂], 22.4 [CH(CH₃)₂], 22.4 [CH(CH₃)₂], 20.7 [CH(CH₃)₂], 20.6 [CH(CH₃)₂], 19.7 [CH(CH₃)₂]. Analysis calculated for C₁₉H₃₅NP₂: C 67.23, H 10.39, N 4.13%; found: C 66.05, H 10.39, N 4.13%. ESI–MS (positive, *m/z*): 340.2322 [C₁₉H₃₅ + H]⁺.

To synthesise complex (**2**), anhydrous FeCl₂ (21 mg, 0.166 mmol) and (**1**) (56 mg, 0.174 mmol) were mixed in tetrahydrofuran (THF; 10 ml) and the mixture was stirred for 8 h at room temperature. During the reaction, the turbid solution turned pale yellow and all components dissolved. The solution was filtered and concentrated to dryness *in vacuo*. The pale-yellow residue was washed thoroughly with pentane. Pale-yellow complex (**2**) was obtained after evaporation of the solvent from the filtrate (70 mg, 91%).

Colourless crystals of (**2**) were obtained by slow evaporation from a THF solution. Analysis calculated for C₁₉H₃₅NP₂FeCl₂: C 48.95, H 7.57, N 3.0%; found: C 48.87, H 7.90, N 2.62%. ESI–MS (positive, *m/z*): 394.206 [C₁₉H₃₅NP₂Fe]⁺.

To synthesise complex (**3**), anhydrous CoCl₂ (25 mg, 0.194 mmol) and (**1**) (60 mg, 0.177 mmol) were mixed in THF (10 ml) and the mixture was stirred for 7 h at room temperature. During the reaction, the colour of the solution gradually changed from light blue to deep blue and all

Table 1
Experimental details.

	(1)	(2)	(3)	(4)
Crystal data				
Chemical formula	C ₁₉ H ₃₅ NP ₂	[FeCl ₂ (C ₁₉ H ₃₅ NP ₂)]	[CoCl ₂ (C ₁₉ H ₃₅ NP ₂)]	[MnBr(CO) ₃ (C ₁₉ H ₃₅ NP ₂)]
<i>M_r</i>	339.42	466.17	469.25	558.30
Crystal system, space group	Monoclinic, <i>P</i> 2 ₁ / <i>c</i>	Triclinic, <i>P</i> $\bar{1}$	Triclinic, <i>P</i> $\bar{1}$	Monoclinic, <i>P</i> 2 ₁ / <i>n</i>
Temperature (K)	150	150	150	150
<i>a</i> , <i>b</i> , <i>c</i> (Å)	16.2905 (5), 6.7510 (2), 18.9112 (6)	8.2907 (1), 10.7222 (2), 13.6434 (2)	8.2603 (2), 10.7220 (3), 13.6314 (3)	10.6732 (5), 15.6935 (8), 15.1651 (7)
α , β , γ (°)	90, 98.2024 (11), 90	87.0826 (6), 80.8448 (6), 75.7315 (6)	86.8728 (10), 80.5491 (10), 75.6607 (10)	90, 96.0732 (8), 90
<i>V</i> (Å ³)	2058.52 (11)	1160.35 (3)	1153.68 (5)	2525.9 (2)
<i>Z</i>	4	2	2	4
Radiation type	Mo <i>K</i> α	Mo <i>K</i> α	Mo <i>K</i> α	Mo <i>K</i> α
μ (mm ⁻¹)	0.21	1.02	1.12	2.25
Crystal size (mm)	0.38 × 0.16 × 0.07	0.40 × 0.39 × 0.35	0.23 × 0.21 × 0.09	0.47 × 0.45 × 0.29
Data collection				
Diffractometer	Bruker APEXII CCD area-detector	Bruker APEXII CCD area-detector	Bruker APEXII CCD area-detector	Bruker APEXII CCD area-detector
Absorption correction	Multi-scan (<i>SADABS</i> ; Bruker, 2014)	Multi-scan (<i>SADABS</i> ; Bruker, 2014)	Multi-scan (<i>SADABS</i> ; Bruker, 2014)	Multi-scan (<i>SADABS</i> ; Bruker, 2014)
<i>T</i> _{min} , <i>T</i> _{max}	0.93, 0.98	0.67, 0.72	0.86, 0.91	0.47, 0.56
No. of measured, independent and observed [<i>I</i> > 2σ(<i>I</i>)] reflections	37883, 4970, 4231	32317, 5588, 5098	27897, 5055, 4435	38793, 5516, 5115
<i>R</i> _{int}	0.032	0.021	0.026	0.019
(sin θ/λ) _{max} (Å ⁻¹)	0.660	0.660	0.639	0.639
Refinement				
<i>R</i> [<i>F</i> ² > 2σ(<i>F</i> ²)], <i>wR</i> (<i>F</i> ²), <i>S</i>	0.035, 0.096, 1.02	0.025, 0.069, 1.05	0.029, 0.076, 1.04	0.025, 0.066, 1.02
No. of reflections	4970	5588	5055	5516
No. of parameters	208	235	235	280
H-atom treatment	H-atom parameters constrained	H-atom parameters constrained	H-atom parameters constrained	H-atom parameters constrained
$\Delta\rho_{\text{max}}$, $\Delta\rho_{\text{min}}$ (e Å ⁻³)	0.69, -0.21	0.35, -0.29	0.55, -0.27	1.27, -1.13

Computer programs: *APEX2* (Bruker, 2014), *SAINT* (Bruker, 2013), *SHELXS97* (Sheldrick, 2008), *SHELXL2014* (Sheldrick, 2015), *XP* in *SHELXTL* (Sheldrick, 2015) and *publCIF* (Westrip, 2010).

components dissolved. The solution was filtered and concentrated to dryness *in vacuo*. The residue was washed thoroughly with pentane. Blue complex (3) was obtained after evaporation of the solvent from the filtrate (yield 65 mg, 78%).

Blue crystals of (3) were obtained by slow evaporation of solvent from a THF/*n*-hexane solution (1:1.2 *v/v*). Analysis calculated for C₁₉H₃₅CoCl₂NP₂: C 48.71, H 7.56, N 3.01%; found: C 48.63, H 7.52, N 2.98%. ESI-MS (positive, *m/z*): 468.0945 [*M*]⁺.

To synthesise complex (4), Mn(CO)₅Br (62 mg, 0.226 mmol) and (1) (161 mg, 0.474 mmol) were mixed in toluene (10 ml) and the mixture was stirred for 24 h at 393 K. During the reaction, the colour of the solution changed from colourless to yellow and gas evolution was observed. The clear yellow solution was filtered and concentrated to dryness *in vacuo*. The residue was washed thoroughly with pentane. Yellow complex (4) was obtained after evaporation of the solvent from the filtrate (yield 78 mg, 62%).

Yellow crystals of (4) were obtained by slow evaporation of solvent from a THF/*n*-hexane solution (1:1.5 *v/v*). ¹H NMR (THF-*d*₈, 300 MHz, 297 K): δ 7.54 (*t*, *J*_{HH} = 8 Hz, 1H, *m*-CH_{py}), 7.25 (*d*, *J*_{HH} = 7 Hz, 1H, *p*-CH_{py}), 7.15 (*d*, *J*_{HH} = 7 Hz, 1H, *o*-CH_{py}), 4.98 (*t*, *J*_{PH} = 10 Hz, 1H, CH), 2.50 (*s*, 3H, py-CH₃), 3.05–3.47 [*m*, 4H, CH(CH₃)₂], 1.25–1.57 [*m*, 24H, CH(CH₃)₂];

³¹P NMR (CDCl₃, 121 MHz, 297 K): δ 42.1 (*s*), 36.7 (*s*); ¹³C NMR (CDCl₃, 75 MHz, 297 K): 216.7 (CO), 158.5 (*i*-C), 154.3 [C_{Ar}(CH₃)], 137.6 (*m*-CH), 121.6 (*p*-CH), 119.6 (*o*-CH), 57.9 (CH), 31.1 [CH(CH₃)₂], 29.6 [C_{Ar}(CH₃)], 28.1 [CH(CH₃)₂], 27.9 [CH(CH₃)₂], 23.9 [CH(CH₃)₂], 20.9 [CH(CH₃)₂], 19.1 [CH(CH₃)₂]. IR (ATR, cm⁻¹): ν(CO) 2008, 1952, 1911. Analysis calculated for C₂₂H₃₅BrMnNP₂O₃: C 47.33, H 6.32, N 2.51%; found: C 46.71, H 6.46, N 2.57%. ESI-MS (positive, *m/z*): 582.0539 [*M* + Na]⁺, 560.0721 [*M* + H]⁺.

2.2. Refinement

Crystal data, data collection and structure refinement details are summarized in Table 1. All H atoms were placed in idealized positions, with C–H = 0.95–1.00 (CH) or 0.98 Å (CH₃), and refined using a riding model, with *U*_{iso}(H) = 1.2*U*_{eq}(C) for CH or 1.5*U*_{eq}(C) for CH₃.

3. Results and discussion

PNP pincer ligands bearing methylene side arms can, in principle, be prepared starting from 2,6-lutidine by deprotonation of the methyl groups and reaction with chlorophosphanes (Kawatsura & Hartwig, 2001). When

research papers

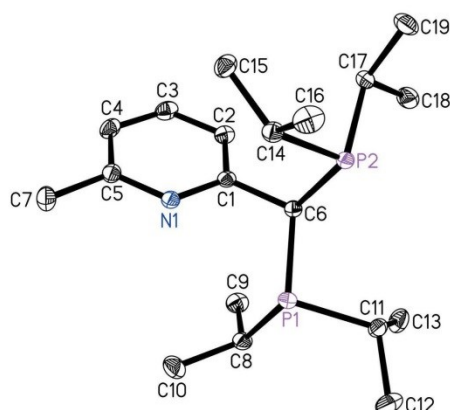


Figure 1

The molecular structure of (1). Displacement ellipsoids are drawn at the 30% probability level. H atoms have been omitted for clarity.

aiming for the synthesis of the neutral PNP pincer ligand 2,6-bis[(diisopropylphosphanyl)methyl]pyridine [ligand (A) in Scheme 1] (Jansen & Pitter, 1999) according to the synthetic protocol described earlier for the similar ligand with terminal *t*-Bu groups (Kawatsura & Hartwig, 2001), we observed that selective formation of the desired ligand (A) does not take place. Instead, significant amounts of PPN ligand (1), formed by twofold phosphorylation of just one of the methyl groups, were obtained (Scheme 1). An explanation is that, after the first phosphorylation step has occurred, deprotonation can take place at the newly formed P(i-Pr)₂CH₂ group to give PPN ligand (1). From *in situ* ³¹P NMR spectra, these two compounds were identified as the main components [δ 12.7 ppm for (A) and 12.9 ppm for (1)] in a ratio of 8:92. After sublimation of the yellow oily mixture, PPN ligand (1) could be isolated in an analytically pure form in a yield of 15%.

Due to structural similarities between (A) and (1), the ³¹P{¹H} NMR spectra are very similar. For a solution of (A) in CDCl₃, a chemical shift of 12.6 ppm was reported, whereas in our case for (1) we observed a singlet resonance at δ 12.9 ppm.

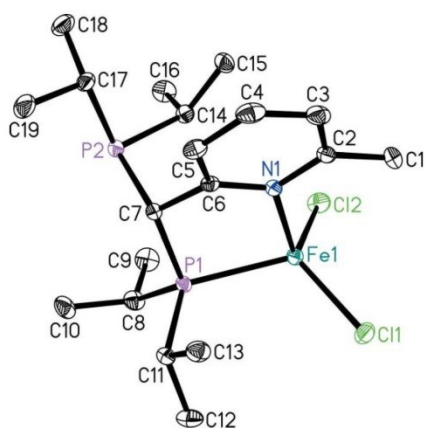


Figure 2

The molecular structure of (2). Displacement ellipsoids are drawn at the 30% probability level. H atoms have been omitted for clarity.

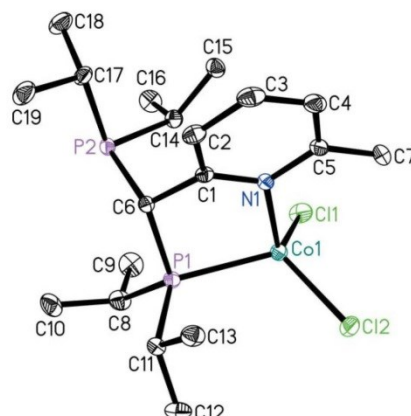


Figure 3

The molecular structure of (3). Displacement ellipsoids are drawn at the 30% probability level. H atoms have been omitted for clarity.

However, in the ¹H NMR spectra, differences became evident, with isolated and well-defined singlet resonances for the intact methyl group (δ 2.47 ppm) and the methine group containing both diisopropylphosphane groups (δ 3.53 ppm).

The molecular structure of (1) is depicted in Fig. 1. It confirms the twofold phosphorylation of one of the methyl groups, resulting in a (diisopropylphosphanyl)methyl fragment which shows slightly distorted tetrahedral geometry at the methine C6 atom. Bond lengths and angles are in the expected range.

With this hitherto unknown ligand in hand, we investigated its coordination chemistry using a series of different 3d metal precursors. In principle, different types of coordination should be possible using ligand (1), namely *P,P*- or *P,N*-bidentate complexation, as well as tridentate coordination *via* both P-atom donors and the N atom. Based on the structure of this ligand, this last coordination mode might be possible but was not observed in this case.

The reaction of FeCl₂ with (1) in tetrahydrofuran (THF) results in the formation of compound (2) with *P,N*-coordination of one PPN ligand to the metal, while CoCl₂ gives the deep-blue isostructural paramagnetic complex (3). Single crystals were obtained from THF solutions for (2) or from a mixture of THF and *n*-hexane for (3). The molecular structures are depicted in Figs. 2 and 3, and selected bond lengths are given in Table 2.

The molecular structure of (2) shows the iron centre in a distorted tetrahedral coordination environment [Cl1—Fe1—N1 = 107.56 (3), Cl1—Fe1—Cl2 = 119.80 (2), Cl2—Fe1—P1 = 118.828 (16), P1—Fe1—N1 = 81.10 (3), N1—Fe1—Cl2 = 109.28 (3) and Cl1—Fe1—P1 = 112.541 (15)°], with the PPN ligand (1) in the *P,N*-coordination mode, thus resulting in a five-membered chelate ring and one of the diisopropylphosphane groups being noncoordinating [Fe1—P1 = 2.4155 (4) and Fe1—N1 = 2.1545 (11) Å]. Upon coordination of ligand (1), the P1—C7—C6 angle is reduced slightly [109.45 (8)°, *cf.* 113.30 (9)° in ligand (1)]. The calculated four-coordinate geometry index τ_4 (Yang *et al.*, 2007) of 0.86 confirms the distorted tetrahedral coordination geometry. Interestingly, for Fe⁰ complexes bearing similar 2-[bis(diphenylphosphanyl)-

Table 2
Selected bond lengths for complexes (2), (3) and (4).

	(2) (<i>M</i> = Fe, <i>X</i> = Cl)	(3) (<i>M</i> = Co, <i>X</i> = Cl)	(4) (<i>M</i> = Mn, <i>X</i> = Br)
<i>M</i> —N	2.1545 (11)	2.0637 (14)	
<i>M</i> —P1	2.4155 (4)	2.3729 (5)	2.3247 (5)
<i>M</i> —P2			2.3351 (5)
<i>M</i> — <i>X</i>	2.2483 (4), 2.2420 (4)	2.2285 (5), 2.2406 (5)	2.5231 (3)

methyl]pyridine ligands, both the described *P,N*-coordination and the *P,P*-binding mode are known (Mague & Krinsky, 2001).

In complex (3), the bonds between the PPN ligand and the Co centre [*Co*1—N1 = 2.0637 (14) and *Co*1—P1 = 2.3729 (5) Å] are slightly shorter than in Fe complex (2), which is in line with the higher electron density at the metal atom is also reflected by the shorter covalent radius for the Co atom (Pyykkö & Atsumi, 2009). Also in this case, complexation of (1) results in a slight conformational change of the ligand, as can be seen, for example, from the reduction of the P1—C6—C1 angle [109.70 (11)°]. For complex (3), the value of τ_4 of 0.90 is slightly closer to the expected value of 1.0 for an ideal tetrahedral coordination geometry than for Fe complex (2). A very similar Co^{II} dichloride complex was reported by Mague & Krinsky (2001) using the 2-[bis(diphenylphosphanyl)methyl]pyridine ligand, with bond lengths *Co*—N = 2.042 (3) and *Co*—P = 2.3756 (10) Å.

A different coordination mode of the PPN ligand was observed in a reaction with Mn(CO)₅Br. Vigorous CO release was observed, resulting in the isolation of yellow complex (4) (Scheme 2). The Mn^I complex is diamagnetic and characteristic ³¹P resonances can be found at 36.7 and 42.2 ppm, most likely due to the presence of two different *P,P*-bound diastereoisomers in solution. NMR analysis of single crystals that were analysed by X-ray crystallography showed that the intense signal at 42.2 ppm can be assigned to the isomer found in the solid state (see below). The IR spectrum of (4) shows three pronounced carbonyl-stretching vibrations at 2008, 1952, and 1911 cm^{−1}, in line with values for other Mn^I tricarbonyl complexes (Spall *et al.*, 2016).

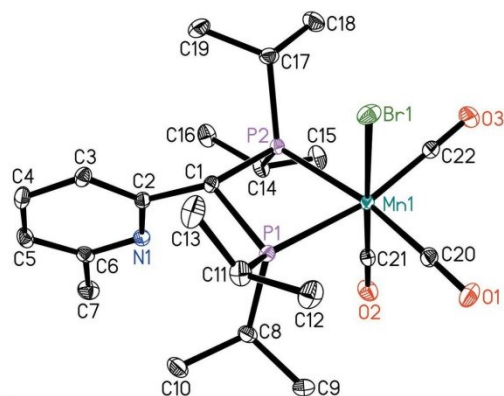


Figure 4
The molecular structure of (4). Displacement ellipsoids are drawn at the 30% probability level. H atoms have been omitted for clarity.

The molecular structure of (4) (Fig. 4) shows the Mn^I fac-tricarbonyl species in a distorted octahedral coordination geometry, with the Br ligand in the axial position. As mentioned above, the PPN ligand adopts a different binding mode, namely *P,P*-coordination, to give a bis(diisopropylphosphanyl)methane chelate ligand with the pyridine ring being noncoordinating. The Mn—P distances are as expected for an Mn^I-bis(phosphane) complex [*Mn*1—P1 = 2.3247 (5) and *Mn*1—P2 = 2.3351 (5) Å]. Compared with free ligand (1), as is well documented for a small-bite-angle bis(phosphane) ligand, significant distortion is observed upon coordination to the Mn centre [*P*1—C1—*P*2 = 95.63 (8)°]. Interestingly, *P,N*-binding has also been observed for group 7 metal(I) complexes, as seen in the Re compound reported by Mague & Krinsky (2001). Another example of a *P,P*-coordinated 2-[bis(diphenylphosphanyl)methyl]pyridine ligand was presented by Lang *et al.* (2002), who investigated the coordination chemistry of that ligand to Pd.

4. Conclusions

We have presented the synthesis and coordination chemistry of the PPN ligand 2-[bis(diisopropylphosphanyl)methyl]-6-methylpyridine. Compounds of this type can be obtained as a side product in the synthesis of well-established PNP pincer ligands. The structures of the metal complexes of this ligand reported here show two different coordination modes, either *P,N* or *P,P*, which differ depending on the metal centre. Whereas for Fe^{II} and Co^{II}, the *P,N*-coordination was found to be preferred, resulting in the formation of isostructural paramagnetic complexes, for Mn^I a bis(phosphane) complex with *P,P*-coordination was isolated. All complexes display one remaining free donor site that could, in principle, be accessible for the coordination of a further metal atom.

Acknowledgements

We thank our technical and analytical staff, in particular Dr Wolfgang Baumann (LIKAT), for support.

Funding information

Funding for this research was provided by: China Scholarship Council (grant No. 20150808083 to DH).

References

- Albrecht, M. & van Koten, G. (2001). *Angew. Chem. Int. Ed.* **40**, 3750–3781.
- Arashiba, K., Miyake, Y. & Nishibayashi, Y. (2011). *Nat. Chem.* **3**, 120–125.
- Boer, S. Y. de, Gloaguen, Y., Reek, J. N. H., Lutz, M. & van der Vlugt, J. I. (2012). *Dalton Trans.* **41**, 11276–11283.
- Boom, M. E. van der & Milstein, D. (2003). *Chem. Rev.* **103**, 1759–1792.
- Bruker (2013). *SAINT*. Bruker AXS Inc., Madison, Wisconsin, USA.
- Bruker (2014). *APEX2* and *SADABS*. Bruker AXS Inc., Madison, Wisconsin, USA.
- Choi, J., MacArthur, A. H. R., Brookhart, M. & Goldman, A. S. (2011). *Chem. Rev.* **111**, 1761–1779.
- Jansen, A. & Pitter, S. (1999). *Monatsh. Chem.* **130**, 783–794.

research papers

- Kawatsura, M. & Hartwig, J. F. (2001). *Organometallics*, **20**, 1960–1964.
- Kinoshita, E., Arashiba, K., Kuriyama, S., Miyake, Y., Shimazaki, R., Nakanishi, H. & Nishibayashi, Y. (2012). *Organometallics*, **31**, 8437–8443.
- Lang, H.-F., Fanwick, P. E. & Walton, R. A. (2002). *Inorg. Chim. Acta*, **328**, 232–236.
- Langer, R., Diskin-Posner, Y., Leitius, G., Shimon, L. J. W., Ben-David, Y. & Milstein, D. (2011). *Angew. Chem. Int. Ed.* **50**, 9948–9952.
- Langer, R., Gese, A., Gesevičius, D., Jost, M., Langer, B. R., Schneck, F., Venker, A. & Xu, W. (2015). *Eur. J. Inorg. Chem.* pp. 696–705.
- Mague, J. T. & Krinsky, J. L. (2001). *Inorg. Chem.* **40**, 1962–1971.
- Montag, M., Zhang, J. & Milstein, D. (2012). *J. Am. Chem. Soc.* **134**, 10325–10328.
- Nelson, S. M., Perks, M. & Walker, B. J. (1976). *J. Chem. Soc. Perkin Trans. 1*, pp. 1205–1209.
- Pyykkö, P. & Atsumi, M. (2009). *Chem. Eur. J.* **15**, 12770–12779.
- Sheldrick, G. M. (2008). *Acta Cryst. A* **64**, 112–122.
- Sheldrick, G. M. (2015). *Acta Cryst. C* **71**, 3–8.
- Shih, W.-C. & Ozerov, O. V. (2015). *Organometallics*, **34**, 4591–4597.
- Spall, S. J. P., Keane, T., Tory, J., Cocker, D. C., Adams, H., Fowler, H., Meijer, A. J. H. M., Hartl, F. & Weinstein, J. A. (2016). *Inorg. Chem.* **55**, 12568–12582.
- Tanaka, R., Yamashita, M. & Nozaki, K. (2009). *J. Am. Chem. Soc.* **131**, 14168–14169.
- Westrip, S. P. (2010). *J. Appl. Cryst.* **43**, 920–925.
- Yang, L., Powell, D. R. & Houser, R. P. (2007). *Dalton Trans.* pp. 955–964.
- Zhang, S., Pattacini, R. & Braunstein, P. (2011). *Inorg. Chem.* **50**, 3511–3522.

5.4. Fe(II) hydrido complex catalysed dehydrogenation of hydrazine borane and insights on the products structure using solid-state NMR and XPS analysis

D. Han, R. Knitsch, F. Anke, M. R. Hansen and T. Beweries

manuscript in preparation.

Contribution to this paper is 50%.

Fe(II) hydrido complex catalysed dehydrogenation of hydrazine borane and insights on the products structure using solid-state NMR and XPS analysis

D. Han,^{†a} R. Knitsch,^{†b} F. Anke,^a L. Ibing,^b M. Winter,^b H. Jiao^a, M. R. Hansen^{*b} and T. Beweries^{*a}

^a Leibniz-Institut für Katalyse an der Universität Rostock e.V., Albert-Einstein-Str. 29a, 18059 Rostock, Germany

^b Westfälische Wilhelms-Universität Münster, Institut für Physikalische Chemie, Corrensstr. 28/30, 48149 Münster, Germany.

Supporting Information Placeholder

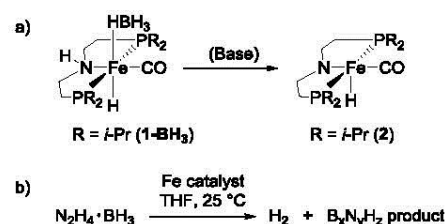
ABSTRACT: The catalytic dehydrogenation of hydrazine borane using molecularly defined PNP Fe(II) hydride complexes [(PNHP)Fe(HBH₃)(H)(CO)] (PNHP = HN[CH₂CH₂P(*i*-Pr)₂], **1-BH₃**) and [(PNP)Fe(H)(CO)] (PNP = N[CH₂CH₂P(*i*-Pr)₂], **2**) is reported. Both catalysts are highly active and recyclable and release up to 2.56 equivalent of hydrogen, giving a thermally unstable solid dehydrogenation product. The isolated B₂N₂H₂ residues were analysed by solid-state NMR spectroscopy combined with DFT calculation of NMR parameters and XPS analysis. A mechanism of hydrazine borane dehydrogenation and polymerisation leading to the residue is presented.

INTRODUCTION

The development of new hydrogen-storage materials that can ideally be used repeatedly in mobile applications is one of the main challenges connected with the nowadays evident increasing worldwide demand for clean and sustainable energy sources.¹ Hydrogen storage in so-called chemical hydrides such as ammonia borane (AB), displaying a very attractive gravimetric hydrogen capacity of 19.6 wt%, was thoroughly investigated in the past and numerous examples for its catalytic dehydrogenation were described.² In this context, the potential of hydrazine borane (HB) was also studied in recent years. First studies on H₂ release from HB included thermolysis³ and hydrolysis⁴, giving ideally up to five equivalents of hydrogen by stepwise hydrolysis of HB and hydrazine decomposition.⁵ Using this approach, formation of thermodynamically stable B-O bonds takes place which can be regarded as problematic when considering rehydrogenation of spent materials. Our group has reported on transition metal catalyzed dehydrogenation of HB using group 4 metallocene complexes⁶ as well as ring-substituted POCOP Ir complexes (POCOP = κ^3 -C₅H₃-2,6-(OPtBu₂)₂).⁷ As the former example only showed very poor activity and formation of N₂, most likely by decomposition of hydrazine, was observed, no non-noble metal catalyst are known for hydrolytic hydrogen release or homogeneous dehydrogenation of HB to date.

Beller and Schneider have developed Fe(II) complexes bearing tridentate PNHP and PNP pincer ligand environments⁸ (PNHP = HN[CH₂CH₂P(*i*-Pr)₂], PNP = N[CH₂CH₂P(*i*-Pr)₂]) which turned out to be a very potent catalyst motif for a series of hydrogenation and dehydrogenation reactions of organic substrates.⁹ As an interesting feature of these complexes, cooperativity between the metal center and the PNP ligand was found to be important for the outcome of the reaction, giving highly active dehydrogenation catalysts for the amido form and hydrogenation

catalysts for the amine form of the ligand (complexes **1-BH₃** and **2**, Scheme 1).



Scheme 1. a) PNP Fe(II) hydrido complexes **1** and **2**. b) HB dehydrogenation using Fe complexes.

Ammonia borane (AB) dehydrogenation using amido complex **2** as a catalyst resulting in the formation of a linear polyaminoborane was presented by Schneider and co-workers.¹⁰ Moreover, in a recent study, we have described the use of complex **1-BH₃** as a precatalyst for the dehydropolymerisation of methylamine borane.¹¹ In this contribution we extend these studies to HB as the substrate and report on the first example of homogeneous dehydrogenation of HB using the above mentioned pincer Fe(II) complexes as noble-metal free, molecularly defined catalysts.

RESULTS AND DISCUSSION

Upon addition of complex **1-BH₃** as the catalyst to HB in THF under an atmosphere of Argon at room temperature, immediate evolution of gas was observed. Simultaneously, the color of the Fe hydrido complex slowly faded from yellow to pale yellow and a white solid precipitated. The progress of the reaction was monitored by volumetric analysis, indicating that complex **1-BH₃** catalyzes the release of approximately one equivalent of H₂ per molecule HB (Figure 1).

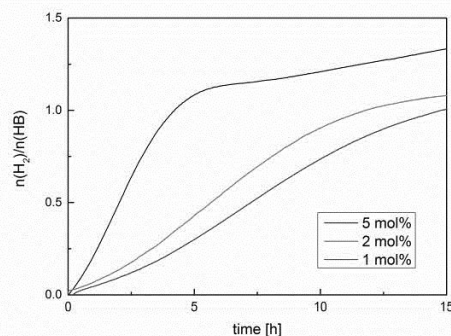


Figure 1. Volumetric curves for dehydrogenation of HB (1.1 mmol) using different concentrations of complex **1-BH₃** in THF at $T = 25\text{ }^{\circ}\text{C}$.

For (POCOP)Ir hydrido complexes as the catalysts full conversion could not be observed using low catalyst loadings of less than 2 mol%.⁷ In the case of Fe complex **1-BH₃**, full conversion (i.e. formation of at least one equivalent of H₂) could also be observed in catalytic runs using lower Fe concentrations. Analysis of the headspace of the reaction mixture indicated that H₂ was the only gaseous product. Formation of N₂ as a product of hydrazine decomposition was not found. In all cases, a significant time of induction was observed with lower activity. In a previous report on methylamine borane dehydropolymerisation¹¹, we have found a similar behavior in THF, which can be traced back to the generation of the active species from complex **1-BH₃**. Here, BH₃ elimination is needed in order to generate the active catalyst species **1**, a Fe(II) dihydrido complex (vide infra). This Lewis base induced BH₃ elimination was also reported earlier by Langer and co-workers.¹² After separation of the insoluble dehydrogenation product from the catalyst solution by filtration, a pale yellow solution was obtained, which upon addition of fresh **HB** was still active for dehydrogenation. ³¹P NMR analysis of this solution showed the presence of complex **2** (δ 116.3 ppm), Fe(II) dihydrido complex (δ 116.7 ppm), PNP ligand (δ -1.0 ppm) and oxidized PNP ligand (δ 52.1 ppm).

As we observed an induction period for **HB** dehydrogenation using complex **1-BH₃**, we next focussed on the investigation of the amido complex **2**, which in principle forms upon BH₃ abstraction from **1-BH₃**, followed by H₂ dissociation. Thus, this complex is likely to be present during **HB** dehydrogenation using **1-BH₃** as precatalyst species as well. In dehydrogenation reactions using the amido complex **2**, significantly more than one equivalent of H₂ evolved in much shorter reaction times than for complex **1-BH₃** (Figure 2). Also, reaction rates at the onset of the dehydrogenation reaction were much higher compared to reaction with **1-BH₃** as the precatalyst (cf. Figures 1 and 2). A maximum of approximately 2.56 equiv. of H₂ was observed in a long term experiment using 5 mol% of **2** after 74 hours. Notably, dehydrogenation of **HB** using both catalyst precursors **1-BH₃** and **2** was found to be a homogeneous process as evidenced by a PMe₃ poisoning experiment (see Supporting Information for details).¹³ In-situ NMR studies at -78 °C showed that both Fe complexes are also active at low temperature, forming the aforementioned Fe(II) dihydrido complex (³¹P: δ 116.7 ppm) and hydrogen (¹H: 4.55 ppm), thus suggesting the presence of a dehydrogenation process that shows essentially no activation barrier (see Supporting Information for details).

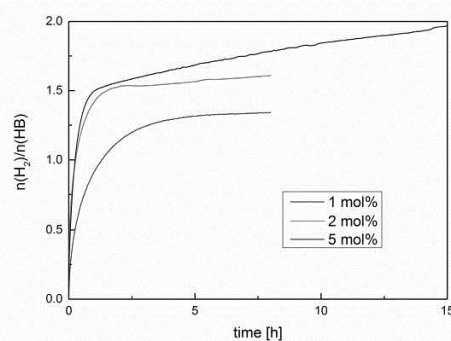


Figure 2. Volumetric curves for dehydrogenation of HB (1.1 mmol) using different concentrations of complex **2** in THF at $T = 25\text{ }^{\circ}\text{C}$.

Interestingly, the B-N material obtained from high-extent hydrogen release (i.e. > 2 equivalents H₂) was found to be rather unstable in air, leading to spontaneous self-ignition. However, when stored under Argon the material did not show any signs of decomposition. Due to the limited stability, detailed characterisation of this dehydrogenation residue was not possible. Also in this case, the separated catalyst solution still showed significant activity in further dehydrogenation runs using fresh substrate.

Release of significantly more than one equivalent of hydrogen at room temperature (Figures 1 and 2) suggests the presence of an additional dehydrogenation step which plays a role especially for higher catalyst loadings. To further evaluate this, we performed dehydrogenation reaction using 2 mol% of complexes **1-BH₃** and **2** at lower ($T = 15\text{ }^{\circ}\text{C}$) and higher temperatures ($T = 40\text{ }^{\circ}\text{C}$) and found that in the latter case rapid release of more than two equivalents of hydrogen takes place (see Supporting Information for details). At $T = 15\text{ }^{\circ}\text{C}$ a maximum of 1.3 equivalents of hydrogen was released, slightly less than at room temperature. We assume that – as suggested by Manners and co-workers for other amine borane adducts¹⁴ – the additional amount of H₂ is caused by metal-free dehydrocoupling of the transient [H₂NNH=BH₂] and higher temperature is needed to overcome the activation barrier for this.

To further investigate the fate of the Fe catalysts **1-BH₃** and **2**, we performed *in situ* NMR studies under reaction conditions, i.e. in an open system with samples taken after certain reaction times. *In situ* NMR spectra using complex **1-BH₃** suggest activation of the precatalyst by BH₃ abstraction as only complex **1-BH₃** was detected at the onset of dehydrogenation. With time, decay of this species and formation of the *trans*-dihydrido complex (¹H: -9.56 ppm; ³¹P: 116.7 ppm) were observed. Also, free hydrazine was detected (¹H: δ 2.95 ppm). In ¹¹B NMR spectra, apart from a decay of the **HB** resonance and the characteristic signal for **1-BH₃**, no other B containing intermediate species was observed. *In situ* NMR experiments using complex **2** in an open system very little amounts of the starting material **2** were detected (see Supporting Information for details). Additionally, ³¹P resonances for two *cis/trans* isomers of the Fe(II) dihydrido complex were observed at δ 113.0 and 116.7 ppm^{9c}, which slowly decayed during dehydrogenation. Multiplet signals in ¹H NMR spectra at -8.7 and -9.56 ppm support this assignment. *In situ* NMR spectroscopy at 195 K (closed J. Young NMR tube) showed that also at low temperature formation of the dihydrido complex **1** and H₂ takes place. In ¹H NMR spectra with **1-BH₃** and **2** as the catalyst apart from the decay of the starting material **HB** formation of free hydrazine was observed. Interactions

of the latter or of BH_3 with the Fe catalysts **1**- BH_3 or **2** were not observed by NMR spectroscopy. In line with this, dehydrogenation reactions with **1**- BH_3 and **2** in the presence of free N_2H_4 or BH_3 did not show significant differences compared to the catalytic runs shown in Figures 1 and 2. In the case of (POCOP)Ir hydrido complex catalysed **HB** dehydrogenation, formation of a hydrazine complex – most likely the resting state of the catalytic cycle – was observed.⁷ Deactivation of the Fe catalyst can be rationalised based on the slow build-up of ^{31}P resonances for the free PNP ligand (δ 1.0 ppm) and its oxidised form (δ 52.1 ppm) in both cases.^{9f}

STRUCTURAL CHARACTERISATION OF THE DEHYDROGENATION PRODUCTS

For characterization of the reactions residue, neither liquid-state NMR nor X-ray diffraction was applicable due to the amorphous nature of the precipitated solid and insolubility in all common organic solvents. Thus, to investigate these residues, we conducted solid-state NMR experiments in combination with XPS analysis. The ^{11}B MAS NMR spectra in Figure 3 of **HB** dehydrogenated using catalyst **1**- BH_3 and **2** reveal two different boron species with ^{11}B isotropic shifts of -7 and -4 ppm. The ^{11}B chemical shifts show that these species correspond to boron in four-fold coordination (BN_xH_y , $x+y=4$) as also observed in our previous work using an Ir-based catalyst.⁷ Surprisingly, both catalyst **1**- BH_3 and **2** lead to essentially the same ^{11}B MAS NMR spectrum (Figures 3) despite their different reaction behavior at 2 mol% catalyst loading (Figures 1 and 2).

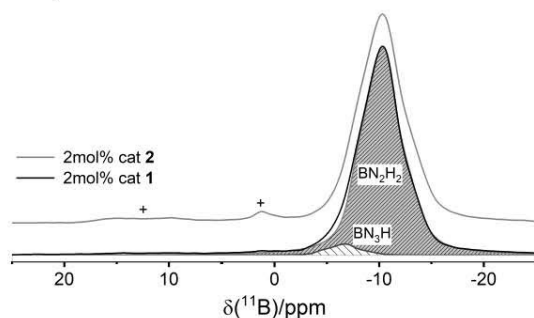


Figure 3. ^{11}B MAS NMR spectra of **HB** samples after abstraction of 1 eq. H_2 using **1**- BH_3 (black) and **2** (grey) as catalysts measured at a magnetic field strength of 11.7 T and a MAS frequency of 25 kHz. ^{11}B subgroups were assigned to the two resonances simulated on basis of MQMAS results (Figure 4). Impurities caused by a reaction of the residue with air are marked with a + sign.

Hence, it is reasonable to assume a common hydrogen abstraction mechanism for both catalysts, leading to similar $\text{B}_2\text{N}_y\text{H}_z$ structures. Additionally, the ^{11}B MAS NMR spectra of **HB** dehydrogenated using 2 or 5 mol% of the catalysts are identical (see Supporting Information for details). As the precipitated solid appears to include identical boron environments independent of the reaction conditions, the following structural discussion will focus only on the dehydrogenation product using 2 mol% of catalyst **2** at an abstraction rate of 1 eq. H_2 . To further increase the resolution and determine the quadrupolar coupling parameters from the overlapping ^{11}B species in the ^{11}B MAS NMR spectrum, we conducted a triple-quantum (3Q)MAS NMR experiment (Figure 4). From this spectrum (Figure 4, top), the extracted horizontal rows give clear proof for the two different boron species in the precipitated solid

(cf. Figure 3 and Figure 4 a, b). Moreover, we extracted the ^{11}B quadrupolar coupling parameters (C_Q and η_Q) for both boron species using the 3QMAS experiments in Figure 4 combined with lineshape deconvolution of the ^{11}B MAS NMR spectrum in Figure 3 (see Table S1). These parameters are comparable to those determined for similar boron species in our recent work using an Ir-based catalyst.⁷

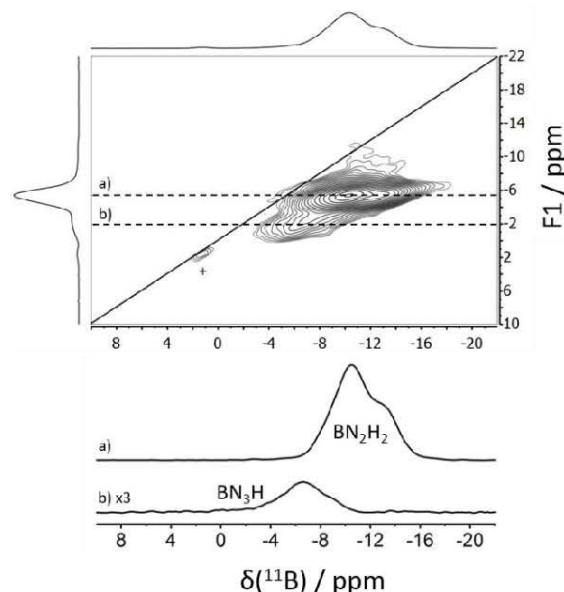


Figure 4. ^{11}B 3QMAS NMR spectrum of **HB** dehydrogenated using 2 mol% of **1**- BH_3 as catalysts up to an abstraction rate of 1.0 eq. H_2 measured at a magnetic field strength of 11.7 T and a MAS frequency of 25 kHz. Both observed ^{11}B slices were extracted at maximum intensity, corresponding to the dashed lines (shown below). An impurity caused by reaction of the residue with air is marked with a + sign. Table S1 summarizes the determined ^{11}B chemical shifts and quadrupolar coupling parameters.

Before linking these boron species and their NMR parameters to the precipitate structure and hydrogen abstraction mechanism it is essential to gain further insight into the atomic composition. To this end we characterized the sample used for the solid-state NMR experiments via XPS analysis as summarized in Table S3. These measurements revealed a significant amount of solvent (THF) incorporated into the structure, which could not be removed even under the high vacuum conditions employed in the XPS measurement. Concerning the atomic ratio of boron to nitrogen (B:N) a ratio close to 1:2 as expected for **HB**, taking into account that no gaseous nitrogen species were detected during the dehydrogenation reaction and that only a minor amount of free N_2H_4 was found in the in situ liquid-state NMR (see Supporting Information for details). However, the experimentally determined B:N ratios can be seen to fall in the range from 1.0 to 1.3, see Table S3. From the work of Goubeau and Ricker who studied the thermolysis of **HB** (up to 1 eq. H_2)¹⁵, this discrepancy can however be understood. In their work, as in this work, they observed an insoluble amorphous solid with a B:N ratio of ~ 1.0 , where large amounts of solvent molecules were incorporated, which upon further dehydrogenation lead to explosive/unstable products.¹⁵ On this basis, we can attribute the additional loss of nitrogen content compared to **HB**, to the

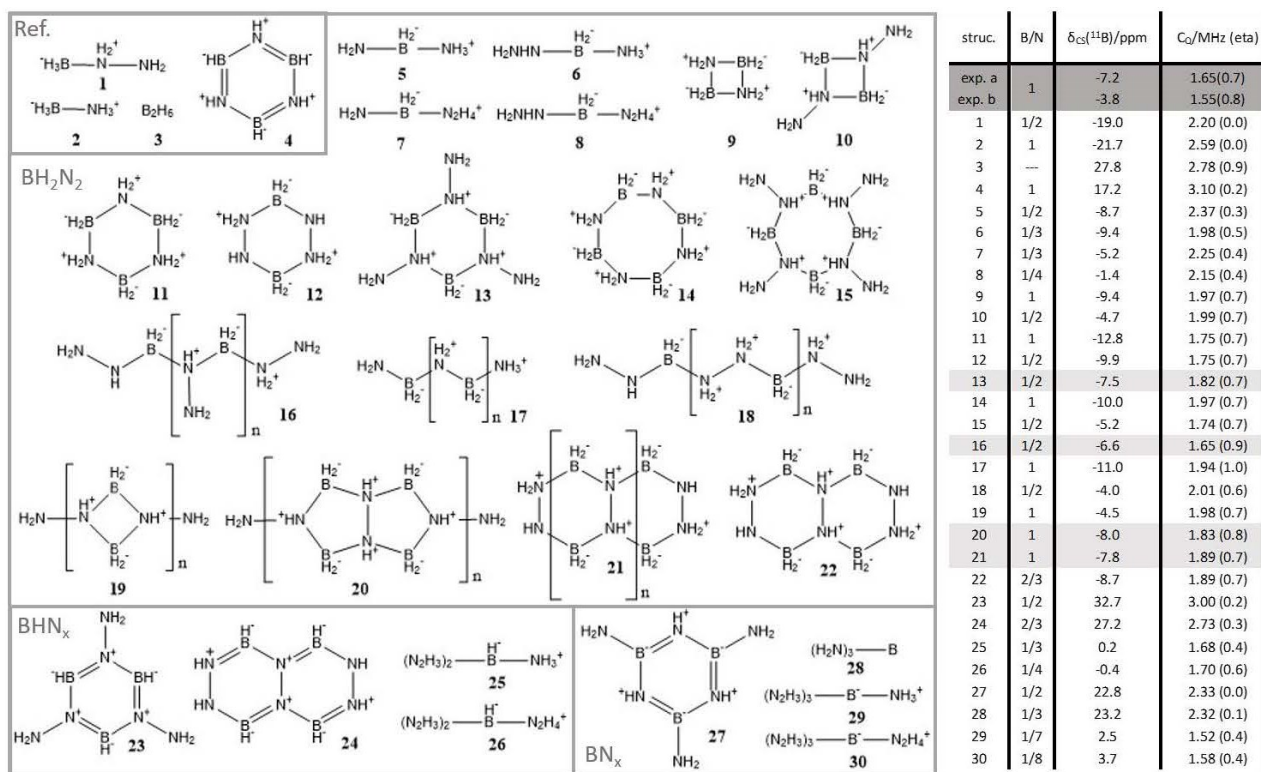


Figure 5. Left: BN_7H_5 structures used for DFT geometry optimization and calculation of ^{11}B NMR parameters (for details See supplemental information). Right: GIAO-DFT calculated ^{11}B parameters using TURBOMOLE with B3-LYP as functional and an Ahlrich def2-TZVP basis set.

release of N_2H_4 molecules that are strongly bound to the precipitate. Such adsorbed N_2H_4 molecules are neither detected in solution-state NMR nor using solid state methods as they are removed when drying the resulting residue. Due to the nature of the precipitate, Goubeau and Ricker further proposed a polymeric structure containing cyclic $\text{B}_2\text{N}_2\text{H}_6$ monomers (cf. Figure 5, 19–21). With these results in mind, we have performed DFT calculations for a series of $\text{B}_x\text{N}_y\text{H}_z$ model structures as summarized in Figure 5. These structures include plausible small clusters and polymeric structures similar to previous work^{15,16} and report the DFT calculations of ^{11}B chemical shifts and quadrupolar coupling parameters (Table 1). Such calculated NMR parameters can be used as structural fingerprints, since they are sensitive to the chemical environment of boron and can be compared to the experimental ^{11}B chemical shifts and quadrupolar coupling parameters determined from Figure 3 and 4. We note that DFT calculations for similar $\text{B}_x\text{N}_y\text{H}_z$ structures have recently been performed by Kobayashi and co-workers¹⁷; however, their work focussed on the calculation and correlation of experimental ^{15}N chemical shifts.¹⁷ Also note that our DFT approach are gas-phase calculations and as such does not include effects from a solid-state packing of the structures. Referencing of the chemical shift calculations, were performed using four different reference structures (1–4 in Figure 5) with known ^{11}B chemical shifts (see Supporting Information for details). The comparison of experimental and calculated ^{11}B chemical shifts (Figure 5) and their associated quadrupolar coupling parameters show that the dominating ^{11}B species at -7 ppm can be assigned to a BH_2N_2 group. The model compounds containing this particular motif with a good agreement between experimental and calculated NMR parameters

are the model structures 13, 16, 20, and 21. However, as discussed above on the basis of the XPS results, the precipitate shows a B:N ratio close to 1 and clearly has a polymeric nature, we can exclude structures 13 and 16. Thus, we conclude that the precipitate most likely consists of five- or six-membered rings as depicted in structures 20 and 21, or also a mixture of both systems taking into account their similar ^{11}B NMR parameters. Goubeau and Ricker assumed that thermal decomposition of **HB** most likely leads to the six-membered ring structure, considering its thermal stability, IR properties, and the fact that solvent molecules are easily incorporated.¹⁵ This is achieved by helical or random-coil-like macrostructures with varying *cis*- and *trans*-isomers of the six-membered rings.

The second ^{11}B species located at -4 ppm was in our previous study attributed to a BHN_3 group due to the increased ^{11}B chemical shift and reduced quadrupolar coupling constant compared to the dominating boron component.⁷ However, taking into account the results from our more extensive DFT calculations of model structures, Figure 5 and Table 1, this minor component can equally well be a BH_2N_2 group, resulting for instance from the adduct formation of a free BH_2 end group with N_2H_4 . Figure 6 presents a possible polymerisation pathway leading to the proposed structure 21 where such free BH_2 end groups are present. The reaction is initiated via the catalytic abstraction of H_2 from one **HB** molecule, resulting in BN_2H_3 , which can then abstract BH_3 from **HB** due to its increased basicity compared to N_2H_4 .¹⁵ $\text{B}_2\text{N}_2\text{H}_6$ is formed after a second catalysed dihydrogen abstraction step. These $\text{B}_2\text{N}_2\text{H}_6$ units can easily undergo cyclic ring closure leading to a more thermodynamically stable product. Further addition of $\text{B}_2\text{N}_2\text{H}_6$ then results

in the polymer formation. The polymerisation to structure 20 can be explained using an analogous reaction pathway.

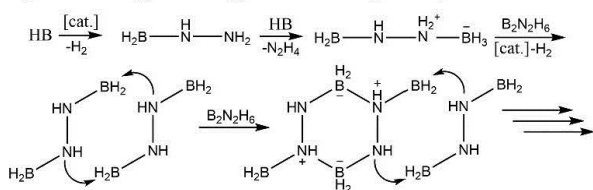


Figure 6. Possible reaction mechanism for abstraction of 1 eq. H_2 from HB leading to polymerisation with six-membered rings as repeating unit.

The homogeneous dehydrogenation leading to only one major BH_2N_2 species might in fact be advantageous for the potential application of HB as a hydrogen storage material as the cyclization of this compound appears to be more likely than for thermodynamically stable boron nitride. For this reason, we investigated the stability of the obtained precipitate in terms of exposure to air to test its sensitivity to moisture and O_2 , especially when stored for an extended period of time. From the ^{11}B MAS NMR spectra acquired for two different samples, one stored in air and the other under argon for four weeks, it can be easily seen that the precipitate stored in air changes its structure significantly, i.e., the precipitate includes two new boron species at 1 ppm and 18 ppm. The ^{11}B chemical shifts as well as their associated quadrupolar coupling parameters show that the boron species at 1 ppm is likely from a $\text{BN}_{4-x}\text{O}_x$ group and that the signal at 18 ppm is due to threefold-coordinated BN_3 . O_x (see Supporting Information for details). Thus, these results show that the reaction with air needs to be excluded when considering the possible application of HB as hydrogen storage material using an abstraction rate of only one equivalent of H_2 . On the other hand, this approach with abstraction of only one equivalent H_2 clearly has the advantage that any formation of explosive residues, due to increased H_2 abstraction¹⁵, can be prevented using proper reaction monitoring. Additionally, the catalytic dehydrogenation of HB compared to thermolysis using the Fe catalysts 1 and 2 can be easily achieved at room temperature.

MECHANISTIC CONSIDERATIONS FROM DFT ANALYSIS

On the basis of our experimental results, we also carried out B3PW91 density functional theory computations to clarify the reaction mechanism, where we discussed and interpreted from experiment to theory and vice versa. In our experiment, we observed the immediate H_2 evolution from the dehydrogenation of hydrazine borane (HB) catalyzed by complex 1- BH_3 as the catalyst in THF under an atmosphere of argon at room temperature. Concurrently, the color of the Fe hydrido complex slowly faded from yellow to pale yellow and a white solid precipitated.

First we computed the thermal dehydrogenation of HB ($\text{H}_2\text{N}-\text{NH}_2-\text{BH}_3 \rightarrow \text{H}_2\text{N}-\text{HN}=\text{BH}_2 + \text{H}_2$). It is found that this reaction is exergonic (-12.13 kcal/mol); indicating a thermodynamically favorable process. In addition, we computed the direct dehydrogenation via a four-membered $[2+2]$ transition state; and the computed free energy barrier is very high (34.97 kcal/mol), revealing the high thermodynamic stability of HB towards dehydrogenation; and therefore catalytic dehydrogenation is necessary. The trimerization of $\text{H}_2\text{N}-\text{HN}=\text{BH}_2$ to borazine ($\text{B}_3\text{N}_3\text{H}_6$) and NH_3 is exergonic by 180.02 kcal/mol.

Since our experimental work showed that both amino complex 1 and amido complex 2 are active catalysts, we computed HB dehydrogenation using 1 and 2 for comparison. The computed results are shown in Figure 5.

For the reaction between complex 1 and HB, we tried to find a double-hydrogen bonding interacted intermediate, i.e.; between the proton of the catalyst N-H bond and the hydride of the BH_3 group as well as between the hydride of the catalyst Fe-H and the proton of the central NH_2 group. We tried several configurations by varying the conformations of the terminal BH_3 and NH_2 group; and the most stable intermediate HB-A has only one hydrogen-bonding between Fe-H and the proton of the central NH_2 group. This hydrogen bonding has a $\text{NH}-\text{HFe}$ distance of 1.505 Å and the hydrogen-bonding is slightly exergonic by 0.20 kcal/mol. It is not possible to get the structure of the intermediate with double-hydrogen bonding. Starting from intermediate HB-A, we tried to get one concerted transition state (HB-TS1) for double H_2 formation to get complex 2 and $\text{H}_2\text{N}-\text{HN}=\text{BH}_2$, but failed. Furthermore, we tried to eliminate one H_2 molecule between the hydrogen bonding via the Frustrated Lewis Pair concept, i.e.; one H_2 molecule between the Fe center and the B center; and optimization for searching the transition state (HB-TS2) leads to the direct formation of an artificial structure with coordinated H_2 ; and removal of H_2 forms intermediate HB-B; and this step is exergonic by 3.59 kcal/mol. Starting from intermediate HB-B (the HB-B-*trans* isomer is less stable by 3.99 kcal/mol) it is also not possible to get the transition state (HB-TS3) for the second H_2 formation. From HB-A to 2 and $\text{H}_2\text{N}-\text{HN}=\text{BH}_2$, the reaction is exergonic by 11.61 kcal/mol. However, the formation of complex C from 2 and $\text{H}_2\text{N}-\text{HN}=\text{BH}_2$ is exergonic by 8.10 kcal/mol; and this is much smaller than the free energy (-180.02 kcal/mol) of the trimerization of $\text{H}_2\text{N}-\text{HN}=\text{BH}_2$ to borazine and release of NH_3 .

Starting from the amido complex 2 and a second HB molecule, we computed the second dehydrogenation cycle. At first, we tried to find a double-hydrogen bonding interacted intermediate (HB-D), i.e.; between the proton of the central N-H bond and the catalyst amido nitrogen center as well as the hydride of the BH_3 group and the Fe center. However, structure optimization results in the formation of intermediate (HB-E), in which the central N-H bond is already broken and the hydrogen atoms is transferred to the amido nitrogen atom as well as one hydrogen bonding between B-H-Fe. In contrast, the formation of the hydrogen bonding complex (HB-F) between the amido nitrogen atom and the central NH_2 group of HB is endergonic by 3.46 kcal/mol, and therefore, not competitive with HB-E. Starting from intermediate (HB-E), we tried to get the transition state for the hydride transfer from B to Fe (HB-TS4), but failed. Structure optimization directly yields catalyst 1 and $\text{H}_2\text{N}-\text{HN}=\text{BH}_2$. All these findings indicate that this dehydrogenation might have very low barrier (if any); and that the reaction can be considered as typical and simple acid and base reaction; and only such type of reaction is in line with our experimentally observed reaction kinetics, i.e.; fast at room temperature and detectable at very low temperature. On the basis of this discussion, we propose a simple acid and base reaction mechanism (Figure 6).

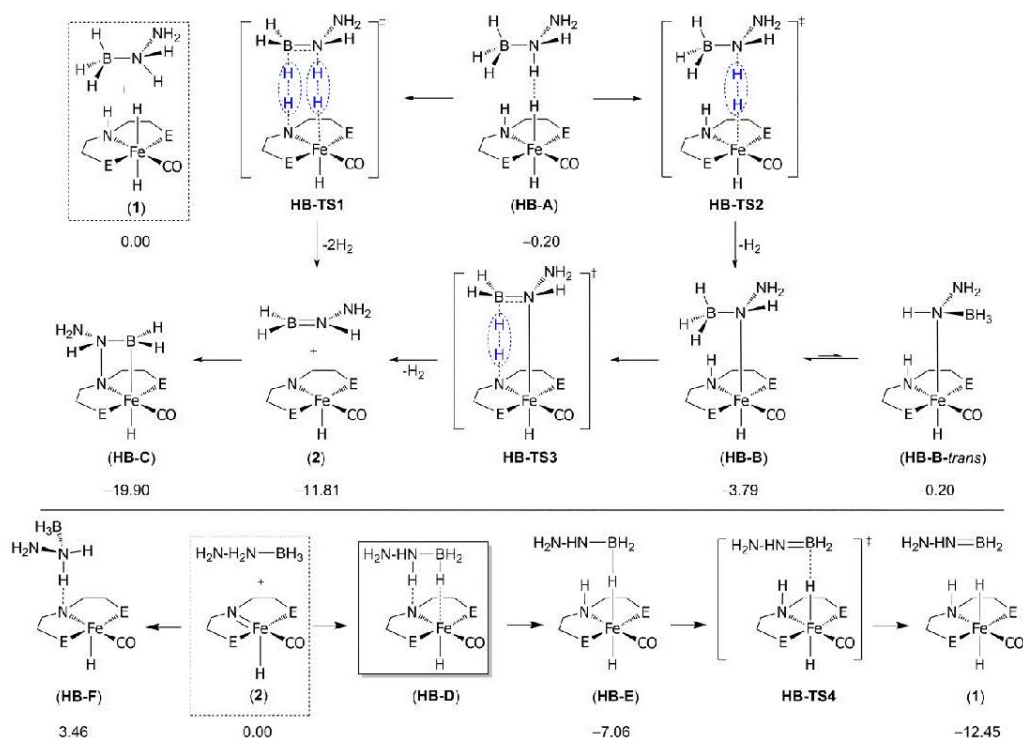


Figure 7. B3PW91 reaction thermodynamics of catalysts 1 and 2 with HB.

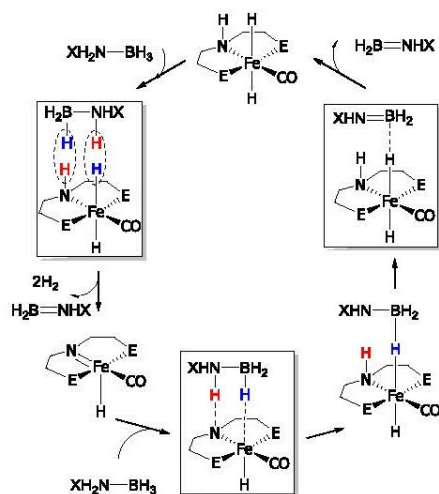


Figure 8. Proposed mechanism for the dehydrogenation of HB ($X = \text{NH}_2$) and AB ($X = \text{H}$) using catalysts 1 and 2.

CONCLUSIONS

We have presented the first study of hydrazine borane dehydrogenation using non-noble metal based homogeneous catalysts at mild conditions. Iron(II) hydrido complexes were found to be very active and recyclable catalysts, releasing at least one equivalent of hydrogen. In cases where significantly more than one equivalent of hydrogen evolved, the obtained solid dehydrogenation product showed signs of decomposition in line with its tentative structural assignment as a material containing highly energetic cyclic unsaturated B-N units containing a nitrogen-nitrogen bond. Solid-state NMR investigation of the solid residue with an abstraction of 1.0 eq. H_2 gave essentially the same ^{11}B spectra for both investigated

residues. This is in line with the suggested common dehydrogenation mechanism of both catalysts. Structural analysis of the precipitate lead to an assignment to a homogeneous polymer with a six-membered or less likely a five-membered ring as repeating unit. These structures were derived from a combination of XPS analysis with solid-state NMR spectroscopy as well as DFT calculations of different $\text{B}_x\text{N}_y\text{H}_z$ structure models. These structural models and calculations might also lead to an improved understanding of boron clusters in similar fields of research. DFT analysis of the first Fe catalysed dehydrogenation step suggests the presence of an essentially barrier-free reaction mechanism that involves acid-base-type interactions between the Fe hydride catalyst and the substrate.

ASSOCIATED CONTENT

Supporting Information

Experimental details, volumetric curves, NMR spectra, details of the DFT calculations.

The Supporting Information is available free of charge on the ACS Publications website.

AUTHOR INFORMATION

Corresponding Author

* mhansen@uni-muenster.de, torsten.beweries@catalysis.de

Notes

† These authors contributed equally.

ACKNOWLEDGMENT

We thank our technical and analytical staff, in particular Andreas Koch, for support. D.H. thanks the China Scholarship Council (file NO. 20150808083) for funding. R.K. acknowledges support by the Fonds der Chemischen Industrie.

REFERENCES

- (1) a) Schlapbach, L.; Züttel, A. *Nature* **2001**, *414*, 353; b) Eberle, U.; Felderhoff, M.; Schüth, F. *Angew. Chem. Int. Ed.* **2009**, *48*, 6608; c) Durbin, D. J.; Malardier-Jugroot, C. *Int. J. Hydrogen Energy*, **2013**, *38*, 14595.
- (2) a) Hamilton, C. W.; Baker, R. T.; Staubitz, A.; Mannes, I. *Chem. Soc. Rev.* **2009**, *38*, 279; b) Staubitz, A.; Robertson, A. P. M.; Sloan, M. E.; Mannes, I. *Chem. Rev.* **2010**, *110*, 4023; c) Beweries, T. in *Organometallics and Related Molecules for Energy Conversion*, ed. Wong, W.-Y., Springer-Verlag Berlin Heidelberg, 2015, pp. 469; d) Rossin, A.; Peruzzini, M. *Chem. Rev.* **2016**, *116*, 8848.
- (3) Hügle, T.; Kühnel, M. F.; Lentz, D. *J. Am. Chem. Soc.* **2009**, *131*, 7444.
- (4) a) Karahan, S.; Zahmakiran, M.; Özkar, S. *Int. J. Hydrogen Energy* **2011**, *36*, 4958; b) Hannauer, J.; Akdim, O.; Demirci, U. B.; Geantet, C.; Herrmann, J.-M.; Miele, P.; Xu, Q. *Energy Environ. Sci.*, **2011**, *4*, 3355; c) Çelik, D.; Karahan, S.; Zahmakiran, M.; Özkar, S. *Int. J. Hydrogen Energy* **2012**, *37*, 5143; d) Çakanyıldırım, Ç.; Demirci, U. B.; Şener, T.; Xu, Q.; Miele, P. *Int. J. Hydrogen Energy* **2012**, *37*, 9722; e) Zhong, D.-C.; Aranishi, K.; Singh, A. K.; Demirci, U. B.; Xu, Q. *Chemical Commun.* **2012**, *48*, 11945; f) Şencanlı, S.; Karahan, S.; Özkar, S. *Int. J. Hydrogen Energy* **2013**, *38*, 14693; g) Zhu, Q.-L.; Zhong, D.-C.; Demirci, U. B.; Xu, Q. *ACS Catalysis* **2014**, *4*, 4261; h) Cléménçon, D.; Petit, J. F.; Demirci, U. B.; Xu, Q.; Miele, P. *J. Power Sources* **2014**, *260*, 77; i) Zhang, Z.; Lu, Z.-H.; Tan, H.; Chen, X.; Yao, Q. *J. Mater. Chem. A* **2015**, *3*, 23520; j) Z. Zhang, Z.-H. Lu, X. Chen, *ACS Sustainable Chem. Eng.*, *3* (2015) 1255.
- (5) Moury, R.; Demirci, U. B. *Energies* **2015**, *8*, 3118.
- (6) Thomas, J.; Klahn, M.; Spannenberg, A.; Beweries, T. *Dalton Trans.* **2013**, *42*, 14668.
- (7) Han, D.; Jösch, M.; Klahn, M.; Spannenberg, A.; Drexler, H. J.; Baumann, W.; Jiao, H.; Knitsch, R.; Hansen, M. R.; Eckert, H.; Beweries, T. *Dalton Trans.* **2016**, *45*, 17697.
- (8) a) Alberico, E.; Sponholz, P.; Cordes, C.; Nielsen, M.; Drexler, H.-J.; Baumann, W.; Junge, H.; Beller, M. *Angew. Chem. Int. Ed.* **2013**, *52*, 14162; b) Koehne, I.; Schmeier, T. J.; Bielinski, E. A.; Pan, C. J.; Lagaditis, P. O.; Bernskoetter, W. H.; Takase, M. K.; Würtele, C.; Hazari, N.; Schneider, S. *Inorg. Chem.* **2014**, *53*, 2133.
- (9) *Selected examples:* a) Werkmeister, S.; Junge, K.; Wendt, B.; Alberico, E.; Jiao, H.; Baumann, W.; Junge, H.; Gallou, F.; Beller, M. *Angew. Chem. Int. Ed.* **2014**, *53*, 8722; b) Bornschein, C.; Werkmeister, S.; Wendt, B.; Jiao, H.; Alberico, E.; Baumann, W.; Junge, H.; Junge, K.; Beller, M. *Nature Commun.* **2014**, *5*, 4111; c) Bielinski, E. A.; Lagaditis, P. O.; Zhang, Y.; Mercado, B. Q.; Würtele, C.; Bernskoetter, W. H.; Hazari, N.; Schneider, S. *J. Am. Chem. Soc.* **2014**, *136*, 10234; d) Chakraborty, S.; Lagaditis, P. O.; Förster, M.; Bielinski, E. A.; Hazari, N.; Holthausen, M. C.; Jones, W. D.; Schneider, S. *ACS Catalysis* **2014**, *4*, 3994; e) Chakraborty, S.; Dai, H.; Bhattacharya, P.; Fairweather, N. T.; Gibson, M. S.; Krause, J. A.; Guan, H. *J. Am. Chem. Soc.* **2014**, *136*, 7869; f) Chakraborty, S.; Brennessel, W. W.; Jones, W. D. *J. Am. Chem. Soc.* **2014**, *136*, 8564.
- (10) Glüer, A.; Förster, M.; Celinski, V. R.; Schmedt auf der Günne, J.; Holthausen, M. C.; Schneider, S. *ACS Catalysis* **2015**, *5*, 7214.
- (11) Anke, F.; Han, D.; Klahn, M.; Spannenberg, A.; Beweries, T. *Dalton Trans.* **2017**, *46*, 6843.
- (12) Schneck, F.; Assmann, M.; Balmer, M.; Harms, K.; Langer, R. *Organometallics* **2016**, *35*, 1931.
- (13) Sonnenberg, J. F.; Morris, R. H. *Catal. Sci. Technol.* **2014**, *4*, 3426.
- (14) Leitao, E. M.; Stubbs, N. E.; Robertson, A. P. M.; Helten, H.; Cox, R. J.; Lloyd-Jones, G. C.; Mannes, I. *J. Am. Chem. Soc.* **2012**, *134*, 16805.
- (15) Goubeau, J.; Ricker, E. Z. *Anorg. Allg. Chem.* **1961**, *310*, 123.
- (16) Moury, R.; Moussa, G.; Demirci, U. B.; Hannauer, J.; Bernard, S.; Petit, E.; van der Lee, A.; Miele, P. *Phys. Chem. Chem. Phys.* **2012**, *14*, 1768.
- (17) Kobayashi, T.; Gupta, S.; Caporini, M. A.; Pecharsky, V. K.; Pruski, M. *J. Phys. Chem. C* **2014**, *118*, 19548.

6. Curriculum Vitae

Personal Information

Name	HAN, DELONG
Date of birth	5th, Jan., 1989
Place of birth	Gansu, China, P. R. China
Nationality	Chinese
Address	Albert-Einstein-Str. 29, 18059 Rostock, Germany
Email	Delong.han@catalysis.de
Phone	+4917645643545



Academic Background

- 10/2014 - PhD student at Leibniz Institute for Catalysis in the department Coordination Chemistry and Catalysis, supervised by PD. Dr. Torsten Beweries, research topic: transition metal catalysed dehydrogenation and dehydrocoupling of amine borane adducts for hydrogen storage and materials chemistry
- 9/2011 – 7/2013 Graduate Student at Inner Mongolia University of Technology in Hohhot, Inner Mongolia (P.R. China) in the group for functional molecular materials of Prof. Dr. Liming Han, research topic: characterization and intermolecular charge transfer in ferrocenyl substituted benzene; synthesis of ferrocenyl substituted isobenzofuranes and isoindoles
- 9/2007 – 7/2011 Studied at Qingdao Agricultural University in Qingdao, Shandong (P.R. China) as undergraduate student

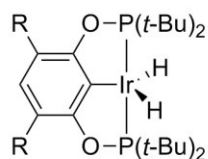
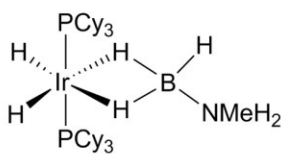
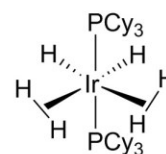
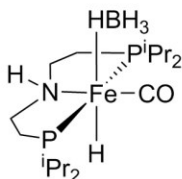
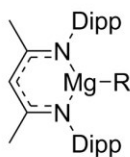
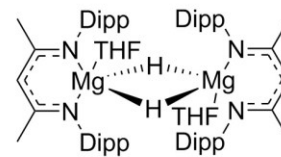
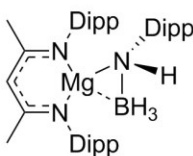
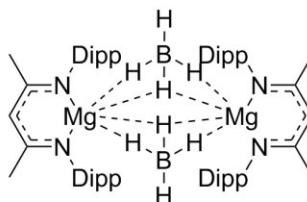
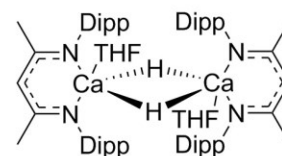
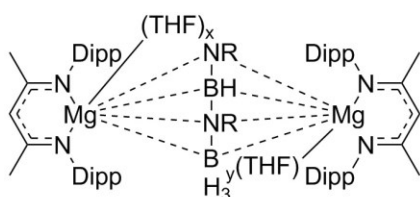
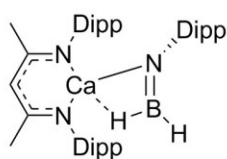
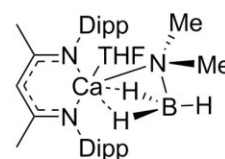
Awards and scholarships

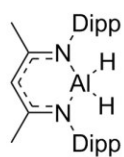
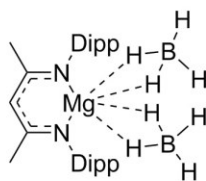
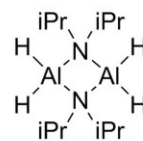
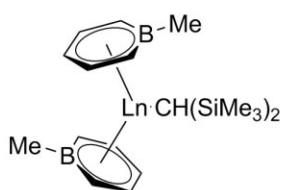
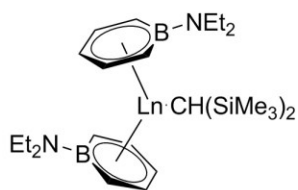
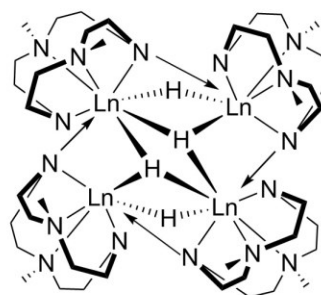
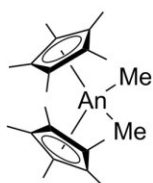
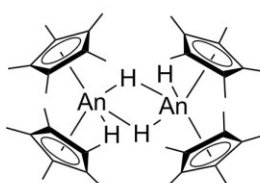
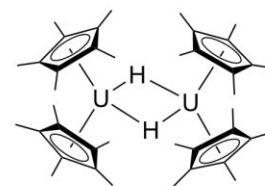
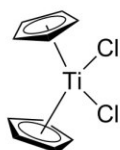
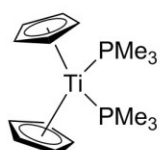
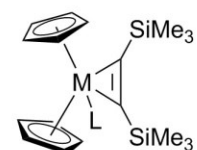
1. Organometallics poster award at 16th International meeting on Boron Chemistry, Hongkong (China) 09.-13.07.2017
2. Full scholarship for PhD studies from The China Scholarship Council (CSC)

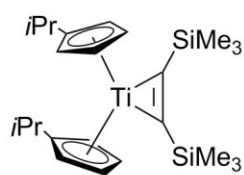
Publications

1. D. Han[†], R. Knitsch[†], F. Anke, H. Jiao, M. R. Hansen*, T. Beweries*, manuscript in preparation.
2. D. Han, B. Andres, A. Spannenberg, T. Beweries*, *Acta Cryst. C* **73**, 917.
3. F. Anke, D. Han, M. Klahn, A. Spannenberg, T. Beweries*, *Dalton Trans.*, **2017**, 46, 6843.
4. D. Han, M. Joksche, M. Klahn, A. Spannenberg, H.-J. Drexler, W. Baumann, H. Jiao, R. Knitsch, M. R. Hansen, H. Eckert, T. Beweries*, *Dalton Trans.*, **2016**, 45, 17697.

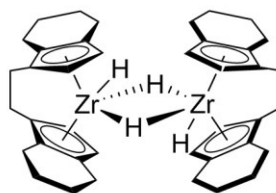
7. Compounds in the dissertation

**1****2****3****4****5** R = nBu**6** R = N(SiMe₃)₂**7****8****9****10****11** R = H, x = 1, y = 1**12** R = *i*Pr, x = 1, y = 0**13** R = Me, x = 1, y = 0**14****15**

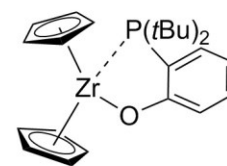
**16****17****18****19** Ln = Y**20** Ln = Lu**21** Ln = Y**22** Ln = Lu**23** Ln = La**24** Ln = Y**25** An = Th**26** An = U**27** An = Th**28** An = U**29****30****31****32** M = Ti, no L**33** M = Zr, L = Pyridine



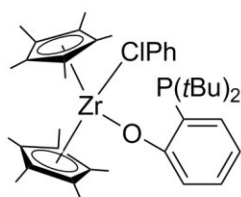
34



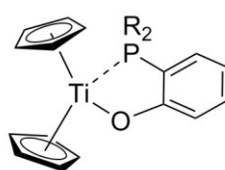
35



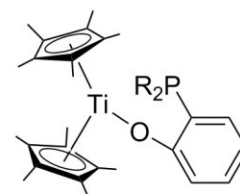
36



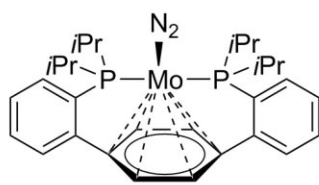
37

38 R = *i*Pr

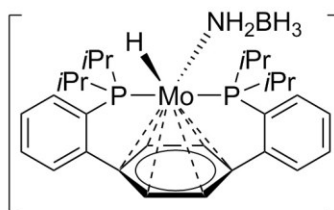
39 R = Ph

40 R = *i*Pr

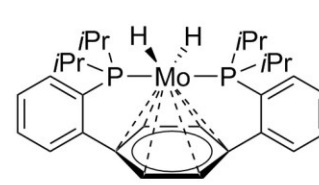
41 R = Ph



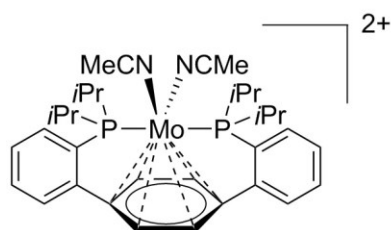
42



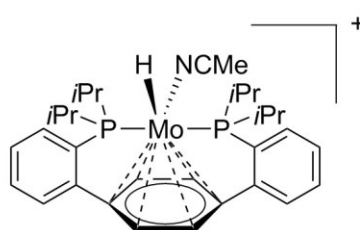
43



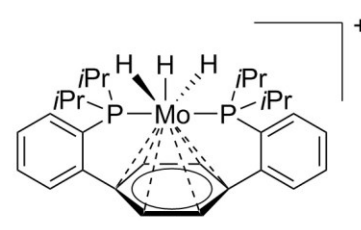
44



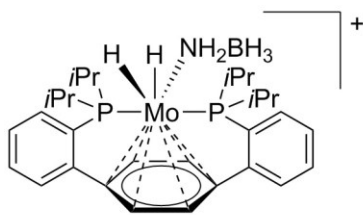
45



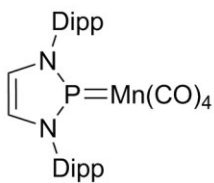
46



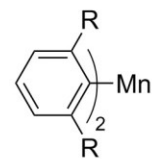
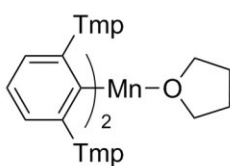
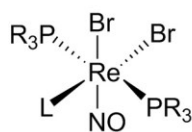
47



48



49

50 R = 2,6-Me₂C₆H₃51 R = 2,4,6-Me₃C₆H₂52 Tmp = 2,4,5-Me₃C₆H₂R = *i*Pr53 L = H₂

54 L = MeCN

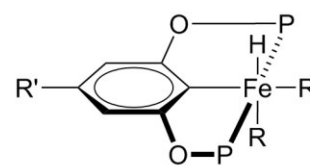
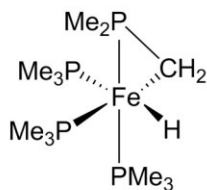
55 L = ethylene

R = Cy

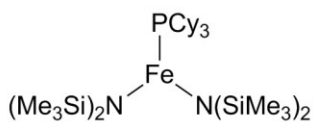
56 L = H₂

57 L = MeCN

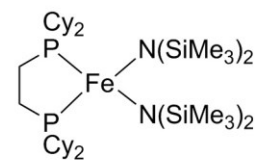
58 L = ethylene

59 R' = H, R = PMe₃60 R' = H, R = PMe₂Ph61 R' = MeO, R = PMe₂Ph

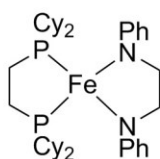
62



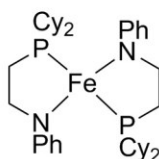
63



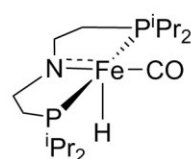
64



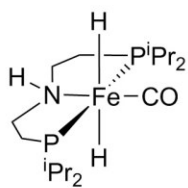
65



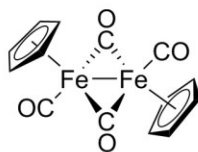
66



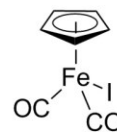
67



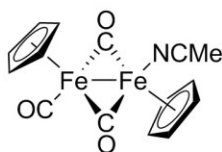
68



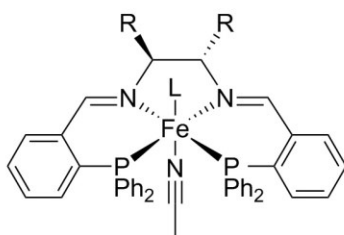
69



70



71

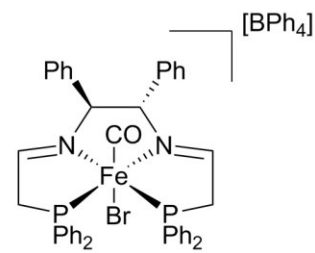


72 L = NMe, R = H

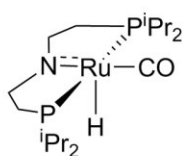
73 L = CO, R = H

74 L = NMe, R = Ph

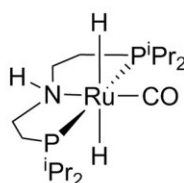
75 L = CO, R = Ph



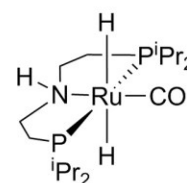
76



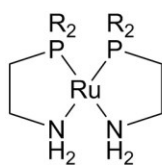
77



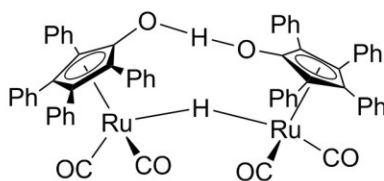
78



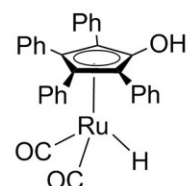
79

80 R = *i*Pr81 R = *t*Bu

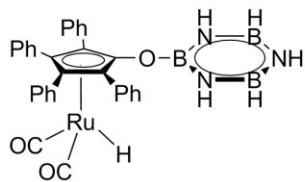
82 R = Ph



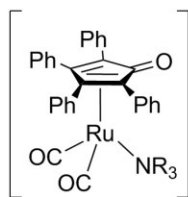
83



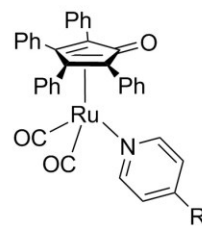
84



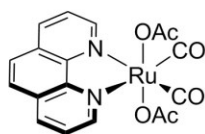
85



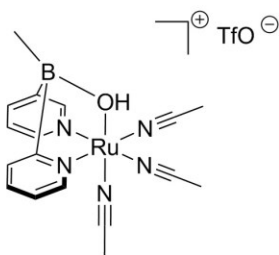
86



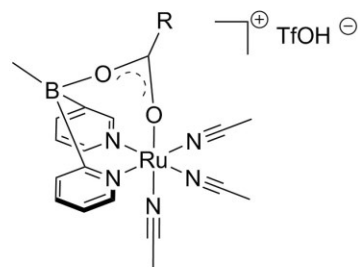
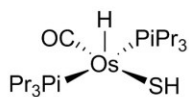
87 R = H

88 R = NH₂89 R = CF₃

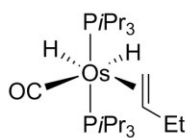
90



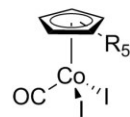
91

92 R = CH₃93 R = CF₃

94

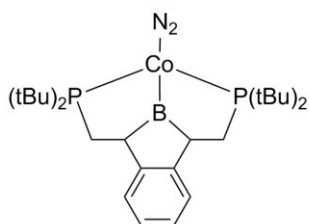


95

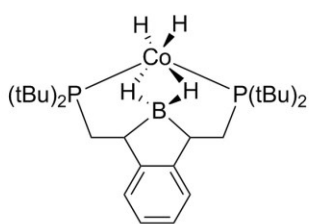


96 R = Me

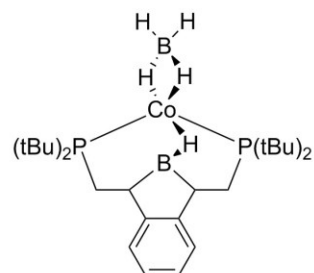
97 R = H



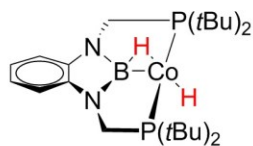
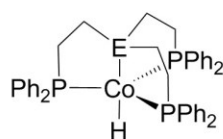
98



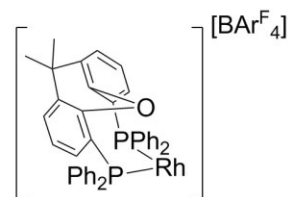
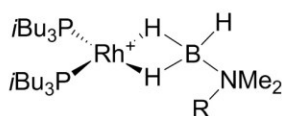
99



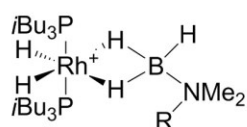
100

**101**

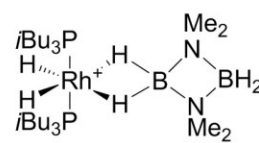
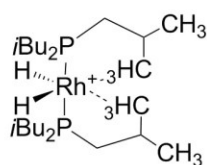
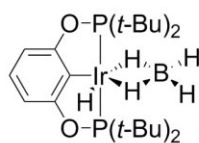
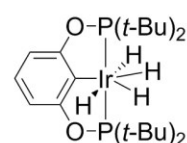
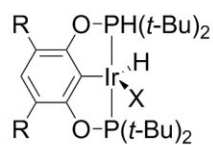
102-N E = N
102-P E = P

**103**

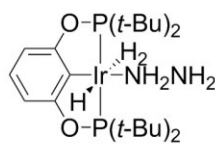
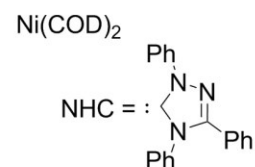
104-1-a R = H
104-2-a R = Me

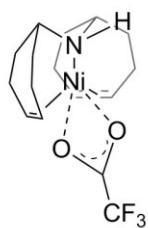
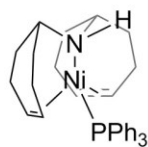
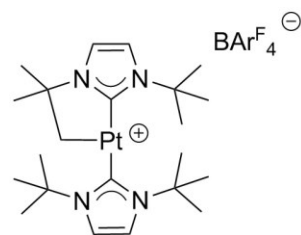
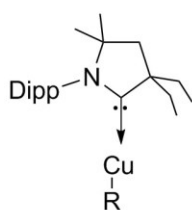


104-1-b R = H
104-2-b R = Me

**104-2-c****104-d****105****106**

R = H **107** X = Cl
 R = *t*-Bu **108** X = H **109** X = Cl
 R = COOMe **110** X = H **111** X = Cl
112 R = CF₃, X = H

**113****114**

**115****116****117****118** R = Cl**119** R = BH₄